Dynamics of Ring Polymers in an Obstacle Environment

A thesis submitted in partial fulfillment of
the requirements for the degree of

Doctor of Philosophy

by

V. S. Balaji Iyer
(Roll No. 03402702)

Under the guidance of
Prof. Vinay A. Juvekar
and
Dr. Ashish K. Lele

DEPARTMENT OF CHEMICAL ENGINEERING
INDIAN INSTITUTE OF TECHNOLOGY–BOMBAY
April 2009

To my Teachers

Thesis Approval

The thesis entitled

Dynamics of Ring Polymers in an Obstacle Environment

by

V. S. Balaji Iyer
(Roll No. 03402702)

is approved for the degree of

Doctor of Philosophy

Examiner	Examiner
Guide	Co Guide

Chairman

Date: _____

Place: _____

INDIAN INSTITUTE OF TECHNOLOGY BOMBAY, INDIA

CERTIFICATE OF COURSE WORK

This is to certify that **V. S. Balaji Iyer** (Roll No. 03402702) was admitted to the candidacy of Ph.D. degree on July 2003, after successfully completing all the courses required for the Ph.D. programme. The details of the course work done are given below.

S.No	Course Code	Course Name	Credits
1	CL 602	Mathematical & Statistical Methods in Chemical Engg	6
2	CL 624	Polymer Processing	6
3	CL 664	Polymer Thermodynamics	6
4	CL 645	Polymer Dynamics	6
5	CLS801	Seminar	4
6	CL 702	Lecture Series	PP
7	HS 699	Communication and Presentation Skills	PP
		Total Credits	**28**

IIT Bombay

Date: Dy. Registrar (Academic)

Abstract

We present three different frameworks for studying the dynamics of flexible non-concatenated ring polymers constrained by an array of obstacles. All the frameworks are developed for an array of fixed obstacles, as in the case of gel, and extended to the case of dynamic obstacles, as in the case of melts and semi-dilute solution. The frameworks, *viz.*

- Pom-Pom Ring (**PPR)**
- Blob-Spring (**BS)**
- Fractal-Gate (**FG)**

are based on three different approaches to dynamics of polymers.

The PPR framework is based on a coarse-grained mean-field approach to dynamics of polymers in the presence of topological constraints. In formulating the PPR framework the similarity of the static structure of the flexible ring polymer in an array of fixed obstacles to that of the ideal randomly branched polymer is exploited using aspects of the pom-pom model for branched polymers. The topological constraints are handled via the mean-field tube model framework. Based on the PPR formulation we obtain expressions for curvilinear diffusion coefficient, self-diffusion coefficient, spectrum of relaxation times and dynamic structure factor. The scaling exponents for the molecular weight dependence of diffusion coefficient and the longest relaxation time obtained using the formulation are shown to be in agreement with previously proposed scaling arguments. Further, the framework is utilized to build a molecular theory of linear viscoelasticity for ring polymers in both an array of fixed obstacles and melt of ring polymers. The linear viscoelastic predictions of the theory are shown to be in close agreement with experiments on melt of ring polymers in the terminal regime. However, the PPR framework based molecular theory does not capture the self-similar dynamics of ring polymers and consequently the power law slopes of gain modulus, at the intermediate frequencies, observed in experiments.

The BS framework is based on a coarse-grained fluctuations approach to dynamics of flexible polymers. In formulating the BS framework ideas developed for the study of dynamics of unentangled fractal polymers is extended to model dynamics of flexible ring polymers in an array of fixed obstacles. The extension is achieved by incorporation of the appropriate friction coefficient to describe the perpetual evolution of the perimeter of a ring polymer as it undergoes Brownian motion in a topologically constrained environment. The framework being based on dynamics of fractal polymers is intrinsically self-similar. The scaling exponents for the molecular weight dependence of self-diffusion coefficient and spectrum of relaxation times obtained based on the framework are shown to be in agreement with the previously proposed scaling arguments. The framework is utilized to derive a constitutive relation and the predictions of the relation are compared with the experimental data on linear viscoelastic response of a melt of ring polymers. The linear viscoelastic response based on the constitutive relation is shown to be in qualitative agreement with experiments on melt of rings.

The FG framework is based on the judicious combination of the fluctuations approach to dynamics of fractals and mean-field approach of handling entanglements. In this the fluctuations approach to dynamics is worked out for an arbitrary section composed of m-blobs with a different friction coefficient from that of BS model. The center of mass of the m-section of chain undergoing such fluctuations is considered to be constrained in a tube corresponding to the trunk of the chain section. The dynamics of the m-section chain is governed by the combination of the fluctuations and 1-D diffusion of the center of mass of the m- section out of the gate of its confinement. Such a combination of dynamics of the chain is shown to yield a molecular weight dependence of curvilinear-diffusion coefficient, relaxation spectrum and longest relaxation time in agreement with previously proposed scaling arguments. Self-similarity in dynamics is considered as a natural consequence of the simultaneous operation of this dynamics at all length scales. It is argued that there are several such sections diffusing from the gates of confinement in the chain and the contribution of the sections to the viscoelastic response is weighted by the number fraction of gates in the chain. The linear viscoelastic response of the chain is then obtained as the superposition of the responses of the sections of the chain. In all these frameworks we have assumed that the ring chain has a Cayley tree structure in the obstacle environment and we have not explicitly accounted for interpenetration of loops of the ring chain.

The addition of ring polymers to a solution of non-concatenated ring polymers beyond the threshold concentration causes introduction of topological constraints. Under such conditions

the change in concentration influences both the static structure and dynamics of ring polymers in a way different from that of linear polymers. Consequently, the diffusion coefficient of ring polymers in a topologically constrained environment can be expected to be different from that of linear polymers. The connection between the dynamics of a flexible ring polymer and its static structure in a topologically constrained environment is elucidated in the PPR, BS and FG frameworks. Here, we present scaling arguments for the concentration and molecular weight dependence of self-diffusion coefficient of ring polymers in semi-dilute solutions, and show that contrary to expectations these scaling relations are identical to what is known for linear polymers. At higher concentrations excluded volume interactions arising from possibilities of segmental overlap can become effective for large ring polymers. In this regime the diffusion coefficient of large ring polymers shows a relatively weaker dependence on concentration and molecular weight.

In a topologically constrained environment the static structure and size of a flexible non-concatenated ring polymer (macrocycle) is known to differ from that of linear polymers. In condensed states such as melt or concentrated solution, ring polymers assume compact conformations ($R \sim N^{\nu}$ with $\nu \approx 0.4$) as compared to that of linear polymers with the same degree of polymerization ($\nu = 0.5$). Upon substituting some of the ring polymers with linear polymers, the ring polymers swell because of local relaxation of the non-concatenation constraint. In the limit of infinite dilution the size of the ring polymer is expected to scale as $R \sim N^{0.5}$. We consider ring-linear blends as ideal semi-dilute solutions of ring polymers in linear polymers and present a scaling argument to capture the size transition. We argue that the size of the ring polymer remains the same as that in Θ-solvent up to the overlap concentration, C_r^*. Beyond C_r^* the size of the ring shrinks according to $R \sim C_r^{\beta}$, where $\beta = 2\nu - 1 = -0.2$ for $\nu = 0.4$.

Contents

List of Tables

List of Figures

Nomenclature

β	Scaling exponent relating size & concentration
ϵ	Measure of extent of reaction
ζ	Friction coefficient of the Rouse bead
ζ_{eff}	Effective friction coefficient
ζ_{eff}^{p}	Effective friction coefficient of the the $(1/p)^{th}$ section of the chain
ζ_{loop}	Friction coefficient of the loop
ζ_{p}	Friction coefficient of the p^{th} Rouse mode
ζ_{blob}	Friction coefficient of a blob
η_0	Zero shear viscosity
ν	Scaling exponent relating size and degree of polymerization
υ	Excluded volume parameter
ρ	Scaling exponent relating backbone size and degree of polymerization
ρ_m	Melt density
τ_{arm}	Relaxation time of a branch arm through 'breathing modes'
τ_b	Relaxation time of a branched Pom-Pom backbone
τ_d	Longest relaxation time based on reptation/$1-D$ diffusion dynamics
τ_e	Relaxation time at the entanglement length scale

τ_0	Relaxation time at the blob length scale
τ_p	Relaxation spectrum based on Rouse dynamics
ψ	Fraction of chain in original tube in mean-field tube model
Ψ	Configurational probability distribution
ω	Frequency of oscillation in an oscillatory shear experiment
ξ	Correlation length
φ	Fraction of reacted B groups
φ_c	Critical fraction of reacted B groups
a	Linear dimension of obstacle
b	Kuhn length of a polymer
C	Concentration of Kuhn segments in solution
C^*	Overlap/Threshold concentration
$C^\#$	Concentration above which topological constraints are activated
C^{ex}	Concentration above which excluded volume interactions are activated
c	Concentration of Kuhn segments in melt
c_b	Concentration of blobs in melt
D	Self-diffusion coefficient
d	Spatial dimension
d_c	Upper critical dimension
d_f	Fractal dimension
d_s	Spectral dimension
D_{loop}	Loop diffusion coefficient

D_P	Curvilinear diffusion coefficient
D_m	Diffusion coefficient from fractal Rouse
f	Functionality of condensation monomer
$\mathbf{f}_n$	Stochastic force on the n^{th} bead in the chain
$\mathbf{f}_p$	Stochastic force on the p^{th} Rouse mode in the chain
G	Relaxation modulus
G^0	Plateau modulus
G'	Gain modulus
G''	Loss modulus
$\mathbf{H}_{nm}$	Mobility tensor
i	Coordinate of Cayley tree
$g(\mathbf{k}, t)$	Dynamic structure factor
$\mathbf{k}$	Wave vector
k	Spring constant
$\mathbb{k}$	Common primitive path of a closed random walk in a Cayley tree
k_B	Boltzmann constant
k_{eff}	Effective spring constant
k_p	Rouse mode spring constant
L	Contour length
L_P	Contour length of the primitive chain
M	Mass of chain
M_e	Entanglement molecular weight

M_0 Kuhn segment molecular weight

N Number of steps in the coarse grained representation of the polymer chain

N_ξ Number of Kuhn segments in a blob of lenght ξ

N_A Avogadro number

N_e Number of Kuhn segments between entanglements

N_K Number of Kuhn segments in the polymer chain

n_m Number fraction of m-mers in AB_{f-1} condensation polymerization

$P(x)$ Probability distribution

p Mode number in Rouse

p_s Mode number in spectral Rouse

q Fourier variable

q_n Number of branch arms

R Size of a polymer

R_{dil} Size in dilute solution

$\mathbf{R}_G$ Position coordinate of the center of mass

R_g Radius of gyration

$\mathbf{R}_n$ Position coordinate of the n^{th} bead in the chain

$\mathbf{R}(s,t)$ Position coordinate associated with point at the curvilinear distance s along the primitive chain at time t

T Temperature in degree K

U Potential of mean force

u_m Probability of finding a A group as part of m-mer in AB_{f-1} polymerization

$u_{m|N-m}$ Probability that a group divides a hyperbranched polymer into m and $N-m$ parts.

$\mathbf{X}_p$	p^{th} Rouse mode
z	Coordination number of Cayley tree lattice
subscript l	Denotes linear polymer chain
subscript r	Denotes ring polymer chain

Chapter 1

Introduction

1.1 Motivation

It is known that many characteristics of crystalline, glassy and fluid states of polymers rely on the special properties generated by the ends of molecules (McLeish, 2003). For instance crystalline polymers almost inevitably have defects due to presence of chain ends and the defects result in local (dislocations, grain boundaries) and global (bending, twisting) distortions of the molecular symmetry with pronounced implications on mechanical and optoelectronic properties (Kübel *et al.*, 2000). The glass transition temperature of polymeric systems is known to be dependent on the number of chain ends in the system. In a dense melt of polymers the ends are known to play an important role in the relaxation of mechanical stresses when it is subject to a strain (McLeish, 2003).

- A natural question of fundamental interest is: **What would be the dynamic response of systems composed of polymers without chain ends - '*endless*' ring chains?**

DNA often naturally occurs in the ring form (called plasmid DNA) and is characterized by the technique of gel electrophoresis (Wasserman and Cozzarelli, 1986). Although the technique has been widely used, the dynamics of plasmid DNA through a gel environment is not well understood. This is in part because of complications that arise in the study of electrophoretic mobility of a plasmid DNA molecule due to its semi-flexible and polyelectrolytic nature. It has been suggested that a flexible ring polymer in any given environment is a convenient model system to start with for understanding the mobility of molecules like DNA (Roovers and Toporowski, 1983). Recent advances in the understanding of concentrated solutions and

melt of ring polymers continue to indicate that these systems possess particular fascination as they promise to furnish yet another class of entangled fluids qualitatively different from linear and branched polymeric systems (McLeish, 2003). More importantly the dynamics of a large ring polymer in an array of fixed obstacles in itself is a poorly understood problem in polymer dynamics. Development of frameworks for studying the dynamics of flexible ring polymers in the presence of obstacles is thus of considerable importance both from a fundamental and application perspective.

The rheological response of a polymeric fluid is connected to the macromolecular architecture of the polymers constituting the fluid. For example, it is known that for a polymeric fluid composed of chains made of chemically identical monomers the linear and branched architecture compositions exhibit strikingly different flow behavior even in viscometric flows. We expect that this is a consequence of influence of the chain-architectural aspects on static and dynamic behavior at a molecular level. Further, the response of the polymeric fluid is also strongly dependent on the density of the chains in the fluid. For example, it is known that the dynamic response of a dilute solution of polymers is very different from that of a dense system like a melt or semi-dilute solution. We expect this to be the consequence of confinement effected by the presence of other chains on statics and dynamics of any given polymer chain in a dense system like that of a melt.

Based on these observations we consider topological constraints that arise in a polymeric system to be of two types *viz.*:

- Internal: Corresponding to the macromolecular architecture such as enchainment and branching.
- External: Corresponding to the confinement of the polymer effected due to presence of other chains/obstacles in its environment.

The study of rheological response on the basis of molecular theory requires formulation of frameworks that can capture the influence of both internal and external topological constraints.

Although rheological response is sensitive to the macromolecular architecture, it is seen to be quite insensitive to the shape of the segmental size or the constructing unit of the polymer. In fact the macroscopic viscosity of linear polymer chains is known to depend on the average coil size of the chain rather than on the shape of the constructing unit (Doi and Edwards, 1986). In order to capture this universality of the response of polymers a coarse-grained picture of the

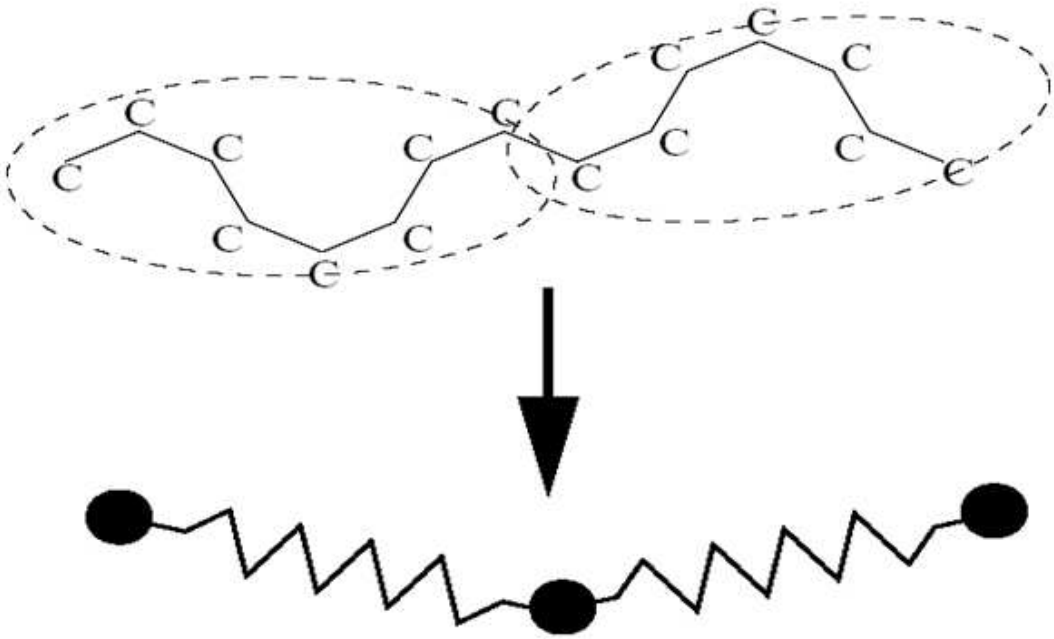

Figure 1.1: Bead-Spring coarse-graining of a polymer chain

polymer as Brownian beads connected by springs is used to understand the dynamics of polymers (Fig:1.1). The coarse graining allows for the macromolecular architecture to be retained while the microscopic details are lumped together into few parameters, like the Kuhn length or persistence length, specifying segmental characteristics.

While the intrinsic architecture can be captured in the bead-spring coarse graining the effect of external topological constraints has to be incorporated through rigorous inter-chain interactions or mean-field interactions. The tube model framework has been the most successful mean-field framework for handling external topological constraints (McLeish, 2003). According to this model the external topological constraints on the polymer can be thought of as constraints that confine the polymer in a tube which restricts mobility in the lateral direction (Fig:1.2). The section of polymer thus confined laterally is however free to move along its length through 1-D diffusion a dynamics known as reptation.

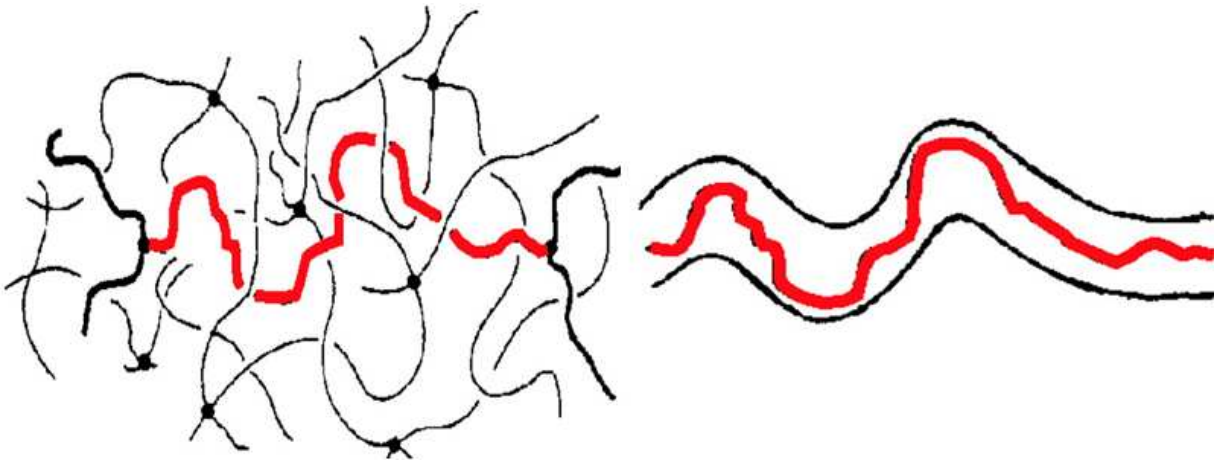

Figure 1.2: Schematic of tube model

1.2 Problem Statement

A linear polymer chain can be considered as a Gaussian chain in both a Θ-Solvent and its melt (see section 2.1). In the case of linear polymer chains, such an uncomplicated static structure, not influenced by presence of obstacles in the environment, makes it easier to fit it into the tube model framework. The application of the concept of reptation is relatively straightforward and highly successful for modeling the dynamics of topologically constrained linear polymers. The reptation dynamics studies have enabled a better understanding of the viscoelastic response of the linear polymeric systems on a coarse grained mean-field molecular theory basis (Doi and Edwards, 1986). Several sophisticated models based on the reptation idea have been developed in the recent past by incorporation of additional relaxation modes (see section 2.2). In the case of structures such as star, branch and rings understanding the Brownian dynamics and consequently the viscoelastic response on a molecular theory basis is complicated by:

- Complexity of the static structures; in the case of rings the static structure is influenced by the presence of obstacles (Khokhlov and Nechaev, 1985).
- The application of the tube model and associated dynamics for branched polymers is far from straightforward and has required an ingenious conceptualization *viz.*, the Pom-Pom polymer, first proposed by McLeish and Larson (1998), to extract the dynamics from such an architecture.

- In the case of rings the absence of free ends, which play an important role in the relaxation mechanism for linear and branched chains, leads to concerns regarding application of reptation or pom-pom dynamics for ring polymeric systems (Roovers, 1988).

The present work is aimed at developing coarse-grained mean-field frameworks for studying dynamics of ring polymers in a topologically constrained environment. The models have three main objectives:

- Obtaining expressions for dynamic properties such as diffusion coefficient and the relaxation spectrum of a non-concatenated ring polymer in the presence of external topological constraints.

- Building constitutive relations to predict the viscoelastic response of such ring polymeric systems.

- Capturing the transition effected by introducing external topological constraints on properties like size, longest relaxation time and diffusion coefficient in ring polymeric systems.

1.3 Scope

The scope of the present work is to develop rigorous frameworks to model the dynamics of flexible non-concatenated rings in an obstacle environment. Specifically, we develop three frameworks:

- Pom-Pom Ring (PPR)

- Blob-Spring (BS)

- Fractal-Gate (FG)

for modeling the dynamics of ring polymers in a topologically constrained environment. We restrict our attention to unknotted flexible ring polymers in the presence of obstacles around them. By flexible we mean that the Kuhn length, b, of the ring chain is much smaller than the linear dimension, a, of the obstacle. At the same time, the ring is constrained because its size R is much larger than a. Thus we consider the dynamics in the limit $b << a << R$. There are two types of obstacles we pay attention to:

- Fixed array of obstacles similar to that of gel.
- Melt/Semi-dilute solution where the obstacles can be dynamic and the average linear dimension of the obstacle is a fit parameter.

Having derived expressions for the dynamic properties of ring polymers from the coarse-grained mean-field frameworks, we use them to explore the effect of concentration on size, longest relaxation time and diffusion coefficient of ring polymers in semi-dilute solutions. The effect of concentration on the size of a ring polymer in a ring-linear blend is also explored by considering the linear polymer as a solvent for the ring chain.

In chapter 3 we give a reptation interpretation to dynamics of ring polymer in a fixed array of obstacles. The reptation interpretation of the dynamics is then combined with aspects of pom-pom model to formulate the PPR framework. The PPR framework thus formulated is then used to derive expressions for diffusion coefficient, relaxation time and dynamic structure factor for a ring polymer in an array of obstacles. Based on the dynamics we develop a constitutive relation to describe the linear viscoelasticity of a ring polymer in a fixed array of obstacles and extend it to the case of melt of ring polymers. Further we consider modifications arising in dynamics due to finer corrections of contour length fluctuations in the reptation interpretation. Finally, we compare the predictions of the PPR model with the scaling model of Obukhov *et al.* (1994) and experimental results of ring polybutadiene KPBD34B3 (Roovers, 1988) and discuss some of the limitations of the model.

In chapter 4 we give a fluctuation interpretation to dynamics of ring polymer in a fixed array of obstacles. The fluctuation interpretation of the dynamics is then combined with aspects of dynamics of polymeric fractals to formulate the BS model. We also present arguments which can be used to view the dynamics of polymeric fractals in terms of predominant length scale dynamics of the Cayley tree ring chain. The BS model is then used to derive expressions for diffusion coefficient and relaxation time for a ring polymer in an array of obstacles. Based on the dynamics we develop a constitutive relation to describe the linear viscoelasticity of ring polymer in a fixed array of obstacles and extend it to the case of melt of ring polymers. Finally, we compare the predictions of the BS model with the experimental results of ring polybutadiene KPBD34B3 (Roovers, 1988) and discuss some of the limtitations of the model.

In chapter 5 we suggest a combination of fluctuation and mean-field approach of handling entanglements to dynamics of ring polymer in a fixed array of obstacles. The framework is bulit

in three steps. First, the fluctuation dynamics of an arbitrary section of the polymeric fractal is worked out with a friction coefficient different from that used in the BS model. In the second step we work out the dynamics of the center of mass of such a fluctuating section diffusing out of a tube of confinement. In the third step the principle of self-similar dynamics is used to generalize the results for all the length scales in the chain and the viscoelastic response is obtained as the the superposition of the response of the sections of the chain. In working out the superposition the number density of tubes in the system is used as a weighting function and is worked out based on the density of Gates associated with the Cayley tree fractal structure.

In chapter 6 we present scaling arguments for elucidating the effect of concentration on statics and dynamics of ring polymers in semidilute solution strating from both Θ and good solvent conditions, First we discuss the effect of concentration on the size of a ring polymer followed by its effects on longest relaxation time in the semi-dilute solution. We combine the results of size and relaxation time dependence on concentration to yield the effect of concentration on diffusion coefficient. We also discuss the effect of volume fraction/concentration of ring polymers in a ring-linear blend on the size of the ring polymer in the blend. Finally, we compare the results of the scaling predictions with simulation results and experiments on diffusion of cyclic DNA in a semidilute solution using the three different models we have presented in the earlier chapters.

Chapter 2

Review of Literature

2.1 Statics

Highly flexible polymers when looked at a sufficiently large scale appear as a random walks (Doi and Edwards, 1986). A flexible linear polymer chain in a Θ-solvent viewed at a large length scale can be considered as an ideal random walk in 3-D with each step of the walk (bond of the chain) having a Gaussian distribution. The problem of getting the end-to-end vector probability distribution for this polymer chain is analogous to the problem of finding the probability distribution of the position of a particle in a general random flight with Gaussian distribution of displacements. Chandrasekhar (1943) in his classic paper titled 'Stochastic Problems in Physics and Astronomy' has worked out the probability distribution of the position in a general random flight with Gaussian distribution of displacements. Based on this analogy an *exact* solution to end-to-end vector distribution can be obtained for any value of number of steps N associated with the polymer chain. The chain model obeying the statistics as worked out based on the analogy is known as the Gaussian chain model. The Gaussian chain is thus a coarse-grained picture of the real chain. Each step of the Gaussian chain is a statistical segment known as the Kuhn segment.

In a good solvent due to favorable solvent monomer interactions the chain is expected to swell. The chain in this case can be represented by a different kind of random walk that is not allowed to intersect. Such a random walk is known as self-avoiding walk (SAW) and is known to have complex mathematical properties that can be investigated using different numerical and analytical approaches (de Gennes, 1979; Doi and Edwards, 1986). In a dense system like that of the melt the situation is expected to be complicated due to increased density and consequently

stronger interactions between monomers. However, it was shown through self-consistent field arguments that the linear polymer chain in 3-D in a dense system obeys the ideal random walk statistics (de Gennes, 1979). Thus, the statistics of a linear polymer chain in its melt can be understood based on the Gaussian chain model.

In section 1.1 we briefly discussed the two kinds of topological constraints, *viz.* internal and external, in polymeric systems. Either type of constraints can modify the physical properties of statistical systems consisting of chain-like objects (Nechaev, 1998). Our concern in this section is to understand the effect of the introduction of internal topological constraint of chain closure (as in a ring) and external topological constraints like obstacles on the statistics of this ring chain. Efforts to understand the statics of topologically constrained ring chain have been made based on analytical theory, computer simulation and experimental studies. We discuss the key efforts to understand the effect of the internal topological constraint of chain closure and the effect of external topological constraints on the ring chain in sections 2.1.1 and 2.1.2 respectively.

2.1.1 Effect of Internal Topological Constraint

The statistics of a ring chain in a Θ-solvent was worked out by Zimm and Stockmayer (1949). They showed that the radius of gyration of the ring chain consisting of N_K Kuhn segments is given by $N_K b^2/12$ - a value exactly half that of the linear chain in a Θ-solvent. Although the chain dimensions are smaller, the scaling exponent, ν, connecting the size of the ring chain, R, to the degree of polymerization remains the same as that of linear chains. Higgins *et al.* (1979) reported small-angle neutron scattering (SANS) experiments in support of the general theoretical approach of Zimm and Stockmayer (1949) to the problem of conformational statistics of flexible ring chains. However, the poly(dimethyl siloxane) ring polymers used in these experiments were of relatively low molecular weight. Recently the reduction in chain size and the similarity in scaling exponents have been verified through SANS and light scattering experiments for telechelic polystyrene ring polymer in the molecular weight range of $20K - 600K$ (Ohta *et al.*, 2006). However, they report a slightly higher ratio of radius of gyration of ring to linear polymer ≈ 0.8 as opposed to the ratio of half expected from the Zimm and Stockmayer (1949) approach.

The deviation from the Zimm and Stockmayer (1949) predictions may be due to the fact that they do not consider the global topological constraint of non-knotting in working out the

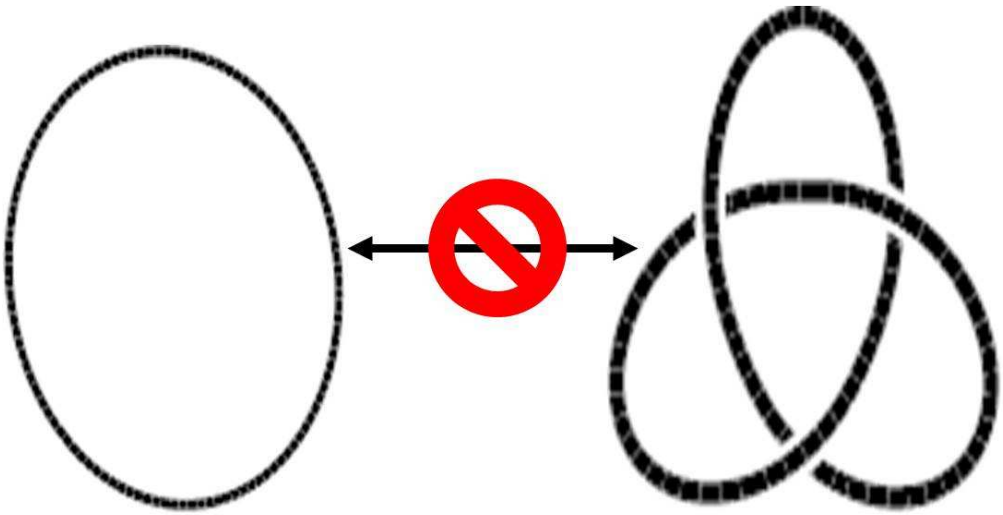

Figure 2.1: Schematic of the non-knotting topological constraint

chain statistics. Cates and Deutsch (1986) pointed out that the global configuration of a ring polymer is restricted to a single knot-type and any change of knot-type involves breaking and reforming of bonds of a polymer which is forbidden (see Figure 2.1). des Cloizeaux (1981) argued that this topological constraint acts in a way similar to that of short-range excluded volume interactions based on consideration of linking numbers of two curves. Deutsch (1999) explored the statics of isolated ring polymers using off-lattice simulations with purely topological interactions and without excluded volume. The off-lattice simulations showed that for rings with $N = 512$ repeat units the scaling exponent of size with number of repeat units for a ring without excluded volume is about ≈ 0.55 whereas the scaling exponent was ≈ 0.59 for $N = 1024$ and $N = 2028$. The result has been verified by simulations of Brown *et al.* (2001) based on Shaffer's algorithm. The scaling exponent close to that of linear SAW for large ring polymers even in the absence of excluded volume interaction is an outcome of purely topological interactions. In a good solvent the ring chain is expected to swell due to the onset of excluded volume interactions in addition to the topological interactions. In this case des Cloizeaux (1981) argues that a long flexible ring chain in a good solvent has size scaling $R \sim N^{\nu}$ with the exponent $\nu \geq \nu_{SAW}$.

2.1.2 Effect of External Topological Constraint

An ideal flexible ring polymer, of size R_{dil} in dilute solution, composed of Kuhn segments of length b, when introduced into an array of fixed obstacles, of linear dimension a, takes a collapsed conformation when $b << a << R_{dil}$ (Khokhlov and Nechaev, 1985). The lattice equivalent to the ideal flexible ring polymer in the obstacle environment is a random walk in a cubic lattice in the presence of obstacles (Khokhlov and Nechaev, 1985; Nechaev, 1998). Such a random walk is equivalent to a closed random walk on a dual lattice without obstacles which has the form of a simple tree known as the Cayley tree (see Figure 2.2) (Khokhlov and Nechaev, 1985; Nechaev, 1998). The structure arising out of the closed random walk on a Cayley tree is known as a lattice animal/tree structure and resembles that of a randomly branched polymer (see Figure 2.3).

Each node of the Cayley tree is attributed a coordinate i, which is the smallest number of steps required to return from a given node to the origin (Figure 2.2). A closed random walk has to have equal distances moved from and to the origin. Thus, for a N step closed random walk on a Cayley tree the "average" coordinate i is of the order of $N^{1/2}$ steps from the origin (Khokhlov and Nechaev, 1985). The spatial size of the ideal ring in the array of fixed obstacles corresponds to a random walk of i steps on the Cayley tree and hence is of order $\sim ai^{1/2} \sim aN^{1/4}$. Nechaev (1998) used the above model of a polymer chain in an array of obstacles to work out the detailed statics of a ring chain in an array of fixed obstacles. The mean-square radius of gyration of a ring polymer in an array of fixed obstacles without excluded volume interactions (ideal) is given by (Nechaev, 1998):

$$\left\langle R_g^2 \right\rangle = \frac{z}{z-2}\frac{\sqrt{2\pi}}{8}a^2\sqrt{N} \tag{2.1}$$

where, z is the coordination number of the Cayley tree lattice and a is the step size of the lattice.

It is seen that the ring chain in an array of fixed obstacles without excluded volume interactions has a size scaling similar to that of an ideal randomly branched polymer (Khokhlov and Nechaev, 1985; Nechaev, 1998). This correspondence in size scaling is expected since the Cayley tree lattice animal structure and the randomly branched polymers are known to belong to the same universality class. The exact correspondence of universality class between the Cayley tree lattice animal and the branched polymer was shown through field theory arguments by Lubensky and Isaacson (1979). They derived the critical exponent of Cayley tree lattice animal above an upper critical dimension $d_c = 8$ and showed that it is in agreement with the the Zimm

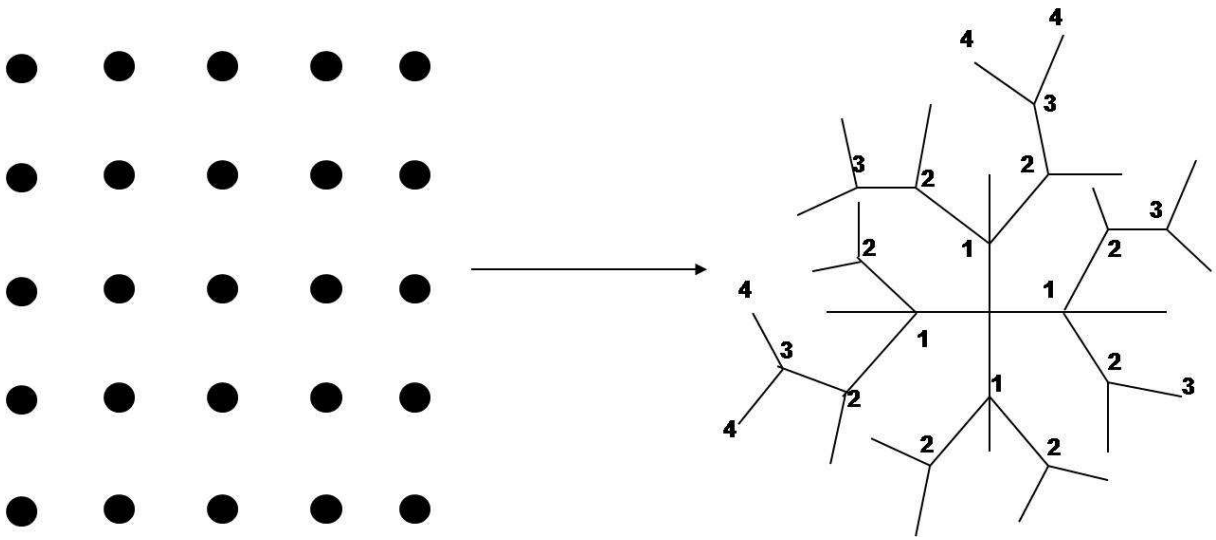

Figure 2.2: Cayley tree mapping of an array of fixed obstacles

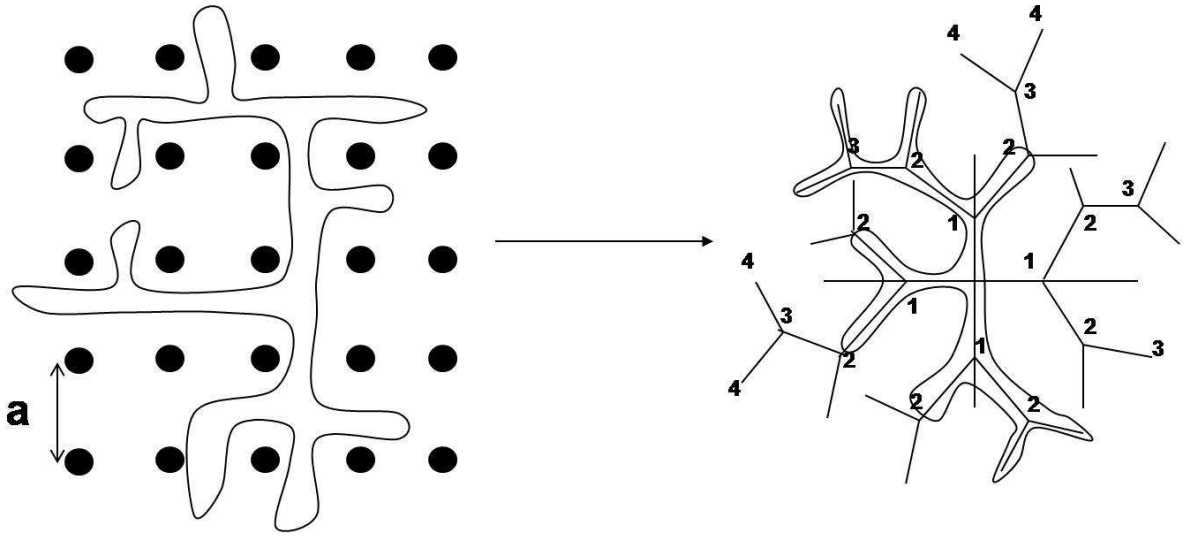

Figure 2.3: Lattice tree structure of a ring polymer in an array of fixed obstacles

and Stockmayer (1949) result of $\nu = 1/4$ for randomly branched polymers.

In the case of large rings in the fixed array of obstacles excluded volume interactions remain active as the network cannot adjust its density to screen out the interactions (Cates and Deutsch, 1986). Parisi and Sourlas (1981) showed that in a good solvent a branched polymer of the same universality class as the lattice animal in $3 - D$ would have a size exponent $\nu = 1/2$. The branched polymers in this case are intrinsically considered to have annealed branch points, *i.e.*, the position of the branch points are allowed to fluctuate (Gutin *et al.*, 1993). The Cayley tree lattice animal structure of a ring chain in a fixed array of obstacles clearly belongs to the annealed branched polymer universality class. Gutin *et al.* (1993) considered branched polymers with quenched (the position of branch point is fixed) and annealed branch points and showed that they belong to different university classes.

A Flory-type estimate of the size scaling of branched polymers with quenched branch points can be achieved based on the balance between the the excluded volume contribution and the elastic contribution to the free energy (Gutin *et al.*, 1993; Daoud *et al.*, 1983). The excluded volume contribution is considered to depend on the repulsive interaction between monomers and consequently increases the size R. If c is the local concentration of monomers, the repulsive energy per unit volume is proportional to the pairs present, *i.e.* c^2 (de Gennes, 1979). In a d dimensional system the internal monomer concentration is given by $c_{int} \approx N/R^d$. The repulsive energy per chain is obtained by integration of the repulsive energy per unit volume over the volume of the chain R^d and is given by (de Gennes, 1979):

$$F_{rep} \approx T\upsilon(T)c_{int}^2 R^d = T\upsilon(T)\frac{N^2}{R^d} \tag{2.2}$$

where υ is a positive quantity having the dimensions of volume known as the excluded volume parameter. The elastic contribution to free energy comes from the entropic consideration that swelling reduces entropy and consequently increases free energy. Thus, the elastic contribution tries to keep the chain in a conformation close to the ideal chain conformation for the chain and resists deviations from the ideal size R_0. The elastic contribution to the free energy is taken analogous to the Flory-type derivation for linear polymers and is given by:

$$F_{el} \approx T\frac{R^2}{R_0^2} \tag{2.3}$$

where R is the size of the chain and R_0 is the unperturbed size of the chain.

The total free energy of the system can be written as the sum of the excluded volume and

the elastic contributions (Gutin *et al.*, 1993; Daoud *et al.*, 1983):

$$F \approx T\upsilon(T)\frac{N^2}{R^d} + T\frac{R^2}{R_0^2} \tag{2.4}$$

The minimization of the free energy between the opposing elastic and excluded volume interactions with respect to the size yields a size scaling of $R \sim N^{\nu}$ where $\nu = 5/[2(d+2)]$ in agreement with that obtained by Isaacon and Lubensky (1980). The exponent ν becomes equal to the classical theory result of Zimm and Stockmayer (1949) at the upper critical dimension of $d_c = 8$. The exponent $\nu = 1/2$ for $d = 3$ a result in agreement with the exact solution of Parisi and Sourlas (1981) and MC simulations of Redner (1979).

A Flory-type estimate of the size scaling for the case of branched polymers with annealed branch points is different from that of the case of quenched branch points. The stretching of the chain in the annealed branch point branched polymer causes rearrangement of branches and changes the characteristic number of bonds between the ends of the branched chain. The free energy contribution due to the change of number of bonds L between two arbitrary fixed ends of the branched polymer has two parts (Gutin *et al.*, 1993):

- Elastic part which resists swelling and increase in R for any given L as it decreases entropy given by TR^2/L
- Rearrangement entropy associated with the rearrangement of branches and consequently the change of L given by TL^2/N

The combination of the free energy contributions due to change in number of bonds with that of the excluded volume free energy contribution yields the free energy of the annealed branched polymer:

$$F_{ann} \approx T\upsilon(T)\frac{N^2}{R^d} + T\frac{R^2}{L} + T\frac{L^2}{N} \tag{2.5}$$

The free energy thus obtained has to be minimized with respect to both L and R. The minimization yields the scaling of L and R with the degree of polymerization N given by $L \sim N^{\rho}$ and $R \sim N^{\nu_{ann}}$ with:

$$\rho = \frac{d+6}{3d+4} \tag{2.6}$$

$$\nu_{ann} = \frac{7}{3d+4} \tag{2.7}$$

It can be seen that at the critical dimension $d_c = 8$ the exponent $\nu_{ann} = 1/4$ remains unperturbed and $\rho = 1/2$. The $\nu_{ann} = 1/4$ is in agreement with the Nechaev statistics for ideal rings in an

array of fixed obstacles discussed earlier. Further the $\rho = 1/2$ suggests the existence of a structure in the ideal Cayley tree ring with its contour length composed of the order of $N^{1/2}$ segments.

The array of fixed obstacles environment discussed so far is akin to a gel where the cross-links in the network act as obstacles confining a chain. In a dense system like melt the ring polymer chain is expected to be confined as a consequence of the density of the system although the obstacles are no longer fixed as in the case of cross-links in a gel. Klein hypothesized three different possible static configurations of a larger flexible ring in a dense system like that of the melt (see Figure 2.4). The first subdivision in Klein hypothesis corresponds to the states of enclosing of obstacles *viz* threaded and non-threaded states. If the ring chain encloses parts of other chains then it is considered to be threaded by other chains as in Figure 2.4(a). If the ring does not enclose parts of other chains it is considered to be non-threaded as in Figure 2.4(b) and (c). The non-threaded state can be further subdivided into ramified and non-ramified states. The ramified state corresponds to the ring being spread out with its structure similar to that of star polymer as in Figure 2.4(b). The non-ramified structure corresponds to that of a double-folded sausage like structure of a ring chain 2.4(c).

It is seen that Klein hypothesis on statics does not explicitly account for the additional topological constraint that arises in the system of melt of rings. This additional topological constraint in the melt of rings is non-concatenation, *i.e.*, the concatenation of any two rings neighbors is prohibited as it involves breaking and reforming of bonds (see Figure 2.5)(Cates and Deutsch, 1986). Cates and Deutsch (1986) conjectured that the rings in a melt of rings possibly do not obey Gaussian statistics due to the non-concatenation constraint.

A Flory-type estimate of the size of a ring chain in its melt was presented by Cates and Deutsch (1986) based on the argument that the topological constraint of non-concatenation tries to squeeze the ring chains which is opposed by the elastic contribution which resists deviations from the ideal size. The quantification of free energy loss due to non-concatenation constraints was done based on the argument that the presence of a ring neighbor to a ring chain causes loss of a degree of freedom (Cates and Deutsch, 1986). If the ring in a melt is of size R then the number of neighbors in the ring in d dimensions would scale as R^d/N. Thus, the free energy penalty that squeezes the rings due to the presence of these neighbors is given by TR^d/N. The elastic contribution to free energy which opposes the squeezing is given by TN/R^2. The

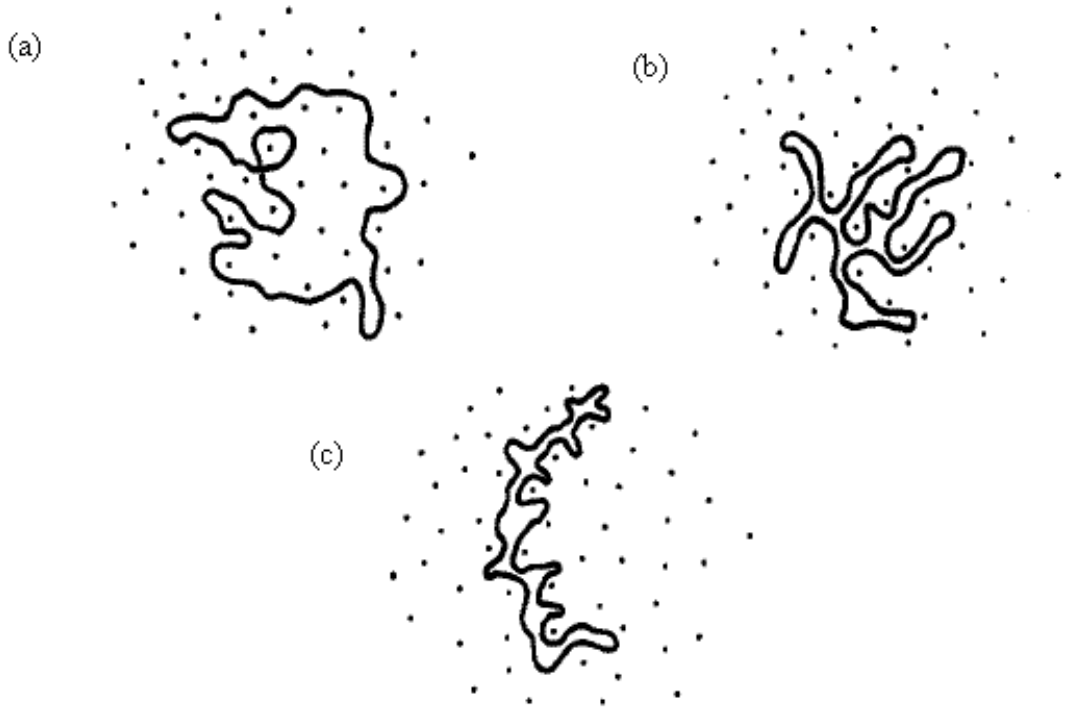

Figure 2.4: Klein hypothesis on the structure of a ring in a melt (Klein, 1986) (a) enclosing obstacles (threaded ring) (b) non-obstacle-enclosing ramified structure with large loops (c) non-obstacle-enclosing non-ramified structure

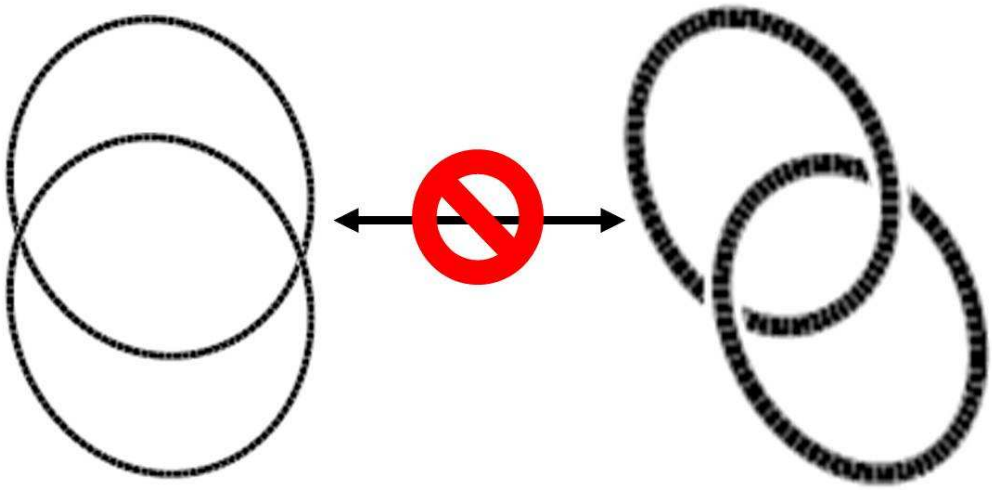

Figure 2.5: Schematic of the non-concatenation topological constraint

combination of the free energies yields:

$$F \approx T\frac{R^d}{N} + T\frac{N}{R^2} \tag{2.8}$$

The minimization of the free energy with respect to size R yields $R \sim N^{2/(d+2)}$ (Cates and Deutsch, 1986). For $d = 3$ this yields $R \sim N^{2/5}$ a scaling which lies between that of an ideal ring in an array of fixed obstacles and an ideal Gaussian chain.

Müller *et al.* (1996) investigated the influence of strong interaction between neighboring ring chains through computer simulations using the bond fluctuation algorithm (Carmesin and Kremer, 1988) for chains up to $N = 512$ statistical segments at a volume fraction of $\phi = 0.5$ and showed that ring chains in the melt are more compact than Gaussian chains. They did a systematic finite-size analysis of the average ring size $R \sim N^{\nu}$ and showed that it yields an exponent $\nu \approx 0.39 \pm 0.03$ in agreement with the Flory-type free energy arguments of Cates and Deutsch (1986). Further, the normalized static structure factor from the simulations, $S(q)/N$, expressed as a function of the characteristic variable $R_g q$ showed an apparent self-similar power-law regime with a fractal dimension of $1/\nu = 1/0.4$. The Gaussian fractal dimension of 2 was ruled out by their structure factor data.

Brown *et al.* (2001) carried out a computer simulation study of the influence of topological constraints on statics and dynamics of both isolated ring polymers and ring polymers in melt. The study was based on a modified bond fluctuation model proposed by Shaffer (1994, 1995) specially designed to simply switch the topological interactions "on" and "off" and ascertain their effects globally. Based on the study they concluded that for isolated ring polymers the absence of topological constraints leads to Gaussian scaling of the ring polymer size $R_g^2 \sim N$ whereas they are present in much more compact conformations in the melt of rings with $R_g^2 \sim N^{0.83}$ a scaling in agreement with that of Müller *et al.* (1996) simulations.

Müller *et al.* (2000) also investigated the influence of persistence length on the structure of ring polymers in their own melt by means of dynamical MC simulations. These simulation were aimed at identifying the regime in which the ring chains behave like lattice animals in a self-consistent network of topological constraints imposed by neighboring rings. They showed that the increase of the persistence length is an effective route to obtain lattice animal structure. Further they plotted the density distribution of the ring around its center of mass and observed that when the Cates and Deutsch (1986) conjecture is obeyed the density near the center decreased with $\sim N^{-0.2}$. When the persistence length was tuned to obtain more compact lattice animal structures the density near the center was seen to become independent of N for a smaller

value of N. They also observed that the asymptotic value of the density near the center reached for stiffer rings was small. Based on these observations they argued that the density of other rings in the correlation hole of a given ring is larger for stiffer rings and there is a possibility of similar strong overlap for large flexible rings. We understand based on these ideas that a very long flexible ring can indeed take a compact lattice animal conformation in its own melt an understanding we implicitly use in our models.

2.2 Dynamics

The connection between the chain structure of a polymer chain and a dynamic property like viscosity of a polymer solution was first discussed by Hermans (1943). He proposed that the continuous change of shape of polymers in a solution may be described by a diffusion process. To this end he considered the distribution of the distance between ends of a polymer chain to be maintained by a force. The force was used to study the diffusion of an end with respect to the other end when the distribution is affected by a streaming flow. He arrived at a new distribution for the distance between chain ends and used it to determine the viscosity and the birefringence corresponding to the flow. The developments in dynamics of dilute solution of polymers has this fundamental idea as the starting point although they vary in the approach to modeling the diffusion process.

We have already mentioned in section 1.1 about the coarse-graining of a polymer chain into a set of beads connected by springs. Such a chain is known as a *Rouse chain* or a *Rouse-Zimm chain*, the names being associated with the authors of two landmark papers in polymer kinetic theory (Rouse, 1953; Zimm, 1956). It is natural to model the motion of the polymer chain by Brownian motion of the beads of the chain as was first proposed by Rouse (1953). Consequently the equation of the motion of the chain can be described either by the Smoluchowski equation:

$$\frac{\partial \Psi}{\partial t} = \sum_n \frac{\partial}{\partial \mathbf{R}_n} \cdot \mathbf{H}_{nm} \cdot \left[k_B T \frac{\partial \Psi}{\partial \mathbf{R}_m} + \frac{\partial U}{\partial \mathbf{R}_m} \Psi \right] \tag{2.9}$$

or the Langevin equation:

$$\frac{\partial}{\partial t} \mathbf{R}_n(t) = \sum_m \mathbf{H}_{nm} \cdot \left(-\frac{\partial U}{\partial \mathbf{R}_m} + \mathbf{f}_m(t) \right) + \frac{1}{2} k_B T \sum_m \frac{\partial}{\partial \mathbf{R}_m} \cdot \mathbf{H}_{nm} \tag{2.10}$$

for the motion of a collection of interacting Brownian particles subject to a potential field U and hydrodynamic interaction governed by the mobility tensor $\mathbf{H}_{nm}$ (Doi and Edwards, 1986). The

Smoluchowski equation describes the time evolution of the conformational distribution of the Brownian particles, Ψ, while the Langevin equation describes the time evolution of position, $\mathbf{R}_n$, of the Brownian particle.

In the Rouse model, the hydrodynamic interaction and the excluded volume interaction are disregarded and the mobility tensor and the interaction potential are written as (Doi and Edwards, 1986):

$$\mathbf{H}_{nm} = \frac{\mathbf{I}}{\zeta}\delta_{nm} \tag{2.11}$$

$$U = \frac{3k_BT}{2b^2}\sum_{n=2}^{N}(\mathbf{R}_n - \mathbf{R}_{n-1})^2 \tag{2.12}$$

Based on the harmonic potential field expression (2.12) and the delta correlated hydrodynamic interaction expression (2.11) the continuous form of Langevin equation can be written as (Doi and Edwards, 1986):

$$\zeta\frac{\partial\mathbf{R}_n}{\partial t} = k\frac{\partial^2}{\partial n^2}\mathbf{R}_n + \mathbf{f}_n \tag{2.13}$$

where $k = 3k_BT/b^2$. In our model approaches we have used this Langevin description of dynamics of a polymer chain with implicit Rouse assumptions.

The extension of the results from the dynamics of the dilute solution to the melt is expected to be difficult due to the many chain effects in the melt. For the case of melt of low molecular weight linear chains the Rouse model discussed earlier gave a fair prediction of the dynamic properties owing to the fact that the hydrodynamic interactions are screened in a dense system like that of the melt. However, it was observed that beyond a critical molecular weight of the chain, $M \geq M_c$, the dynamics of the linear chains changed drastically to give a (ZSV) as $\sim M^{3.4}$ (Ferry, 1980) as opposed to the $\sim M$ scaling expected from the Rouse dynamics. The understanding of this dynamic response of melt of linear chains was arrived at on the basis of the fundamental ideas of de Gennes (1971) and Doi and Edwards (1978a,b,c, 1979). We review these ideas briefly here as they are of key value in understanding the effect of external topological constraints on dynamics of polymeric systems.

de Gennes considered the motion of a single polymer molecule performing wormlike displacements inside a strongly cross-linked polymer gel. In a classical scaling argument de Gennes considered that the polymer chain consisting of gas of non-interacting 'kinks' or length-defects along its contour. He argued that as these kinks diffuse along the contour of the chain they cause the 1-D diffusion of the chain along its contour. This type of motion was called

'reptation' by de Gennes after the latin *reptare*, to creep (Doi and Edwards, 1986). Based on the idea he showed that there are two characteristic time scales that are associated with such dynamics:

- The equilibration time for the defect concentration $\sim M^2$.
- The time required for the complete renewal of the chain conformation $\sim M^3$

Further he conjectured that the idea of reptation in fixed obstacles can be extended to the case of melts.

Doi and Edwards combined the mathematical formulation of entanglement effect on the entropy of very long flexible molecules developed by Edwards (1967a,b) with the de Gennes (1971) idea of reptation to study the dynamics of long flexible linear molecules in concentrated systems like the melt. The formulation involves two significant simplifications:

- The many-body problem of the topological constraints arising due to chain interactions is simplified into a tube mean-field.
- The dynamics of the chain can be visualized as a simple 1-D diffusion of a polymer chain in a tube mean-field.

Based on the combination of these ideas they arrived at a constitutive relation which showed that the ZSV in such a system scales as the time required for the renewal of the chain conformation and thus scales as $\sim M^3$ a value close to that observed in experiments.

We have already mentioned the success of this simplification in understanding dynamics of entangled polymeric systems and its specific application to linear chain systems in section 1.2. However, the immediately noticeable shortcoming of the first order reptation theory is that it predicts that the ZSV scales as M^3 while numerous experiments give ZSV $\sim M^{3.4}$ (Ferry, 1980). It was suggested that with the complete suppression of the transverse motion the reptation dynamics may provide only an upper bound to the the viscosity and certain transverse motions through the tube mesh may be important for chains of intermediate molecular weights (Graessley, 1980). The transverse motions are expected to be faster processes that reduce the viscosity relative to the asymptotic limit. However, the fast process become less important for high molecular weight chains so the viscosity in the intermediate molecular weights increases faster than the asymptotic M^3 limit to meet it from below (Milner and McLeish, 1998). It

was suggested that the $M^{3.4}$ scaling of viscosity observed reflects this approach to the asymptotic limit of the reptation process in the intermediate molecular weights (Graessley, 1980). Doi (1983) identified the fast process as contour length fluctuations, *i.e.*, the fluctuation-driven stretching and contraction of the chain and showed that its incorporation gives the $M^{3.4}$ scaling for the viscosity in the intermediate molecular weight regime of $10M_c \leq M \leq 100M_c$.

In arriving at the results discussed so far it is seen that the nature of the tube is not explicitly considered. Klein (1978) noted that the strands of the tube mesh of the tube model are parts of other chains which diffuse similarly and hence the lifetime of each entanglement forming the tube is in itself comparable with the disengagement time for the entire chain. This is strictly true only in the case of monodisperse systems. In a polydisperse system this is clearly not the case since the disengagement time of shorter chains is lower than the long chains and consequently these chains can release the constraints on the longer chain before the longer chains disengage from the tube of confinement through reptation. The release of constraints by the shorter chains allows parts of the longer chain to relax through transverse motions. Marrucci (1985) considered such release of constraints to cause an increase in the diameter of the confining tube a relaxation mechanism termed as tube dilation and worked out the corrections based on this idea. This model served as an inspiration to develop more rigorous ideas of 'double reptation' independently developed by Tsenoglou (1991) and des Cloizeaux (1990a,b). In fact the des Cloizeaux (1990a) double reptation model has been shown to describe quantitatively the linear viscoelastic response of melts containing two molecular weights of the same homopolymer. Although advance models (Likhtman and McLeish, 2002; Rubinstein and Colby, 1988) with superior accounting of the effects of constraint release have been developed the des Cloizeaux double reptation idea has been found to be easier to implement (Pathak *et al.*, 2004).

2.2.1 Effect of Internal Topological Constraint

Kramer (1944) generalized Hermans (1943) formulation of the dynamics of a linear macromolecule to the case of macromolecules of architectures like branched and ring polymers. The dynamics of ring polymers in dilute solution with hydrodynamic interactions was first explored by Bloomfield and Zimm (1966). They considered the ring chain as a Gaussian coil and did perturbation calculations for dynamics of the ring chain. Fukatsu and Kurata (1966) worked out the dynamics of ring macromolecules in solution through a different approach and arrived at similar results as Bloomfield and Zimm (1966). They predicted that the ratio of intrinsic

viscosities of ring chain solution to that of the linear chain solution is 0.5 in the free-draining limit and 0.645 in the non free-draining case.

Ring molecules were less familiar at the time of work of Zimm and Stockmayer (1949) and interest in their dynamics was suppressed till the time when the interest was rekindled by the experimental work of Roovers and Toporowski (1983); Roovers (1985a). Weist *et al.* (1987) rederived and extended some of the results of the previous investigators without the restriction of the asymptotic limit of $N = \infty$ where N is the number of beads in the bead-spring model of the ring polymer chain. Further they obtained the complete constitutive equation, the relaxation spectrum, and viscometric properties for a dilute solution of Hookean-spring rings without hydrodynamic interactions. The results of Weist *et al.* (1987) was extended to the case of Hookean-spring rings with hydrodynamic interactions by Liu and Öttinger (1987). Both these works pointed out to dynamics of a ring chain similar to that of the Rouse/Zimm linear chain with only the alteration of the relaxation spectrum of the ring chain effected by the chain closure constraint.

2.2.2 Effect of External Topological Constraint

We have already discussed reptation in a tube model, its success and the improvements achieved by incorporation of additional relaxation modes for systems composed of linear chains in section 2.2. We also discussed the difficulties associated with applying the tube model and reptation dynamics to the case of systems composed of branches and ring chains in section 1.2. However, the kink-defect diffusion mechanism employed in the development of the idea of reptation of a confined linear polymer has been found to be useful in developing scaling models for a confined ring chain (Cates and Deutsch, 1986; Rubinstein, 1986; Obukhov *et al.*, 1994). Thus, it is illustrative to look at the kink-defect diffusion mechanism as first applied to the motion of a confined linear chain and consider its extension to the case of the confined ring chain.

Consider a linear chain made up of N segments containing kink-defects of stored length a. Consider that initially there exists a gradient of density of defects in the chain and as the defects diffuse from the center of the chain towards the ends the chain attains an equilibrium density of defects. The entire chain has this equilibrium density of defects after a certain time *viz.* the equilibration time. The defects have to move a distance of order of the contour of the chain $\sim N$ and consequently a mean-square distance of $\sim N^2$ to diffuse out of the ends. The local diffusion jump is independent of the length of the chain and can be considered as a

constant, D_{loc}. Thus, the equilibration time of the defects is given by the mean-square distance over which the defects have to move to diffuse out of the ends divided by the diffusion constant associated with the local diffusion process, *i.e.*, $\tau_R \sim N^2$. This equilibration time corresponds to the Rouse relaxation time of the chain.

The number of defects in such a chain is expected to be proportional to the contour length of the chain $L \sim N$. When a single defect moves by a distance a it causes a segment along the contour length to have a mean-square displacement a^2. Such a motion of a segment in the chain causes the center of mass of the entire chain to have a mean-square displacement of $(a/N)^2$. In the chain there are N such non-interacting defects and consequently the mean-square motion of the center of mass due to the simultaneous motion of all the defects is given by:

$$\Delta s_{c.o.m} \sim N \left(\frac{a}{N}\right)^2 \sim \frac{a^2}{N} \tag{2.14}$$

This entire motion happens in the time scale of relaxation τ_0 of the stored length a. The curvilinear diffusion coefficient of the chain is thus given by:

$$D_c \sim \frac{\Delta s_{c.o.m}}{\tau_0} \sim N^{-1} \tag{2.15}$$

The longest relaxation time of the chain is the time taken for the chain to completely diffuse out of its original tube of confinement along the chains contour L and is thus given by:

$$\tau_{rep} \sim \frac{L^2}{D_c} \sim N^3 \tag{2.16}$$

Thus we obtain the N^3 scaling of the longest relaxation time. The self-diffusion coefficient of the chain can then be worked out based on the idea that in the time scale τ_{rep} the linear chain moves through a spatial distance of the order of its radius of gyration and hence:

$$D \sim \frac{R_g^2}{\tau_{rep}} \sim N^{-2} \tag{2.17}$$

We have already seen in section 2.1.2 that a ring chain in the presence of an array of fixed obstacles takes a collapsed Cayley tree structure. Cates and Deutsch (1986) considered the diffusion of kink-defects in such a Cayley tree ring chain and worked out the self-diffusion coefficient of an excluded volume ring with $R \sim N^{1/2}$ scaling as $D \sim N^{-2}$. They argued that in the equilibration time scale $\sim N^2$ although a single kink-defect moves along the entire contour of the chain it moves a spatial distance of only the size of the Cayley tree chain R. Thus the mean-square displacement of the center of mass of the chain in the time scale of equilibration

τ_R is given by R^2/N^2. Considering that the equilibration time of defects in rings is the same as that of linear chains they arrived at at a scaling of the center of mass diffusion coefficient due to single kink-defect as:

$$D_0 \sim \frac{R^2}{N^2 \tau_R} \sim \frac{R^2}{N^4} \tag{2.18}$$

They argued that the number of kink-defects is proportional to the perimeter of the chain N and all these kink-defects diffuse over the time scale of equilibration τ_R and consequently the center of mass diffusion coefficient due to the diffusion of all the kink-defects is given by:

$$D \sim N D_0 \sim \frac{R^2}{N^3} \sim N^{2\nu(d)-3} \tag{2.19}$$

where, $\nu(d)$ is the size exponent of the Cayley tree ring in d dimension. This yields for an excluded volume Cayley tree chain in $d = 3$ with $R \sim N^{1/2}$ a diffusion coefficient scaling as $D \sim N^{-2}$ a scaling identical to that of the ideal linear chain in expression (2.17). This yields for an ideal Cayley tree chain with $R \sim N^{1/4}$ a diffusion coefficient scaling as $D \sim N^{-5/2}$ a result independently arrived at by Nechaev *et al.* (1987) and Rubinstein (1986).

The Cates and Deutsch (1986) scaling result for diffusion coefficient, expression (2.19), can be arrived at by an alternate argument as envisaged by Rubinstein (1986). He considered that the motion of all the kink-defects along the perimeter of the chain contribute to the center of mass motion in a way similar to that of the motion of kink-defects along contour of the linear chain (Rubinstein, 1986). This yields the longest relaxation time of the ring chain to be the same as that of the linear chain, *i.e* $\tau_r \sim N^3$, as the only difference between the linear and the ring chain is in the geometry of the contour which does not affect the kink-defects diffusion contribution to the center of mass motion. In this time scale τ the center of mass undergoes a mean-square displacement of the order of its size and hence the self-diffusion coefficient is given by:

$$D \sim \frac{R^2}{\tau} \sim N^{2\nu(d)-3} \tag{2.20}$$

An insightful refinement of the contribution of the diffusing kink-defects to the center of mass motion in a Cayley tree ring chain was proposed by Obukhov *et al.* (1994). They pointed out that the kink-defect diffusion mechanism in the earlier works (Cates and Deutsch, 1986; Rubinstein, 1986) fails to account for the evolution of the shape of the perimeter as the kink-defects move around it. Further they argued that such a variability of shape of the perimeter can serve to alter the density of kink-defects in the system and consequently alter the mechanism of kink-defect diffusion and its contribution to the center of mass motion of the chain. In order to

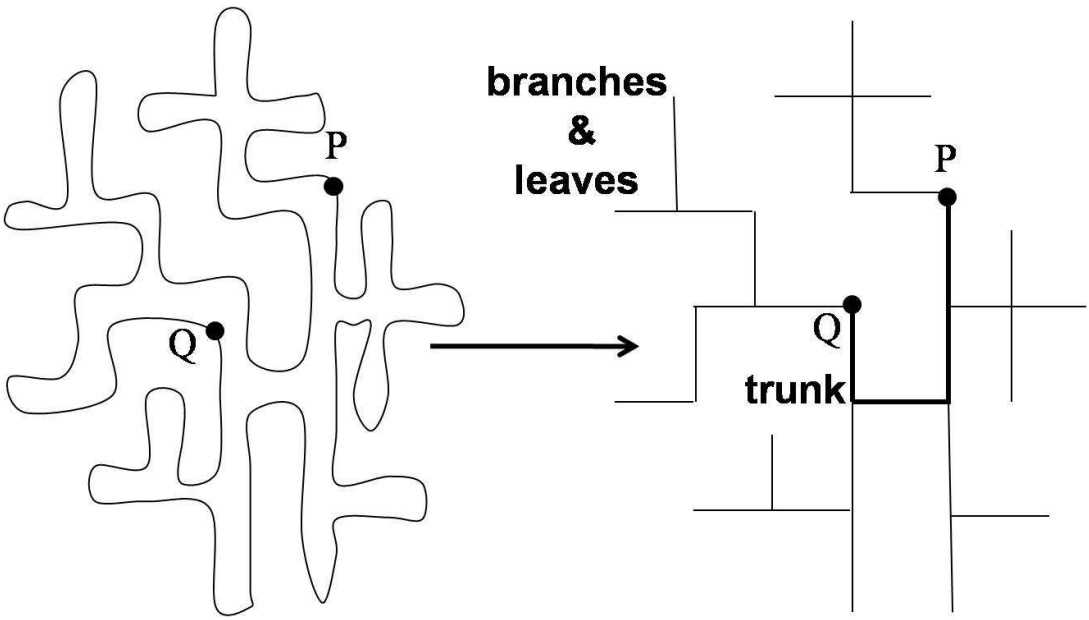

Figure 2.6: Division of a section of a Cayley tree ring into trunk, branches and leaves

understand this difference in mechanism they suggested a shift in focus from the local effect of kink-defect diffusion which causes perpetual changes of conformation to its effect on the most durable feature associated with any section of the polymer.

In order to aid this shift of focus they first divided the Cayley tree structure of the ring chain into substructures *viz.*, trunk, branches and leaves (see Figure 2.6). They argued that the kink-defect diffusion first rearranges the leaves, then the branches and finally the trunk. Further they divided the kink-defect diffusion effects into two distinct parts:

- Diffusion within the branches and leaves which do not contribute to the center of mass motion of the chain.
- Diffusion along the trunk which leads to center of mass motion of the chain.

The branches and leaves were thus considered to act as reservoirs of kink-defects while the dynamical evolution of the trunk causes the center of mass motion of the chain. Consequently a shift of focus to the dynamical evolution of the durable feature, *i.e.*, the trunk of the chain and the refinement of the contribution of the kink-defect diffusion to center of mass motion of the chain section was achieved.

Based on this refined idea Obukhov *et al.* (1994) considered a general section of the Cayley tree ring between two points P and Q consisting of n segments (see Figure 2.6). They argued

that the portion of the lattice tree corresponding to the section can be divided into trunk and branches where the trunk is a random walk of length $m \sim n^{1/2}$. When a single defect moves by a distance 'a' it causes a segment along the trunk to have a mean-square displacement a^2. Such a motion of a segment in the chain causes the center of mass of the section to have a mean-square displacement of $(a/n)^2$. In the trunk there are m such non-interacting defect reservoirs and consequently the mean-square motion of the center of mass due to the simultaneous motion of all the defects is given by:

$$\Delta s_{c.o.m} \sim m \left(\frac{a}{n}\right)^2 \tag{2.21}$$

This entire motion happens in the time scale of relaxation τ_0 of the stored length a. The curvilinear diffusion coefficient of the chain is thus given by:

$$D_c(n) \sim \frac{\Delta s_{c.o.m}}{\tau_0} \sim n^{-3/2} \tag{2.22}$$

Considering the entire ring chain its trunk contains $M \sim N^{1/2}$ and has a $D_c(N) \sim N^{-3/2}$. The longest relaxation is the time taken for the complete reorientation of the trunk of the ring chain and is given by:

$$\tau_r \sim \frac{M^2}{D_c(N)} \sim N^{5/2} \tag{2.23}$$

Thus we obtain the $N^{5/2}$ scaling of the longest relaxation time. The self-diffusion coefficient of the chain can then be worked out based on the idea that in the time scale τ_r the ideal ring chain moves through a spatial distance of the order of its radius of gyration $R_g \sim N^{1/4}$ and hence:

$$D \sim \frac{R_g^2}{\tau_r} \sim N^{-2} \tag{2.24}$$

We hence forward refer to the Obukhov *et al.* (1994) scaling arguments described in fair detail as Duke-Obukhov-Rubinstein (DOR) scaling arguments.

Obukhov *et al.* (1994) studied the dynamics of ring chain based on the numerical simulations through variant of the repton model (Rubinstein, 1987; Duke, 1989). In this study the motion of ring chain of N_a segments in a lattice of obstacles was investigated with the use of a certain set of rules for defect motion (see Obukhov *et al.* (1994) for details of the rules). The equilibrium statistics based on this model yielded the radius of gyration of the chain scaling as $R \sim N_a^{\nu}$ with $\nu = 0.28 \pm 0.02$ for $N_a > 100$ - a value close to the Nechaev (1998) results for ideal Cayley tree ring chains of $\nu = 0.25$. In dynamics the relaxation behavior of the chain was investigated by determining the fraction, f, of the original lattice tree bonds that remain after a time t and it was found that:

- The substantial fraction of the chain relaxed quickly which is expected due to the fast relaxation of branches and leaves.

- At long times there is a single exponential decay corresponding to this fraction given by $f = f_0 \exp(-t/\tau_r)$ where $\tau_r \sim N_a^{2.6\pm0.1}$ and $f_0 \sim N_a^{0.5\pm0.1}$. These results are consistent with the DOR scaling results for longest relaxation time equation (2.23) and the consideration of a predominant length scale of order $N_a^{0.5}$ respectively.

The diffusion coefficient scaling, $D \sim N_a^{-2.1\pm0.1}$, was also found to be consistent to that of the results of the DOR scaling expression (2.24). Further, the curvilinear transport of a chain segment was investigated and it was found that the average mean-square displacement of the segment along the contour is related to the time scale of motion by $\langle l^2 \rangle \sim t^\gamma$ where $\gamma = 0.8 \pm 0.04$. Obukhov *et al.* (1994) pointed out that inversion of equation (2.23) for an arbitrary section of the chain with a contour length, l, is expected to yield $l \sim t^{2/5}$ a result in concurrence with this simulation result. We can consider this final result as an indication of the similarity of dynamics of the Cayley tree ring at all length scales.

Note: Although the kink-defect diffusion mechanism scaling arguments have been employed to understand the dynamics of such Cayley tree rings the problem of equilibration of defects has not been considered explicitly. This is probably due to the absence of free ends which play an important role in such equilibration.

So far we have discussed scaling models for dynamics of Cayley tree rings in an obstacle environment. In the rest of this section we discuss ideas that can be considered as a relevant aid to developing rigorous frameworks for entangled Cayley tree ring polymers. Klein (1986) conjectured that the dynamics of the ramified structure of a ring in a melt (see Figure 2.4) is similar to that of a star polymer and hence is likely to have diffusion coefficients comparable to that of entangled star polymers as arrived at in the light of tube model. In section 2.1.2 we have already discussed the correspondence of the universality class of the Cayley tree structure and randomly branched polymers which have annealed branch points. We have also seen in section 2.1.2 that according to Müller *et al.* (2000) simulations large ring polymers in a melt of identical ring chains are likely to have a lattice tree like structure. Thus, it is useful to review the application of tube model to branched polymers in our quest for formulation of rigorous frameworks for the addressing the entangled dynamics of a Cayley tree ring chains.

In section 1.2 we briefly mentioned the ingenious conceptualization of Pom-Pom polymer

worked out by McLeish and Larson (1998) for application of tube model to study the dynamics of branched polymers. In the Pom-Pom polymer model McLeish and Larson (1998) considered an idealized molecules that has a single back bone with multiple branches emerging from both ends. In a melt of such a polymer the branches and the backbone are entangled with surrounding molecules and are thus confined in a tube. In order to study the dynamics of such an entangled chain, McLeish and Larson (1998), considered how an ensemble of mutually entangled pom-pom polymers reconfigure the orientation by escaping from their orignal tube constraints. They argued that in such a polymer the backbones do not relax initially as the branch points act as effective pinning points to the motion of the backbone. However, the branch arms of the chain are free to relax through deep retractions known as 'breathing modes' which occur by random formation of unentangled loops (Pearson and Helfland, 1984).

The branch points of the chain remain pinned till the arms relax completely through the 'breathing modes' after which the arms essentially act like solvents. Thus, the effective friction to curvilinear diffusion of the chain is located at the branch points rather than distributed along the chain. Based on this physical idea McLeish and Larson (1998) calculated the diffusion coefficient of the branch point by noting that the branch point moves a distance of order a into the tube of constraints in the time scale of relaxation of the arm, τ_{arm} and hence $D_c = (1/2)a^2/\tau_{arm}$. Considering the presence of q_n such arms to linearly increase the drag on the branch point they used the Einstein argument to calculate the drag as:

$$\zeta_b = \frac{k_B T}{D_c} = 2k_B T \frac{\tau_{arm}}{a^2} q_n \tag{2.25}$$

Based on this modification of friction and considering that relaxation of the backbone happens when the branch point diffuses in a dilated tube of constraints to traverse a mean-square distance between the branch points, L^2, they arrived at the relaxation time of the backbone to be of the order $\tau_b \sim L^2 q_n \tau_{arm}$. The relaxation time thus obtained was used in a single relaxation mode expression for the relaxation modulus (McLeish and Larson, 1998).

2.2.3 Polymeric Fractals

Polymers are known to be self-similar (fractal) objects, *i.e.*, the conformation of the smaller sections of a polymer chain when magnified look the same as the conformation of the whole chain (Rubinstein and Colby, 2003). Such fractal objects are known to have non-integer dimensions associated with them (Muthukumar, 1985). In order to understand the idea of non-integer

dimensions we first consider the idea of dimensions from an abstract perspective. A point is a dimension less object, a line an one dimensional object and a plane a two dimensional object. If we take a point and consider an arbitrary continuous translation of it in space according to a certain rule which specifies the location of the point at each moment we obtain a line. A line thus obtained is composed of infinite point locations in space. A plane can similarly be obtained by translation of the line and is composed of infinite lines.

We can continue this operation of adding infinite number of lower dimensional objects to obtain a higher dimensional object. In our arguments so far we have just considered adding infinity of lower dimension objects to arrive at an integer dimensional higher dimension object but not explicitly mentioned the kind of infinity of these objects we have added. We note that there are several kinds of infinities that exist and the specific kind of addition we have considered so far corresponds to the infinity of set of real number of objects. However, it is possible to add other kind of infinities of points or lines. An illustration of a different kind of infinity corresponds to that of a Cantor ternary set (WIKIPEDIA, 2009) obtained by an iterative operation that removes an *open* middle one-third of real numbers between two real numbers, *i.e.*, if we start with the *closed* set of real numbers [0,1] then the operation removes values between the open set (1/3, 2/3) leaving the set [0,1/3] and [2/3,1] in the first iteration and removes values between (1/9, 2/9) and (7/9, 8/9) in the second iteration and so on. The set of values generated by such an iterative operation can be shown to be infinite but the values in the set are sparse in contrast to the values in the set of real numbers and the infinity corresponding to this sparsely populated set is different from the infinity of set of real number. Adding as many points or lines as there are values in a Cantor ternary set corresponds to adding a different kind of infinity. In such a case we obtain objects with non-integer dimensionality. The structures of our concern, the Gaussian chain and the Cayley tree, are such objects.

The geometrical structure of such fractal objects is characterized by their fractal dimensionality d_f – the exponent that relates the mass of a given structure to the spatial size of the structure: (Muthukumar, 1985):

$$M \sim R^{d_f} \tag{2.26}$$

The fractal dimension is associated with the volume of the fractal object through the size R and does not contain information about the internal connectivity of the object. The idea of spectral dimension was introduced to take into consideration the scaling properties of both volume and connectivity in calculation of density of states in a fractal object (Alexander and Orbach, 1982;

Muthukumar, 1985). The topological structural properties of the fractals are hence characterized by the spectral (fracton) dimensionality d_s, which is defined by (Muthukumar, 1985):

$$N_t \sim t^{d_s/2} \tag{2.27}$$

where N_t is the number of distinct sites in the fractal visited by a random walk up to a time t. Although the fractal dimension is known for a large class of fractal objects the exact value of d_s is known only for a limited class of such objects.

Muthukumar (1985) presented a theoretical study of the screening of hydrodynamic interactions and the viscosity of solutions of arbitrarily branched polymers. In this study the general problem was posed as a study of dynamics of polymeric fractals and a scaling relation for the spectral dimension in terms of the fractal dimension for an arbitrarily branched polymer was obtained. We have already seen in section 2.2 concerning discussion on Rouse chain that the equation of motion for a segment depends on the potential force exerted on the segment. This force depends on the nature of the branching, structure of the fractal and consequently on the distribution function of the position vectors of the various cross link junctions, $P_c(\mathbf{R}_i)$. Muthukumar argued that although the distribution function $P_c(\mathbf{R}_i)$ is different for every fractal the global dynamical features of the polymeric fractal can be worked out based on the potential of the mean force acting on a segment instead of working on with the microscopic cross-link distributions.

In order to achieve this he considered a linear Gaussian chain and considered the equation of motion of a segment, s, of a chain of lengths L, similar to that of Rouse Langevin description expression (2.13). For this chain the original equation of motion postulated by Rouse (Rouse, 1953) in terms of the Fourier components given by:

$$\left(\zeta\frac{\partial}{\partial t} + \frac{3k_BT}{l}q^2\right)\mathbf{R}(q,t) = \mathbf{f}(q,t) \tag{2.28}$$

was arrived at by using the probability distribution of the Gaussian chain in terms of Fourier components written as:

$$P(\mathbf{R}) = \aleph \exp\left(-\frac{3}{2}\int \frac{dq}{2\pi}\frac{R^2(q)}{\langle R^2(q)\rangle}\right) \tag{2.29}$$

$$\left\langle R^2(q)\right\rangle = lq^{-2} \tag{2.30}$$

where, the Fourier components $\mathbf{R}(q)$ are given by:

$$\mathbf{R}(q) = \int_0^L ds\ \exp(iqs)\mathbf{R}(s) \tag{2.31}$$

and the Fourier variable $q = 2\pi p/L$ is inversely proportional to the total length and consequently the mass of the linear chain.

The average in the expression (2.30) scales as the square of mass of the chain since $q \sim L^{-1}$. We can consider this average to be composed of two contributions (a) corresponding to that of the mean-square size of the object (b) corresponding to the mass of the object. Since the mean-square end-to-end distance of a Gaussian chain is proportional to $L \sim L^{2\nu}$ with $\nu = 1/2$ the size contribution is given by $\sim q^{-2\nu}$. The mass contribution to the average is always given by $q^{-1} \sim M$. For the Gaussian chain which is self-similar at all length scales the average can be written as $\langle R^2(q)\rangle = lq^{-(2\nu+1)}$ and consequently the equation of motion in terms of the Fourier component can be written as (Muthukumar, 1985):

$$\left(\zeta\frac{\partial}{\partial t} + \frac{3k_BT}{l}q^{2\nu+1}\right)\mathbf{R}(q,t) = \mathbf{f}(q,t) \tag{2.32}$$

Muthukumar (1985) proposed that the equation of motion of any branched fractal object without excluded volume interactions can be written in the form of equation (2.32) where the term containing $q^{2\nu+1}$ accounts for the potential of mean force on the fractal object.

In deriving an expression for the spectral dimension in terms of the fractal dimension Muthukumar (1985) conjectured that the generalized Rouse equation for branched polymers can be written as:

$$\left(\zeta\frac{\partial}{\partial t} - \frac{3k_BT}{l}\nabla_s^2\right)\mathbf{R}(s,t) = \mathbf{f}(s,t) \tag{2.33}$$

where, ∇_s is the generalized Laplacian in d_s dimensional space. In addition considering that a general Rouse mode variable q_s can be defined to be the Fourier conjugate variable to arc length in the space of spectral dimension, d_s, he proposed that equation (2.33) transforms to:

$$\left(\zeta\frac{\partial}{\partial t} + \frac{k_BT}{l}q_s^2\right)\mathbf{R}(q_s,t) = \mathbf{f}(q_s,t) \tag{2.34}$$

Comparing expressions (2.32) and (2.34) he arrived at a relationship between spectral and fractal dimensions given by:

$$\frac{2}{d_s} = \frac{2}{d_f} + 1 \tag{2.35}$$

The relationship (2.35) is arrived at based on several conjectures and the rigorous defence of the conjectures is beyond the scope of the present work. However, we consider the validity of the relationship (2.35) for polymeric fractals of our concern as a measure of correctness of the conjectures and hence briefly consider its validity for the Gaussian and the Cayley tree chain. In the case of Gaussian chain it is known that they have a fractal dimension $d_f = 2$ (Muthukumar,

1985; Rubinstein and Colby, 2003). According to the relationship (2.35) the spectral dimension of the Gaussian chain is given by $d_s = 1$ – a result in agreement with that reported by Alexander and Orbach (Alexander and Orbach, 1982). From the size scaling, $R \sim N^{1/4}$, of the ideal Cayley tree ring structure it is clear that they have a fractal dimensionality $d_f = 4$. The spectral dimension of this chain using expression (2.35) is calculated to be $d_s = 4/3$ – a result that was recently shown to be correct for critical percolation on Cayley trees (Barlow and Kumagai, 2005) and generic ensembles of infinite trees (Durhuus *et al.*, 2007).

Note: The spectral dimension of a fractal object appears to be independent of the space dimension d on which the fractal object is generated by means of a random walk (Alexander and Orbach, 1982; Meakin and Stanley, 1983). The generating function associated with the 'number of distinct sites visited' expression (2.27) is known to be related to the Laplacian in random geometry applications (Durhuus *et al.*, 2007). Thus the spectral dimension may be considered as the appropriate dimension for writing a generalized Rouse equation of form (2.34).

We can also analyze the dynamics of polymeric fractals framework developed by Muthukumar (1985) in terms of its relationship to viscoelastic response of branched polymers. In order to carry out this analysis we consider the microscopic expression for stress in a polymeric system which depends on the correlations between the Fourier components of position and can be shown to be given by:

$$\sigma_{\alpha\beta} = \frac{c}{N} \sum_{q} \frac{3k_B T}{l} q^{2\nu+1} \left\langle R_\alpha(q,t) R_\beta(q,t) \right\rangle \tag{2.36}$$

where, c/N is a measure of density of chains in the system. The Fourier component correlations for any branched fractal object without excluded volume interaction can be obtained using the equation of motion (2.32). Based on the solution to expression (2.32) for simple shear flow the relaxation modulus of an hyperbranched polymer can be shown to be given by:

$$G(t) = \frac{c}{N} k_B T \sum_{q} \exp\left(-\frac{t}{\tau_q}\right) \tag{2.37}$$

where,$\tau_q = (l\zeta/6k_BT)q^{-(2\nu+1)}$. The complex modulus corresponding to the relaxation modulus expression (2.37) can be shown to be:

$$G^*(\omega) = \frac{c}{N} k_B T \sum_{q} \left[\frac{i\omega\tau_q + \omega^2\tau_q^2}{1+\omega^2\tau_q^2}\right] \tag{2.38}$$

The melt rheology of hyperbranched polyesters has been shown to be accurately modeled

by expression, arrived at by Rubinstein *et al.* (1989), given by (Suneel *et al.*, 2002):

$$G^*(\omega) = \frac{d_s G_0}{2}\, i\omega \int_{\epsilon_N}^{\epsilon_x} \frac{(\epsilon/\epsilon_x)^{(d_s/2)-1}}{i\omega + \epsilon} \frac{d\epsilon}{\epsilon_x} \tag{2.39}$$

where, G_0 is the unrelaxed shear modulus, ϵ is the inverse of the relaxation time, ϵ_N and ϵ_x are long and short time cutoffs corresponding to the relaxation time of the entire polymer chain and the sections between branch points respectively. It can be shown that the expression (2.38) arrived at from the dynamics of polymeric fractals framework is similar to the expression (2.39) used in the modeling of melt rheology of hyperbranched polyesters. Thus, the dynamics of polymeric fractals framework may be considered as a useful starting point for looking at dynamics of the Cayley tree ring chain.

2.3 Viscoelasticity and Diffusion

We have already mentioned in section 2.2.1 the triggering of interest in dynamics of ring polymer by the work of Roovers and Toporowski (1983); Roovers (1985a,b, 1988); Roovers and Toporowski (1988). Roovers and Toporowski (1983) prepared narrow molecular weight ring polystyrene (PS) through anionic polymerization and used the techniques of ultracentrifugation sedimentation and gel permeation chromatography to monitor the purity of rings. It was shown that polymers of molecular weights up to 45×10^5 could be synthesized using the experimental protocol. They further pointed out that the the probability of knot formation and concatenation in the synthesis protocol is marginally small (Roovers and Toporowski, 1983). The rheological characterization of a melt of polystyrenes synthesized indicated that the loss modulus, G'', of the ring chain was always lower than that of the linear polymers over the entire frequency regime (Roovers, 1985b). Based on this observation and the relation between plateau modulus G_N^0, loss modulus G'' and loss modulus contribution from the glassy state, G_s'', Roovers and Toporowski (1983) argued that the plateau modulus for ring melt should be half that of the linear melt and hence the rings are not as effectively entangled as linears. This can be considered as the first experimental indication for the altered structure of a ring chain in its melt.

The synthesis of rings was extended to the formation of polybutadiene (PBD) rings (Roovers and Toporowski, 1988) which are known to have an entanglement molecular weight smaller than that of PS and hence are expected to entangle even at relatively low molecular weights as compared to PS. Roovers (1988) in his paper on viscoelastic properties of ring PBD made several interesting observations:

- G' and G'' values of the ring melt about 5 times lower than that of the corresponding linear melt – an indication of weak entanglement effects in ring melts.

- The zero-shear viscosity (ZSV) of ring PBD sample KPBD34B3 about an order of magnitude lower than the linear melt composed of PBD of about the same molecular weight – an indication of faster dynamics of rings.

- ZSV of ring-linear blends of PBD shows a steep change in viscosity due to linear contamination and a maxima in viscosity with varying fraction of linear chains – an indication of rapid slowing of dynamics due to compatibility of ring and linear chains

These observations established ring polymers as a class of entangled fluids different from that of the linear chains.

McKenna and co-workers carried out extensive rheological measurements on melts of macrocyclic polystyrene chains over a broad range of molecular weights from below the critical molecular weight for entanglement M_c to well above this value. Two of their main research papers McKenna *et al.* (1987, 1989) are summarized here. In their earlier paper McKenna *et al.* (1987) reported the temperature and molecular weight dependence of ZSV of several fractions of macrocyclic polystyrene samples synthesized in different laboratories, and have compared their results with those obtained independently by Roovers (1985b) at around the same time. The dilute solution properties of these macrocyclic polystyrene fractions were first extensively measured by size exclusion chromatography, light scattering and limiting solution viscosity. It was found that most of the macrocyclic chains showed $g = [\eta_c] \,/\, [\eta_l] = 0.66$ at or near the theta-condition. Here $[\eta_c]$ and $[\eta_l]$ are respectively the limiting viscosities of solutions of cyclic and linear polystyrene chains. The experimentally observed value of g is in agreement with theoretical expectations for cyclic polymers. Also at these conditions the molecular weight dependence of the limiting viscosity, as defined by the Mark-Howink exponent, for the macrocycles was the same as that for the linears namely 0.5. They further noticed that the exponent for the Roovers rings was 0.46. They attributed this lower value to the possibility that the Roover rings were knotted since they were prepared by cyclization at below theta-temperature. Assuming that the dilute solution properties are a true reflection of the purity of macrocycles, McKenna *et al.* (1987) proceeded to measure their ZSV in melt state. This was done by using the highly sensitive Plazek rheometer that is coupled with an essentially frictionless magnetic bearing and a highly sensitive strain measurement tool. This enabled them to impose very small strain rates

and thereby measure ZSV with great precision. They observed that the temperature dependence of the ZSV of macrocycles and linears were similar to within measurement errors and could be fitted to the Vogel exquation. Further, the molecular weight dependence of the ZSV was also identical for the macrocycles and linears at both below and above the entanglement molecular weight M_c, which was also observed to be indistinguishable for macrocycles and linears. The ZSV data could be fitted by the following equation:

$$\log \eta_0 = logA + \frac{B}{T - T_\infty} + s \log M_w \tag{2.40}$$

The value of the exponent s was seen to be equal to 3.4 for both chain architectures. The actual value of ZSV of macrocycles was a factor of two lower than for linears of similar molecular weights for $M < M_c$. Above M_c the ZSV was observed to be only slightly lower than for linears of similar molecular weights. In comparison the Roover rings had lower ZSV and a stronger, almost exponential, increase in ZSV with molecular weight. It was argued by McKenna *et al.* (1987) that the lower ZSV of Roover rings was because of their highly knotted topology while the stronger dependence on molecular weight was a result of contamination with linear chains. The latter was indeed confirmed by Roovers in a later paper.

In a subsequent paper McKenna *et al.* (1989) reported refined results on the dilute solution properties and creep compliance in melt state of the same polystyrene macrocycles obtained from various sources. The macrocycles were characterized by (i) gel permeation chromatography for molecular weight distribution, (ii) static light scattering for weight average molecular weight, (iii) theta temperature by measuring the second virial coefficient, and (iv) intrinsic viscosity. While for most macrocycles the intrinsic viscosities were found to be nearly 0.66 times that of linear counterparts and showed a $M_w^{0.5}$ dependence, both of which are in agreement with theory, there were some macrocyclic fractions for which the intrinsic viscosities were almost identical to their linear counterparts. However theta temperature measurements for all macrocycle fractions showed that $\theta_{rings} = 28.5°C$ while that for linears was $34°C$. The depression of the theta-temperature for rings compared to linears is in agreement with theoretical predictions. These results showed that while all fractions seemed to show 'ring-like' features the dilute solution properties cannot be considered as a guaranteed indicator of purity of the ring samples. In other words, the dilute solution properties of rings are not highly sensitive to the presence of a small amount of linear contamination. Such contamination is inevitable in the synthesis procedure of macrocycles by ring closure in dilute solution. Coupling between chain ends occurs predominantly for individual molecules (intra-chain) in dilute solutions resulting

in rings. However, inter-chain coupling leading to long linear chains cannot be entirely ruled out. Also there is a statistical chance of deactivation of the chain ends resulting in short linears. McKenna *et al.* (1989) showed that creep compliance of melt state could be a sensitive probe for detecting the presence of linear contaminants. The presence of linear chains causes a lowering of compliance in the rubbery regime compared to pure macrocycles. Further, they measured the ZSV of the macrocycle fractions once again and found that the 'good' fractions (in terms of purity) showed a slightly higher exponent of 3.9 instead of the previously measured value of 3.4. Also the value of M_c for the macrocycles was found to be twice that of linears, a result that is again different than their previously reported result (McKenna *et al.*, 1987). In other words they reported that the value of plateau modulus of their macrocycles was a factor of two lower than that for linear chains, which was in agreement with the Roovers data. Finally, they also carefully prepared blends of macrocyclic and linear polystyrenes and measured their ZSV. They observed that the ZSV of blends was a very strong function of the composition of linears. Specifically they observed that $\eta_{blend}/\eta_{linears} \approx \phi_{linear}^{5.6}$.

We have already discussed in detail the DOR scaling arguments describing the dynamics of ring polymer in an array of fixed obstacles in section 2.2.2. Based on these scaling arguments, Rubinstein and Colby (Rubinstein and Colby, 2003) proposed a constitutive relation for describing the linear viscoelastic response of a melt of such ring chains as (Problem 9.32 of the Polymer Physics book):

$$G(t) \sim \frac{c}{N_e} k_B T \left(\frac{\tau_0}{t}\right)^{2/5} \exp\left(-\frac{t}{\tau_r}\right) \tag{2.41}$$

This constitutive relation has recently been shown to be successful in modeling the linear viscoelastic response of ring PS (Kapnistos *et al.*, 2008). Our derivation of this relation is outlined below. Assuming self similar dynamics, a ring chain is considered to be comprised of $p = 1, 2, ..., N$ independent relaxation modes; the p^{th} mode corresponds to relaxation of N/p blobs and has a relaxation time given by:

$$\tau_p \sim \tau_0 \left(\frac{N}{p}\right)^{5/2} \tag{2.42}$$

The stress relaxation modulus at time τ_p is expected to be proportional to the thermal energy and the number density of blobs, and is thus given by $G(\tau_p) \sim k_B T(p/N)$. A simple substitution for p from the mode-relaxation time equation (2.42) gives:

$$G(\tau_p) \sim k_B T \left(\frac{\tau_0}{\tau_p}\right)^{2/5} \tag{2.43}$$

This suggests that for any time $t < \tau_1$ the relaxation modulus would scale as $G(t) \sim t^{-2/5}$. Including now the exponential decay term representing the stress decay due to relaxation of the entire ring chain, we arrive at the relation (2.41). A more detailed discussion of the the idea of relaxation of a ring chain in an array of fixed obstacles and melts as proposed by Kapnistos *et al* is deferred to the chapter 5.

Among polymers DNA is rather unique in that it is naturally found in a number of different topological forms, including linear, supercoiled circular, relaxed circular, knotted circular and branched (Robertson and Smith, 2007c). The method of observing dynamics of DNA by fluoroscently staining the DNA molecule embedded in a background of unstained DNA was first suggested by Chu (1991). The first such observation of reptation like dynamics of a DNA molecule in an entangled DNA solution was carried out by Perkins *et al.* (1994) using fluorescent microscopy to directly observe the motion of the stained DNA. This study established DNA molecules as an excellent system for studying polymer dynamics. Since then fluorescent microscopy of stained DNA molecules has been used extensively to probe the effect of topological constraints on polymer dynamics of linear chain systems (Teixeira *et al.*, 2007). Robertson and Smith (2007b,c) were the first to investigate the effect of topology of a circular DNA on its diffusion. In a series of experiments they measured the diffusion coefficients of linear and relaxed circular DNA molecules by tracking the Brownian motion of single molecules with fluorescence microscopy.

In studying the effect of length and concentration on diffusion coefficient Robertson and Smith (2007b,c) considered four different systems (a) linear tracers surrounded by linear molecules $(L-L)$ (b) circular tracers surrounded by linear molecules $(C-L)$ (c) linear tracers surrounded by circular molecules $(L-C)$ and (d) circular tracers surrounded by circular molecules $(C-C)$. In their measurements they found that for DNA molecules of 6 kbp and 11 kbp the diffusion coefficient D of the tracers was largely insensitive to the topology. However for 25 kbp and 45 kbp circular DNA surrounded by linear molecules are slowed down considerably and diffuse 100 times slower than the circular tracer surrounded by circular molecules (Robertson and Smith, 2007c). Largest diffusion coefficients were reported for the system of circular tracers surrounded by circular molecules and a decrease of diffusion coefficient was effected by addition of linear molecules. Linear tracers surrounded by linear molecules was found to have an order of magnitude slower diffusion coefficient than circular tracers surrounded by circular molecules.

The observations can be neatly summarized by the relationship $D_{C-C} > D_{L-C} >> D_{L-L} >> D_{C-L}$ (Robertson and Smith, 2007b). Based on these observations Robertson and Smith (2007c) proposed that the free ends of molecules play a critical role in generating entanglements that retard diffusion and the strongly hindered diffusion of circular DNA molecule is caused by threading of the ends of the molecules through the ring chain. The increase in viscosity of ring chains with addition of linear chains reported by Roovers (1988) may be understood on the basis of the strong influence of such threading. Further, for the case of $L - L$, $L - C$ and $C - C$ Robertson and Smith (2007b) reported a cross over of diffusion coefficient from a scaling consistent with the Rouse model to a scaling consistent with the reptation model $D \sim L^{-2}C^{-1.75}$ at ~ 6 times the molecular overlap concentration. It is interesting to note that the concentration scaling of diffusion coefficient D for $L - L$ and $C - C$ are identical in spite of the difference of order of magnitude in their values.

Based on the observation that $D_{C-C} > D_{L-C}$ Robertson and Smith (2007c,b) supported the Klein (1986) conjecture that constraint release would be negligible in circular melts. They also found the concentration threshold to be insensitive to topology while viscoelasticity experiments in the case of ring melts indicate that ring chains in a melt are less effectively entangled. The way to reconcile this anomaly is to consider an intermediate regime of concentrations where topological constraints are not active in compacting rings. The structure of the circular molecule is collapsed when the concentrations goes beyond this regime wherein topological constraints become active leading to compaction and consequently to a faster diffusion mechanism with considerable contributions to relaxation through release of constraints. In chapter 6 we focus on the scaling arguments for diffusion coefficients of $C - C$ systems to gain a better understanding of these observations.

In an interesting follow up of their diffusion studies Robertson and Smith (2007a) measured the forces confining a single molecule embedded within a concentrated solution of long relaxed circular DNA using optical tweezers. In order to determine the confining force a probe in the concentrated solution was subjected to different values of transverse displacements at different rates and the induced force on the probe was measured. The force versus displacement curve thus obtained from these measurements was used to construct the potential per unit length confining the transverse displacements and a characteristic confining distance was determined from this potential. Robertson and Smith (2007a) observed that the confinement distance of circular DNA a_c is less than the confinement distance associated with the linear DNA a_l and is

given by $a_c = 0.75a_l$. They also observed a non-linear force for large displacement of the probe in circular DNA as opposed to that of linear DNA which showed a linear response. This points out to compaction of the circular DNA and a non-Gaussian structure of circular molecules in a concentrated system.

The relaxation of the confinement effects was carefully probed in these experiments and it was observed that confinement effects decayed rapidly in circular DNA as compared to linear DNA (Robertson and Smith, 2007a). However, the time scale of persistence of the confinement field was much larger than Rouse time scale of relaxation of the circular DNA. Based on these observations they concluded that there exists a tube like confinement field similar to that of linears in circular chains however the time scale associated with this confinement field is much smaller than that associated with the linear chain. Interestingly they also pointed out for displacements larger than the length scale of confinement the confining force of the circular polymers was much smaller than that of the linear polymers. The PPR framework developed in chapter 3 considers a tube like confining field for the ring chains which is in fact shown to be short lived than that of the linear chain.

Chapter 3

Pom-Pom Ring Model: Mean Field Approach to Ring Dynamics

3.1 DOR Scaling Arguments: Reptation Interpretation

Scaling arguments for dynamics of ring polymers in an array of fixed obstacle (gel) have been worked out for both ideal (Obukhov *et al.*, 1994) and excluded volume (Cates and Deutsch, 1986) rings. These arguments are based on the kink-diffusion picture discussed in section 2.2.2 wherein a polymer in an array of obstacles diffuses due to motion of 'length defects' or kinks along its contour. The consequent diffusional motion of a linear chain along its contour is similar to that of a snake (reptile) and was termed as 'reptation' by de Gennes (1971). In the kink-diffusion mechanism for dynamics of a linear chain the number of kinks in the chain is considered to be proportional to the contour length of the chain and diffusion of each kink has a specific contribution towards the center of mass motion of the polymer chain.

In the case of ring chains we have seen that there are two different approaches for kink-diffusion based scaling arguments (see section 2.2.2). The difference in the two approaches can be seen to arise in terms of contribution of diffusion of each kink towards center of mass motion of the chain. Cates and Deutsch (1986) propose a linear like kink-diffusion mechanism in which the diffusion of all the kinks along the contour of the chain contribute to the center of mass motion. Obukhov *et al.* (1994) argue that the kink-diffusion mechanism for ring chains is different from that of linear chains as opposed to Cates and Deutsch (1986). They propose a distinct mechanism of kink-diffusion for ring chains wherein all the kinks along the contour do not contribute to the center of mass motion (see section 2.2.2).

There arise differences in the scaling results for ring chains due to (a) variations in static configuration and (b) due to the mechanism of kink-diffusion. For an ideal ring polymer in an array of fixed obstacles the DOR scaling arguments yields diffusion coefficient, $D \sim N^{-2}$, and longest relaxation time, $\tau_d \sim N^{5/2}$ (Obukhov *et al.*, 1994). A linear like diffusion of kinks for an ideal ring polymer in an array of fixed obstacles yields $D \sim N^{-5/2}$ and $\tau_d \sim N^3$ (Nechaev *et al.*, 1987). For an excluded volume ring in an array of fixed obstacles both the scaling arguments yield diffusion coefficient, $D \sim N^{-2}$, and longest relaxation time, $\tau_d \sim N^3$ (Cates and Deutsch, 1986).

We do intuitively expect that the absence of free ends could cause local accumulation of kinks and hence is likely to alter the kink-diffusion mechanism on a global level and consider the DOR scaling arguments as a basis for the PPR framework. We have seen that the mechanism of kink-diffusion according to DOR scaling hinges on the Cayley-tree structure of the ring polymer (see section 2.2.2). The relaxation of branches and leaves is fast and causes only local rearrangements which do not contribute to the center of mass motion while the relaxation of trunk by diffusion along its contour causes center of mass motion. A reptation interpretation can be given to the DOR scaling arguments considering that this diffusion of the trunk along its contour is similar to the reptation of a linear chain with the difference that the trunk has a modified friction associated with it due to the presence of loops along its contour. The dynamics of the trunk, the most predominant length scale, effected through its diffusion governs the longest relaxation times of the system (Figure 3.1).

3.2 Pom-Pom Ring Framework

We formulate the Pom-Pom Ring (PPR) framework based on reptation interpretation of the DOR scaling model. Based on the formulation we predict the dynamics and viscoelastic response of ring polymers in topologically constrained environment. Following the DOR scaling the PPR formulation considers the ring chain in a fixed array of obstacles to assume a Cayley-tree structure which can be broken down to substructures *viz.* trunk, branches and leaves with the relaxation of different substructures happening at different time scales. However, the dynamics of different substructures are coupled in a specific way. In arriving at this coupling we consider that for an ideal ring of $N = N_K/N_e$ blobs with each blob composed of N_e Kuhn segments in an array of fixed obstacles there exists a characteristic length scale that constitutes

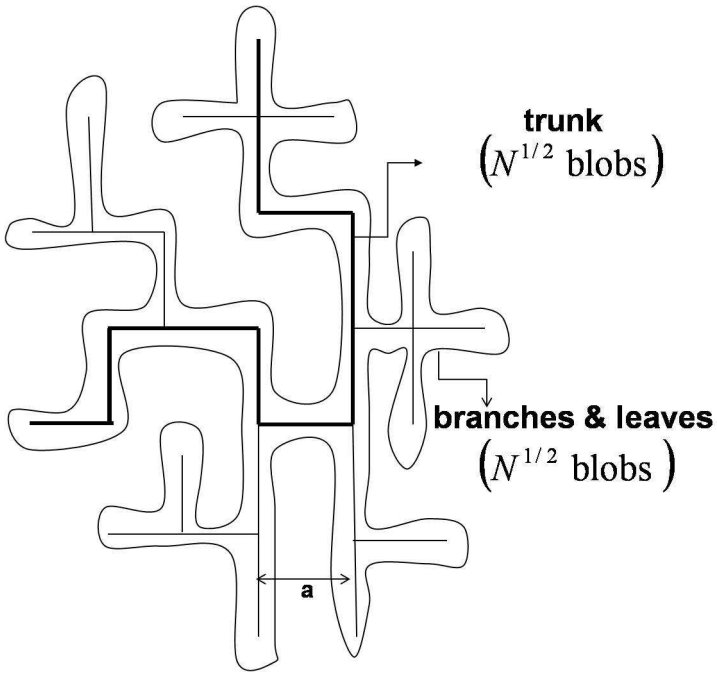

Figure 3.1: Trunk, branch and leaf structures of a lattice tree

the primary trunk of the Cayley-tree structure. The primary trunk of the ring Cayley-tree can be unambiguously determined (Obukhov *et al.*, 1994) and is the most endurable hypothetical structure among the substructures of the ring Cayley-tree. Further, the leaves and branches of the Cayley-tree constitute loops that are attached to the primary trunk at loop points, similar to branches attached to branch points in a branched polymer (Figure 3.2). Given the similarity of the lattice-tree structure to the randomly branched polymer we may now invoke the pom-pom model to describe the dynamics of the ring polymer.

According to the pom-pom model for branched polymers the branches, if entangled, relax through an arm retraction mechanism, which is the only mechanism allowed by a constricting branch point, and the relaxation times are exponentially dependent on the arm molecular weight (McLeish and Larson, 1998; Klein, 1986). Shorter branches, not so entangled, may relax through Rouse modes (Karayiannis and Mavrantzas, 2005). The relaxation of entangled backbone of the branched polymer is constrained by the presence of branch points and can happen only after the relaxation of the branch arms. Thus, the branches add substantially to the friction of the backbone and in the case of the pom-pom model the friction is essentially located at the ends of the backbone (McLeish and Larson, 1998; Karayiannis and Mavrantzas, 2005). In the case of the ideal ring polymer we assume that the primary trunk of the self-similar

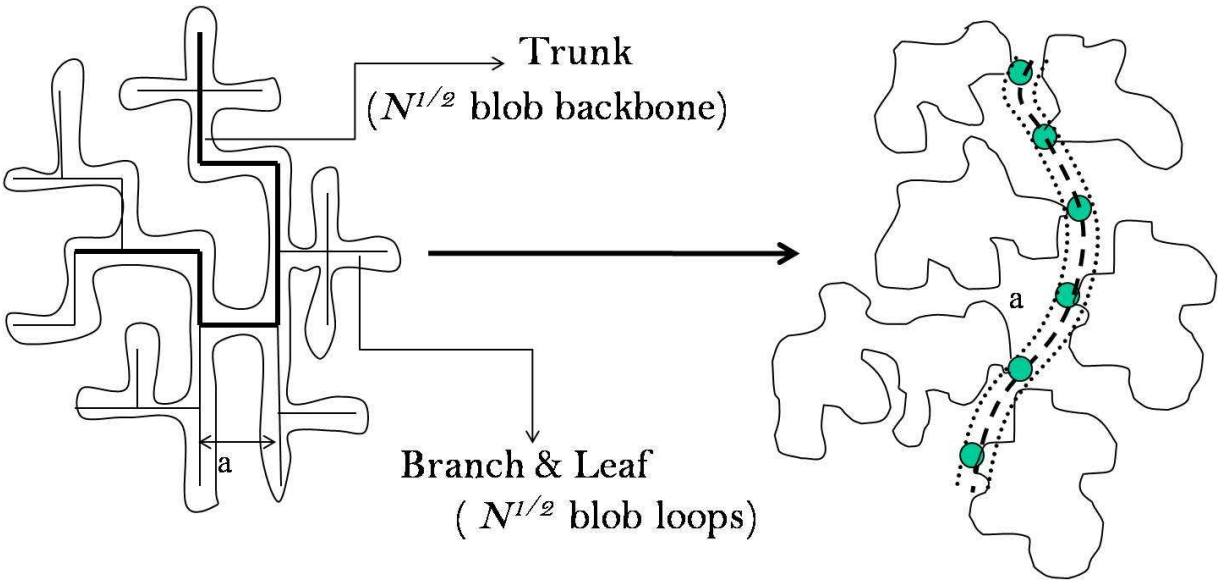

Figure 3.2: Model chain for studying dynamics of the ring chain in an array of fixed obstacles

lattice-animal/Cayley-tree is entangled with the array of obstacles, while the loops take a much more collapsed conformation and are hence not entangled and their dynamics is entirely Rouse like. This assumption is valid if the loops are small and therefore not sufficiently entangled. At any point of time for a trunk segment to move, it requires that the loop attached to the specific trunk segment, relaxes completely and allows for the loop point to move. Thus, the dynamics of the trunk may be affected in a way similar to that of the backbone of the branched polymer. The loops act as frictional constraints for the motion of the trunk.

The primary trunk, viewed in light of the closed random walk on the Cayley tree, can be identified with the steps leading to the 'average' coordinate i, of the closed random walk, which is of order of $N^{1/2}$ steps (see section 2.1). This means that if there is a random walk of N steps with each step of length a then the predominant length scale, *i.e.*, the primary trunk, has a length of order $N^{1/2}a$. We consider that there are N_e Kuhn segments associated with the length scale a and with assumption of Gaussian statistics at this length scale we have $N_e = a^2/b^2$, where b is the Kuhn length of the polymer. The assumption of Gaussian statistics at the length scale a is valid for an ideal chain if the topological constraints are considered to be ineffective at the length scale a. The length of the primary trunk is thus given by:

$$L_P = N^{1/2}a = \left(\frac{N_K}{N_e}\right)^{1/2} a = N_K^{1/2} b \tag{3.1}$$

In this the trunk is a hypothetical mass less object defining the predominant length scale in the

framework. The number of loops accommodated on the hypothetical primary trunk is expected to be proportional to the number of steps in the primary trunk and is of order $N^{1/2}$. Considering the mass of the ring chain to be entirely contained in the loops an average loop would be composed of $N_{loop} = N/N^{1/2} = N^{1/2}$ blobs.

On the basis of the physical picture described above we formulate the Pom-Pom Ring (PPR) framework for studying dynamics of ring polymers. First, we formulate a modified primitive chain for the ring polymer as follows:

1. The primitive chain is constituted by the primary trunk of the lattice tree composed of $N^{1/2}$ blobs with a constant contour length, L_P, given by expression (3.1).

2. Each segment of the primitive chain has attached to it a loop. On an average each loop contains $N^{1/2}$ blobs. We assume that the loops are unentangled because of their collapsed conformation

3. The primitive chain is entangled and can move along itself with a curvilinear diffusion coefficient determined from dynamics of a modified Rouse chain.

4. The primitive chain has the conformation of a random walk, *i.e.*, the tangents at different points along the trunk are uncorrelated.

Second, using the pom-pom analogy (McLeish and Larson, 1998), the diffusion coefficient of a loop point, D_{loop}, is given by $D_{loop} \sim a^2/\tau_{loop}$, where $\tau_{loop} \sim a^2(N^{1/2})^2\zeta_{blob}$ is the longest Rouse relaxation time of the loop attached to the loop point. Using the Einstein argument the drag on a loop point is given by:

$$\zeta_{loop} = \frac{k_B T}{D_{loop}} \approxeq N\zeta_{blob} \tag{3.2}$$

where ζ_{blob} is the friction coefficient of a single blob in the loop. Thus, the modified Rouse chain which constitutes the primitive chain has each of its segments having a friction coefficient of order $N\zeta_{blob}$.

The friction coefficient of a blob, ζ_{blob}, can be derived from the understanding that it consists of N_e unentangled Kuhn segments (beads), which are undergoing the usual Rouse or Zimm dynamics depending on the environment in the pore of the array of obstacles. Assuming Rouse dynamics for the beads, the longest relaxation time, τ_0, of the blob scales as $\sim b^2 N_e^2 \zeta$. The blob of characteristic length a relaxes in time τ_0. The diffusion coefficient of the blob is given

by $D_{blob} \sim (a^2/\tau_0) \sim 1/N_e\zeta$. From the Einstein argument the blob friction coefficient can be obtained using the scaling for blob relaxation time and is given by:

$$\zeta_{blob} = \frac{k_B T}{D_{blob}} \approxeq N_e \zeta \tag{3.3}$$

where, ζ is the friction coefficient of a single Kuhn segment.

In the above arguments we have reduced the structure of the ring polymer to its primary hierarchical level consisting of a primary trunk of $N^{1/2}$ blobs having $N^{1/2}$ number of loops attached to it, each consisting of, on an average, $N^{1/2}$ blobs. In other words we have not explicitly invoked the self-similar structure of the lattice tree. We show in Appendix (A.5) that if the relaxation of the lattice tree ring chain is assumed to occur in a hierarchical manner with the larger substructures relaxing only after the smaller substructures attached to them have relaxed, then such an explicit accounting of the lattice tree structure, while invoking the Einstein argument and the modified Rouse dynamics consistently at each hierarchical level, indeed gives a friction coefficient of a primary trunk segment scaling as $N\zeta_{blob}$. The current framework is thus self-consistent. However, in the rest of the discussion we will concern ourselves only with the description of the dynamics of the primary trunk.

3.3 Diffusion Coefficient and Relaxation Spectrum

3.3.1 Curvilinear Diffusion Coefficient

In the Cayley tree structure of the ring chain the trunk is an hypothetical structure determined by the relative positions of the loops (see Figure 3.2). The PPR framework facilitates a view of the dynamics of the ring chain through the dynamics of the primary trunk of the Cayley tree confined in the tube of obstacles. In this view point the rearrangement of a loop can be thought of as equivalent to the motion of the ring chains trunk along its contour. Such a motion of the trunk along its contour has a curvilinear diffusion coefficient associated with it.

To determine the curvilinear diffusion coefficient of the primitive chain (trunk) we begin with the dynamics of the modified Rouse chain constituting the primitive chain. We start with the force balance, *i.e.*, the Langevin equation, for the n^{th} bead of the chain experiencing an effective friction of $\zeta_{eff} = \zeta_{loop}$,

$$\zeta_{eff} \frac{\partial \mathbf{R}_n}{\partial t} = k_{eff} \frac{\partial^2 \mathbf{R}_n}{\partial n^2} + \mathbf{f}_n \tag{3.4}$$

where, $\mathbf{R}_n$ is the position coordinate of the n^{th} blob. The left hand side of equation (3.4) is the friction force on the blob, the first term on the right hand side corresponds to the entropic spring force on the blob and $\mathbf{f}_n$ is the stochastic force on the blob. In the PPR formulation loops are considered to contribute only to the friction of the primitive chain and the potential between blobs is not affected by the presence of loops. The primitive chain being a Gaussian has an effective spring constant given by $k_{eff} = 3k_BT/a^2$. However, the effective friction coefficient is given by $\zeta_{eff} = \zeta_{loop}$ as argued in the previous section.

From fluctuation-dissipation theorem we have the moments of the stochastic force ($\mathbf{f}_n$) experienced by the modified Rouse bead given by:

$$\begin{aligned} \langle \mathbf{f}_n(t) \rangle &= 0 \\ \langle (f_{n\alpha}(t) f_{n\beta}(t')) \rangle &= 2\zeta_{eff} k_B T \delta(n-m) \delta_{\alpha\beta} \delta(t-t') \end{aligned} \tag{3.5}$$

We decouple the set of equations (3.4), $n = 1, 2, ..., N^{1/2}$, using the normal coordinate transformation (Appendix equations (A.1) to (A.4) with $\nu = 1/4$). The decoupled equations (A.7) and (A.8) are solved to determine the modified Rouse modes and the relaxation spectrum.

The diffusion coefficient of the modified Rouse chain is defined by:

$$D_P = \lim_{t\to\infty} \frac{1}{6t} \left\langle (\mathbf{R}_G(t) - \mathbf{R}_G(0))^2 \right\rangle \tag{3.6}$$

where, $\mathbf{R}_G$ is the position of the center of mass of the chain. The position of the center of mass of the chain corresponds to the zeroth Rouse mode, $\mathbf{X}_0$:

$$\mathbf{R}_G = \frac{1}{N^{1/2}} \int_0^{N^{1/2}} dn\, \mathbf{R}_n = \mathbf{X}_0 \tag{3.7}$$

Thus, the diffusion coefficient is given by:.

$$D_P = \lim_{t\to\infty} \frac{1}{6t} \sum_\alpha \left\langle (X_{0\alpha}(t) - X_{0\alpha}(0))^2 \right\rangle \tag{3.8}$$

From the solution to the zeroth normal mode equation (A.10) we obtain (see Appendix A equation (A.10)):

$$\left\langle (X_{0\alpha}(t) - X_{0\alpha}(0))^2 \right\rangle = \frac{1}{\zeta_0^2} \int_0^t dt \left\langle f_{0\alpha}(t) f_{0\alpha}(t) \right\rangle \tag{3.9}$$

Using the fluctuation-dissipation theorem (3.5) and the normal coordinates (A.2) we obtain the correlation of the center of mass stochastic force:

$$\langle f_{0\alpha}(t) f_{0\beta}(t') \rangle = 2\zeta_0 k_B T \delta_{\alpha\beta} \delta(t-t') \tag{3.10}$$

Using the stochastic force correlation (3.10) and $\zeta_0 = N^{1/2}\zeta_{eff} = N^{1/2}\zeta_{blob}$ in equation (3.9) we obtain the mean square displacement of the center of mass (expression for friction ζ_0 is obtained from Appendix A section A.2 using $\nu = 1/4$):

$$\left\langle (X_{0\alpha}(t) - X_{0\alpha}(0))^2 \right\rangle = 2\frac{k_B T}{N^{1/2}\zeta_{eff}}\delta_{\alpha\alpha}t \tag{3.11}$$

Substituting equation (3.11) in equation (3.8) we obtain

$$D_P = \frac{k_B T}{N^{1/2}\,\zeta_{eff}} \tag{3.12}$$

Using $\zeta_{eff} = \zeta_{loop} = N\zeta_{blob}$ we have:

$$D_P = \frac{k_B T}{N^{3/2}\zeta_{blob}} = \frac{a}{b}\frac{k_B T}{N_K^{3/2}\zeta} \tag{3.13}$$

where we have used expression (3.3) for ζ_{blob}. The diffusion coefficient, D_P, obtained from the modified Rouse dynamics of the trunk, can be considered to correspond to the diffusional rearrangement of all the loops along the contour of the trunk. The DOR scaling arguments (Obukhov *et al.*, 1994) have $N^{1/2}$ kinks diffusing over a linear dimension, a, to give the center of mass curvilinear diffusion coefficient scaling as $N^{1/2}(a/N)^2 \sim N^{-3/2}$, a scaling satisfied by equation (3.13).

3.3.2 Relaxation Spectrum and Self-Diffusion Coefficient

The higher order modified Rouse modes correspond to the rearrangements of parts of the primitive chain. This can be considered to be associated with the loop rearrangements along parts of the contour of the trunk. The higher order modified Rouse modes can be determined from the decoupled normal mode equations (see Appendix A equation (A.15)), $p = 1, 2, ...$ The modified Rouse relaxation spectrum for the primitive chain is given by (see Appendix A equation (A.18)):

$$\tau_p = \frac{1}{p^2}\frac{1}{3\pi^2}\frac{a^4}{b^2}\frac{\zeta}{k_B T}N^2 = \frac{1}{p^2}\frac{1}{3}\frac{b^2}{\pi^2}\frac{\zeta}{k_B T}N_K^2 \tag{3.14}$$

The relaxation spectrum (3.14) is same as the Rouse relaxation spectrum for a linear chain (Doi and Edwards, 1986).

We now consider the case where the primitive chain of length $L_P = N^{1/2}a = N_K^{1/2}b$ is confined in a tube formed by the array of obstacles and relaxes by reptation dynamics similar to that of a linear chain. The reptation dynamics of a chain is tracked through the time evolution

of the time correlation function:

$$\phi(s,s';t) = \left\langle (\mathbf{R}(s,t) - \mathbf{R}(s',0))^2 \right\rangle \tag{3.15}$$

where, $\mathbf{R}(s,t)$ is the position vector of a bead at a curvilinear distance s along the primitive chain at time t. Analogous to the Doi and Edwards (1986) formulation, for linear polymers, the curvilinear diffusion coefficient of the PPR primitive chain is given by the diffusion coefficient of the modified Rouse chain D_P. The evolution of the correlation function (3.15) is governed by the one dimensional diffusion equation given by (Doi and Edwards, 1986):

$$\frac{\partial}{\partial t}\phi(s,s';t) = D_P \frac{\partial^2}{\partial s^2}\phi(s,s';t) \tag{3.16}$$

The associated initial and boundary conditions for this equation are given by (Doi and Edwards, 1986):

$$\phi(s,s';0) = a|s-s'| \tag{3.17}$$

$$\frac{\partial}{\partial s}\phi(s,s';t)|_{s=L_p} = a \tag{3.18}$$

$$\frac{\partial}{\partial s}\phi(s,s';t)|_{s=0} = -a \tag{3.19}$$

The initial condition is based on the consideration that the primitive chain is Gaussian at time $t = 0$ and the mean square distance between two points on the Gaussian chain is proportional to $|s - s'|$. The boundary conditions are flux conditions at the primitive chain ends and have been discussed by Doi and Edwards (1986).

We use the curvilinear diffusion coefficient of the PPR primitive chain given by equation (3.13) to determine the self-diffusion coefficient and longest relaxation time of the ring polymer in a fixed array of obstacles as (Appendix A section A.3 with $\nu = 1/4$):

$$D = \frac{1}{3}\frac{b^2}{a^2}\frac{k_BT}{N^2\zeta} = \frac{1}{3}\frac{a^2}{b^2}\frac{k_BT}{N_K^2\zeta} \tag{3.20}$$

$$\tau_d = \frac{1}{\pi^2}\frac{a^4}{b^2}\frac{\zeta}{k_BT}N^{5/2} = \frac{1}{\pi^2}\frac{b^3}{a}\frac{\zeta}{k_BT}N_K^{5/2} \tag{3.21}$$

The self-diffusion coefficient corresponds to the diffusion of center of mass of the ring chain over a length scale of the size of the ring chain, R, which causes the primitive chain to completely relax its orientation. The longest relaxation time corresponds to the time taken for this diffusion. According to the DOR scaling arguments (Obukhov *et al.*, 1994) the longest relaxation time of the trunk of the lattice tree structure scales as $\tau \sim N^{5/2}$, a scaling satisfied by

equation (3.21). The ring diffuses and moves a distance of order of its size, R, in this time. The self diffusion coefficient of the ring given by $R^2/\tau \sim N^{-2}$ has a scaling satisfied by equation (3.20).

3.4 Dynamic Structure Factor

A direct measure of the dynamics of entangled chains is assessable via the technique of neutron spin echo (NSE) (McLeish, 2002b). NSE is a neutron scattering technique that exploits the neutrons intrinsic angular momentum, or spin, to access extremely high-resolution inelastic scattering. In this experiment polarized neutrons are guided through identical magnetic fields before and after scattering. Due to inelastic scattering the neutrons stay either longer or shorter in the second magnetic field altering the polarization of the scattered neutrons. Thus the energy transfer in the scattering is coded into the spin of the scattered neutrons and the energy and the momentum of the individual neutrons may be independently recorded. Fourier transformation of the energy transfer gives the time-dependent correlation. The final intensity depends on the motion of the scattering centers. Both coherent and incoherent signals may be independently accessed (McLeish, 2002b). The coherent signals provide information on single-segment diffusion and the incoherent signals provide information on segment-segment correlations. The dynamic structure factor based on coherent signals is given by (McLeish, 2002b; Doi and Edwards, 1978a):

$$g(\mathbf{k},t) = \frac{1}{L_P^2}\int_0^{L_P} ds \int_0^{L_P} ds' \left\langle \exp\left[i\mathbf{k}.\left(\mathbf{R}(s,t) - \mathbf{R}(s',0)\right)\right]\right\rangle \tag{3.22}$$

The dynamic structure factor, $g(\mathbf{k},t)$, extracted from the time correlation measurements, can be determined from the reptation picture. In this case the evolution of structure factor corresponds to evolution of the hypothetical trunk of the ring polymer. Based on the reptation formulation we obtain $g(\mathbf{k},t)$ as (Doi and Edwards, 1978a):

$$g(\mathbf{k},t) = \sum_p \frac{2\mu}{\alpha_p^2(\mu^2+\alpha_p^2+\mu)} \sin^2\alpha_p \exp\left(-4\frac{D_P t \alpha_p^2}{L_P^2}\right) \tag{3.23}$$

where,

$$\mu = \frac{k^2}{12} L_P a \tag{3.24}$$

α_p are the positive solutions of the equation:

$$\alpha_p \tan\alpha_p = \mu \tag{3.25}$$

There are two limits at which the dynamic structure factor can be obtained:

- For $\mu << 1$, *i.e.*, $k^2 L_P a << 1$ we focus at large wavelength limit and a length scale larger than the size of the polymer chain and $g(\mathbf{k}, t)$ is given by:

$$g(\mathbf{k}, t) = \exp(-Dk^2 t) \tag{3.26}$$

- For $\mu >> 1$, *i.e.*, $k^2 L_P a >> 1$ we focus at a smaller length scale than the size of the polymer chain and $g(\mathbf{k}, t)$ is given by:

$$g(\mathbf{k}, t) = \frac{12}{k^2 a L_P} \psi(t) \tag{3.27}$$

where, $\psi(t)$ is the fraction of chain in the original tube at time t (see Appendix equation (A.31)). In this formulation since we are concerned with only the motion of the longest length scale, *i.e*, the entangled primary trunk, equation (3.27) above is applicable for magnitude of wave vectors in the range $N^{-1/2} < k^2 < N^{-1/4}$.

3.5 Constitutive Relation

In frequency sweep experiments the stress response of the system is explored as a function of frequency at a given constant strain amplitude. The low frequency regime, also known as the terminal regime, corresponds to the long time response of the system. The high frequency regime corresponds to the short time response of the system. The response of the system at different time scales is expected to be connected to the response of the constituent polymer chains in the system at these time scales. From a reductionist point of view a constitutive relation connecting the stress and deformation in the system can be obtained based on understanding of the dynamics of the constituent polymer chain at long and short times. The dynamics of the polymer chain in turn is understood in terms of the dynamics of the coarse-grained primitive chain.

When a polymer chain is subjected to a stress the short time response of the chain is dictated by the dynamics of small sections of the primitive chain. Below the obstacle linear dimension, a, the primitive chain does not experience the effect of constraints and motion of the sections of the chain below this length scale is described by the modified Rouse dynamics discussed in section (3.3.1). The time scale of relaxation associated with the length scale, a, is

the same as the time taken for the coarse-grained Rouse blob to have an average mean square displacement of a^2. Based on the modified Rouse formulation the time taken for this mean square displacement of the blob along the trunk is given by (use $\nu = 1/4$ in Appendix equation (A.42)):

$$\tau_e = \frac{\pi}{12}\frac{a^4}{b^2}\frac{\zeta}{k_B T}N = \frac{\pi}{12}\, a^2\frac{\zeta}{k_B T}N_K \tag{3.28}$$

For times $t > \tau_e$ the primitive chain starts encountering obstacles and hence dynamics is no longer governed by modified Rouse dynamics beyond this time scale. For length scales longer than linear dimension of the obstacle, a, the response of the polymer chain to an applied stress is dictated by the cooperative motion of the primitive chain through reptation (see sections 3.3.2 and A.3).

The stress in the system at any point of time is proportional to the orientation memory of the chain and the density of oriented chains. The orientation memory for the primitive chain is expressed in terms of the tangent vector correlations along the primitive chain. The density of the primitive chains in the system is given by $c_{Pb}/N^{1/2}$, where, $c_{Pb} = c_P/N_e$ is the concentration of blobs along the trunk of the Cayley tree ring and c_P is the concentration of Kuhn segments along the trunk. The product of the density of the oriented primitive chains in the system and the orientation memory yields the microscopic expression for the stress tensor given by:

$$\sigma_{\alpha\beta} = \frac{c_{Pb}}{N^{1/2}}k_{eff}\int_0^{N^{1/2}} dn \left\langle \frac{\partial R_{n\alpha}}{\partial n}\frac{\partial R_{n\beta}}{\partial n}\right\rangle \tag{3.29}$$

The stress response of the system has to be obtained in two steps because of the distinct dynamics scenario at different length scales. For time scales $t < \tau_e$ the stress response is obtained from modified Rouse dynamics and for $t > \tau_e$ the reptation picture is invoked. For the case $t < \tau_e$, we may use normal coordinates to simplify equation (3.29) and obtain:

$$\sigma_{\alpha\beta} = \frac{c_{Pb}}{N^{1/2}}\sum_p k_p \left\langle X_{p\alpha}X_{p\beta}\right\rangle \tag{3.30}$$

We now impose a homogeneous deformation gradient $\bar{v}(\mathbf{r},t) = \bar{\bar{\kappa}}(t).\mathbf{r}$. Under such a deformation the Langevin equation for the p^{th} normal coordinate, $\mathbf{X}_p$, becomes:

$$\frac{\partial \mathbf{X}_p}{\partial t} = -\frac{k_p}{\zeta_p}\mathbf{X}_p + \frac{1}{\zeta_p}\mathbf{f_p} + \bar{\bar{\kappa}}(t).\mathbf{X}_p \tag{3.31}$$

From the Langevin equation (3.31) we obtain the equation for the correlation $\langle X_{p\alpha}X_{p\beta}\rangle$ as:

$$\frac{\partial}{\partial t}\left\langle X_{p\alpha}X_{p\beta}\right\rangle = -2\frac{k_p}{\zeta_p}\left\langle X_{p\alpha}X_{p\beta}\right\rangle + 4\frac{k_B T}{\zeta_p}\delta_{\alpha\beta} + \kappa_{\alpha\mu}\left\langle X_{p\mu}X_{p\beta}\right\rangle + \kappa_{\beta\mu}\left\langle X_{p\alpha}X_{p\mu}\right\rangle \tag{3.32}$$

Equation (3.32) can be solved to obtain $\langle X_{p\alpha} X_{p\beta} \rangle$ for any given homogeneous deformation gradient. For homogeneous shear where $\bar{\bar{\kappa}}(t)$ is given by:

$$\begin{bmatrix} 0 & \kappa(t) & 0 \\ 0 & 0 & 0 \\ 0 & 0 & 0 \end{bmatrix}$$

we have the equation for the xy component of the correlation given by:

$$\frac{\partial}{\partial t} \langle X_{px} X_{py} \rangle = -2 \frac{k_p}{\zeta_p} \langle X_{px} X_{py} \rangle + \kappa(t) \left\langle X_{py}^2 \right\rangle \tag{3.33}$$

Considering that under the imposed deformation the chain conformation remains close to its equilibrium conformation, we have $\left\langle X_{py}^2 \right\rangle = k_B T / k_p$, using which the solution to equation (3.33) is obtained as:

$$\langle X_{px} X_{py} \rangle = \frac{k_B T}{k_p} \int_{-\infty}^{t} dt_1 \exp\left(-2 \frac{(t - t_1)}{\tau_p} \right) \kappa(t_1) \tag{3.34}$$

Substituting equation (3.34) in equation (3.30) we obtain:

$$\sigma_{xy} = \frac{c_{Pb}}{N^{1/2}} k_B T \sum_p \int_{-\infty}^{t} dt_1 \exp\left(-2 \frac{(t - t_1)}{\tau_p} \right) \kappa(t_1) \tag{3.35}$$

The phenomenological expression for stress tensor in terms of the relaxation modulus is given by:

$$\sigma_{xy}(t) = \int_{-\infty}^{t} dt_1 G(t - t_1) \kappa(t_1) \tag{3.36}$$

Comparing equation (3.35) with equation (3.36) we obtain:

$$G(t) = \frac{c_{Pb}}{N^{1/2}} k_B T \sum_p \exp\left(-2 \frac{t}{\tau_p} \right) \tag{3.37}$$

For the case $t > \tau_e$ the reptation picture is invoked wherein the stress memory in the system at any time corresponds to the fraction of the chain in the original tube at that time (see Appendix section (A.3)). From the reptation formulation the fraction of chain in a given tube, $\psi(t)$, and the associated relaxation modulus, $G(t)$, are given by (Doi and Edwards, 1986):

$$\psi(t) = \frac{8}{\pi^2} \sum_{p(odd)} \frac{1}{p^2} \exp\left(-p^2 \frac{t}{\tau_d} \right) \tag{3.38}$$

$$G(t) = G^0 \psi(t) \tag{3.39}$$

At time $t = \tau_e$ the modified Rouse dynamics expression (3.37) gives the relaxation modulus $G(\tau_e)$:

$$G(\tau_e) = \frac{c_{Pb}}{N^{1/2}} k_B T \sum_p \exp\left(-2\frac{\tau_e}{\tau_p}\right) \tag{3.40}$$

Moving from a discrete to continuous representation in terms of p we have:

$$G(\tau_e) = \frac{c_{Pb}}{N^{1/2}} k_B T \int_0^\infty dp \ \exp\left(-2\frac{\tau_e}{\tau_p}\right) \tag{3.41}$$

Evaluation of the integral in expression (3.40) using expression (3.14) for the relaxation spectrum yields:

$$G(\tau_e) = \frac{c_{Pb}}{\sqrt{2}\pi} k_B T = \frac{c_P}{N_e\sqrt{2}\pi} k_B T \tag{3.42}$$

From reptation dynamics expression (3.39) the relaxation modulus at time $t = \tau_e$ is given by $G(\tau_e) = G^0\psi(\tau_e)$. For large N we can see from equations (3.21) and (3.28), that the time scale $\tau_e << \tau_d$, which makes it reasonable to assume that $\psi(\tau_e) = 1$. By comparison of $G(\tau_e)$ from modified Rouse dynamics and reptation we determine the value of the constant G^0 as given in equation (3.43). Then the expression for relaxation modulus for time $t \geqq \tau_e$ is given by equation (3.44):

$$G^0 = \frac{c_P}{\sqrt{2}\pi} k_B T \frac{b^2}{a^2} \tag{3.43}$$

$$G(t) = \frac{4\sqrt{2}}{\pi^3} c_P k_B T \frac{b^2}{a^2} \sum_{p(odd)} \frac{1}{p^2} \exp\left(-p^2\frac{t}{\tau_d}\right) \tag{3.44}$$

where, we have used $N_e = a^2/b^2$.

In the case of linear polymers a similar derivation of constitutive relation has been done based on the Rouse and reptation dynamics by Doi and Edwards (1986). The final expression for constant G^0 and the relaxation modulus $G(t)$ are given by:

$$G^0 = c k_B T \frac{b^2}{a^2} \tag{3.45}$$

$$G(t) = \frac{8}{\pi^2} c k_B T \frac{b^2}{a^2} \sum_{p(odd)} \frac{1}{p^2} \exp\left(-p^2\frac{t}{\tau_d}\right) \tag{3.46}$$

In the linear chain expressions (3.45) and (3.46) the prefactor $1/\sqrt{2}\pi$ which naturally arises in the derivation of G^0 is uniformly dropped. If the prefactor $1/\sqrt{2}\pi$ is similarly dropped in expressions (3.43) and (3.44) for ring chain we obtain:

$$G^0 = c_P k_B T \frac{b^2}{a^2} \tag{3.47}$$

$$G(t) = \frac{8}{\pi^2} c_P k_B T \frac{b^2}{a^2} \sum_{p(odd)} \frac{1}{p^2} \exp\left(-p^2\frac{t}{\tau_d}\right) \tag{3.48}$$

In our calculations we drop the prefactor $1/\sqrt{2}\pi$ for ring chains in order to be consistent with the Doi and Edwards (1986) formulation for linear chains.

3.6 Melt of Ring Polymers

The analysis for the fixed array of obstacles worked out in the previous sections can be extended to the scenario of melt of ring polymers. The extension of the analysis is achieved on the basis of the assumption that the structure of a ring chain in its melt can be described as consisting of a longest characteristic length scale (the primitive chain) having fast relaxing friction-contributing loops attached to it. Based on scaling arguments and computer simulations (Cates and Deutsch, 1986; Müller *et al.*, 1996, 2000) the size of the ring chain in melt, R, is determined to be of order $\sim N^{\nu}$, where ν can lie between the extremes of $1/4$ and $1/2$ (see section 2.1.2). The primitive chain and the modified Rouse chain of the PPR framework can be appropriately modified with the change in static structure. In the case of rings in a melt environment since $R \sim N^{\nu}a$, where ν can lie between $1/4$ and $1/2$, the characteristic length scale, *i.e*, the length of the primitive path is expected to be of order $N^{2\nu}a$. Considering that there are N_e Kuhn segments associated with the length scale a and the chain obeys Gaussian statistics at this length scale we have $N_e = a^2/b^2$. The length of the primary trunk is given by:

$$L_P = N^{2\nu}a = \left(\frac{N_K}{N_e}\right)^{2\nu} a = N_K^{2\nu}\frac{b^{4\nu}}{a^{4\nu-1}} \tag{3.49}$$

The number of loops along the primary trunk is of order $N^{2\nu}$ as it is expected to be proportional to the length of the primary trunk. Considering the mass of the ring chain to be entirely contained in the loops an average loop would be composed of $\sim N/N^{2\nu} = N^{1-2\nu}$ blobs.

We formulate a modified primitive chain for the ring polymer in a melt as follows:

1. The primitive chain is constituted by the primary trunk of the lattice tree composed of $N^{2\nu}$ blobs with a constant contour length, L_P, given by expression (3.49).

2. Each segment of the primitive chain has attached to it a loop. On an average each loop contains $N^{1-2\nu}$ blobs. We assume that the loops are unentangled because of their collapsed conformation.

3. The primitive chain is entangled and can move along itself with a curvilinear diffusion coefficient determined from dynamics of a modified Rouse chain.

4. The primitive chain has the conformation of a random walk *i.e.* the tangents at different points along the trunk are uncorrelated.

It can be shown that the modified primitive chain has a curvilinear diffusion coefficient given by (see Appendix A.2):

$$D_P = \frac{k_B T}{N^{2-2\nu}\zeta_{blob}} = \left(\frac{a}{b}\right)^{2(1-2\nu)} \frac{k_B T}{N_K^{2-2\nu}\zeta} \tag{3.50}$$

while the relaxation spectrum of the modified Rouse chain remains the same as given by expression (3.14). We use the curvilinear diffusion coefficient of the PPR primitive chain given by equation (3.50) to determine the longest relaxation time of the ring polymer in a melt as (see Appendix A.3):

$$\tau_d = \frac{1}{\pi^2}\frac{a^4}{b^2}\frac{\zeta}{k_B T}N^{2\nu+2} = \frac{1}{\pi^2}\frac{b^{4\nu+1}}{a^{4\nu}}\frac{\zeta}{k_B T}N_K^{2\nu+2} \tag{3.51}$$

The self-diffusion coefficient of the primitive chain remains the same as given by expression (3.20).

Note: In case of the excluded volume ring in an array of fixed obstacles since $R \sim N^{1/2}$ (Cates and Deutsch, 1986) the trunk is expected to be composed of N blobs. The excluded volume ring formulation can be thought of as a trunk composed of N loops each containing one blob. Equation (A.11) of Appendix A.2 shows that for this case indeed $\zeta_{loop} = \zeta_{blob}$. The structure of the excluded volume ring is expected to be similar to that of the non-obstacle-enclosing non-ramified structure of a ring hypothesized by Klein (1986) (Figure 2.4). For this structure we would expect dynamic scalings similar to that of linear chains because the structure is like that of a double folded ring and the dynamics is expected to be like that of reptation of a double folded linear chain (Klein, 1986). Monte Carlo simulations by Cates and Deutsch (1986) confirms that dynamic scalings for excluded volume rings in a fixed array of obstacles is similar to that of linear chains.

In melt the linear dimension a of the obstacle corresponds to the entanglement length scale and is determined from the entanglement molecular weight; an experimentally obtained parameter in the tube model. The entanglement molecular weight is obtained from the plateau modulus, G^0, data and for linear polymers can be calculated using the expression of form (Fetters *et al.*, 2006):

$$M_e = \frac{\rho_m N_A k_B T}{G^0} \tag{3.52}$$

From entanglement molecular weight the average number of Kuhn segments present between entanglements, N_e, can be calculated. The primitive chain formulation intrinsically assumes

and requires a Gaussian structure between entanglements according to which $a^2 = N_e b^2$. As long as N_e remains the same for ring polymers and linear polymers the entanglement spacing a for them remains the same.

If we consider, c_{Pb}, the concentration of number of blobs lying along the trunk of the ring chain then the number of trunks per unit volume in the melt is $c_P/(N^{2\nu})$ since the trunk contains $N^{2\nu}$ blobs. The number of rings per unit volume is given by the concentration of number of blobs per unit volume divided by the number of blobs per ring, c_b/N. Considering that the number of trunks should be the same as number of rings we equate the number of trunks and number of ring chains:

$$\begin{aligned} \frac{c_{Pb}}{N^{2\nu}} &= \frac{c_b}{N} = \frac{c}{N_e N} \\ \frac{c_P}{N_e} &= \frac{c_b}{N^{1-2\nu}} = \frac{c}{N_K^{1-2\nu}} \left(\frac{b}{a}\right)^{4\nu} \end{aligned} \tag{3.53}$$

where, c is the concentration of Kuhn segments in the chain. Substituting for c_P in equation (3.48) we obtain:

$$\begin{aligned} G(t) &= \frac{8}{\pi^2} \frac{c}{N^{1-2\nu}} k_B T \frac{b^2}{a^2} \sum_{p(odd)} \frac{1}{p^2} \exp\left(-p^2 \frac{t}{\tau_d}\right) \\ &= \frac{8}{\pi^2} \frac{c}{N_K^{1-2\nu}} k_B T \frac{b^{4\nu}}{a^{4\nu}} \sum_{p(odd)} \frac{1}{p^2} \exp\left(-p^2 \frac{t}{\tau_d}\right) \end{aligned} \tag{3.54}$$

It is clear from the above expression that the density is diluted by a factor of order $1/N^{1-2\nu}$ when we consider only density of blobs along the trunk of the ring chain. Thus we expect the viscoelastic response of the ring melt to be smaller than the response of linear melt by a factor of order $1/N^{1-2\nu}$.

The zero shear viscosity (ZSV) is proportional to the product of the relaxation time and the value of modulus at the relaxation time (Rubinstein and Colby, 2003). Based on the Doi and Edwards (1986) formulation the ZSV is then given by:

$$\eta_0 \approx G^0 \tau_d \tag{3.55}$$

(ZSV) measurements on polybutadiene rings of MW $6.0 \times 10^4 g/mol$ indicate that the ZSV of ring melt is approximately 10 times lower than that of the corresponding linear melt (Roovers, 1988). This lowering of viscosity can be shown to be caused by density dilution associated with the relaxation response of the ring chain. The ratio of ZSV of a ring melt to that of linear melt is given by:

$$\frac{\eta_{0r}}{\eta_{0l}} = \frac{G_r^0}{G_l^0} \frac{\tau_{dr}}{\tau_{dl}} \tag{3.56}$$

where subscripts r and l denote the values associated with the ring chain and the linear chain respectively.

The ratio G_r^0/G_l^0 can be obtained using expressions (3.47), (3.45) and (3.53) as:

$$\frac{G_r^0}{G_l^0} = \frac{1}{N_K^{1-2\nu}} b^{4\nu-2} \frac{a_l^2}{a_r^{4\nu}} \tag{3.57}$$

The relaxation time for linear chains is given by (Doi and Edwards, 1986):

$$\tau_{dl} = \frac{1}{\pi^2} \frac{b^4}{a_l^2} \frac{\zeta}{k_B T} N_K^3 \tag{3.58}$$

The ratio τ_{dr}/τ_{dl} is obtained using expressions (3.51) and (3.58) as:

$$\frac{\tau_{dr}}{\tau_{dl}} = \frac{1}{N_K^{1-2\nu}} b^{4\nu-2} \frac{a_l^2}{a_r^{4\nu}} \tag{3.59}$$

Thus for large N_K, given $\nu < 1/2$, we have $\tau_{dr} < \tau_{dl}$. Using expressions (3.57) and (3.59) in equation (3.56) the ZSV ratio between melt of ring and melt of linear is given by:

$$\frac{\eta_{0r}}{\eta_{0l}} = \frac{1}{N_K^{2(1-2\nu)}} b^{8\nu-4} \frac{a_l^4}{a_r^{8\nu}} \tag{3.60}$$

We have already seen that beyond the time τ_e the primitive chain starts encountering obstacles and the entanglement dynamics of the chain has to start beyond this time scale. In the absence of obstacles the chain would relax through Rouse dynamics and the longest relaxation time of the chain would be given by τ_1. The ratio τ_1/τ_e can be considered as a measure of the strength of confinement of the chain. Using the expressions (A.19) and (A.42) in the Appendix we obtain the ratio as:

$$\frac{\tau_1}{\tau_e} = \frac{4}{\pi^3} \frac{b^{8\nu}}{a^{8\nu}} N_K^{4\nu} \tag{3.61}$$

According to the expression (3.61) the ratio τ_1/τ_e for $\nu < 1/2$ scales weakly as $N_K^{4\nu}$ in comparison to the scaling of N_K^2 for linear chains. This implies a weaker strength of confinement in a ring chain melt as compared to that of linear chain melt. Simulations of Müller *et al.* (1996) indicates an entanglement crossover in a dense system of ring chains at higher values of N_K as compared to a dense system of linear chains; a signature of weaker strength of confinement in a ring chain melt.

3.7 Contour Length Fluctuations

The first assumption in the PPR formulation is that the primitive chain has a constant contour length. In reality, the contour length of the primitive chain fluctuates with time, and the fluctuation sometimes plays an important role in various dynamical processes (Doi and Edwards,

1986). Contour length fluctuation (CLF) reduces the disengagement time (longest relaxation time) for the primitive chain from its tube of confinement and hence reduces the viscosity. Thus, we expect the theory based on the PPR formulation to over-predict relaxation time and viscosity. In the PPR formulation the longest relaxation time scaling, without CLF, is given by $\tau_d \sim \bar{L}_P^2/D_P$. The average contour length is $\bar{L}_P = N_K^{2\nu} b^{4\nu}/a^{4\nu-1}$ and the curvilinear diffusion coefficient is $D_P \sim N_K^{2\nu-2}$. This yields $\tau_d \sim N_K^{2\nu+2} b^{4\nu+2}/a^{4\nu}$ for the ring without CLF. Given that the trunk is a Gaussian chain made up of $N^{2\nu}N_e = N_K^{2\nu}N_e^{1-2\nu}$ Kuhn segments it can be shown that the average of fluctuation of the length of its contour is given by (Doi and Edwards, 1986):

$$\Delta\bar{L}_P = \frac{1}{\sqrt{3}} N_K^{2\nu} \frac{b^{2\nu}}{a^{2\nu-1}} \tag{3.62}$$

The relaxation time is reduced by CLF corrections and is given by (Doi and Edwards, 1986):

$$\begin{aligned} \tau_d^{CLF} &\simeq \frac{(\bar{L}_P - \Delta\bar{L}_P)^2}{D_P} \\ \tau_d^{CLF} &\simeq \left(\frac{N_K^{2\nu+2} b^{4\nu+2}}{a^{4\nu}} - \frac{2}{\sqrt{3}} \frac{N_K^{\nu+2} b^{2\nu+2}}{a^{2\nu}} + \frac{N_K^2 b^2}{3} \right) \frac{\zeta}{k_B T} \end{aligned} \tag{3.63}$$

In equation (3.63) the first term corresponds to the scaling without CLF corrections the second and third terms correspond to corrections effected by CLF. It can be seen that CLF induced corrections are significant for finite N_K and with the increase in the value of N_K the corrections become less significant. Further, CLF introduced corrections are expected to be considerable in the case of more collapsed ring when the trunk has longer loops associated with it. For example, consider the comparison between the case of $\nu = 2/5$ and $\nu = 1/4$ we have:

$$\begin{aligned} \tau_d^{CLF} &\simeq \left(\frac{N_K^{14/5} b^4}{a^2} - \frac{2}{\sqrt{3}} \frac{N_K^{12/5} b^3}{a} + \frac{N_K^2 b^2}{3} \right) \frac{\zeta}{k_B T} \qquad \left(\nu = \frac{2}{5}\right) \\ \tau_d^{CLF} &\simeq \left(\frac{N_K^{5/2} b^{18/5}}{a^{8/5}} - \frac{2}{\sqrt{3}} \frac{N_K^{9/4} b^{14/5}}{a^{4/5}} + \frac{N_K^2 b^2}{3} \right) \frac{\zeta}{k_B T} \qquad \left(\nu = \frac{1}{4}\right) \end{aligned} \tag{3.64}$$

As the ring becomes more collapsed it can be seen that the exponent of N_K in the second term (correction term) approaches the exponent in the first term.

3.8 Results and Discussion

The PPR framework based expressions for the curvilinear diffusion coefficient, self-diffusion coefficient and longest relaxation time for an ideal ring in an array of fixed obstacles, are in good agreement with the DOR scaling (Obukhov *et al.*, 1994) (see Table 3.1). The framework

Quantity	Scaling (Obukhov *et al.*, 1994)	PPR
Curvilinear diffusion coefficient.	$\sim N^{-3/2}$	$D_P = \frac{k_B T}{\zeta} N_k^{-3/2}$
Self-diffusion coefficient.	$\sim N^{-2}$	$D = \frac{1}{3}\frac{k_B T}{\zeta}\frac{a^2}{b^2} N_K^{-2}$
Longest relaxation time	$\sim N^{5/2}$	$\tau_d = \frac{1}{\pi^2}\frac{b^3}{a}\frac{\zeta}{k_B T} N_K^{5/2}$

Table 3.1: Comparison between the DOR scaling and the expressions derived using the PPR framework.

is general in the sense that as long as the static structure of the ring can be described in terms of a longest characteristic length scale, *viz.*, the primary trunk, and collapsed loops attached to it, appropriate modifications can be incorporated into the framework in terms of the size of the trunk and the loops. The longer the trunk the larger would be the number of loops associated with it but the smaller would be the size of the loops.

The scaling relations of the dynamic quantities appropriately change with the change in static structure (Table 3.2). In general our interest in this chapter was restricted to studying the dynamics of the longest length scale of the ring structure. The primary trunk was modeled as a modified Rouse chain for which the fast relaxing loops associated with it contribute only to the friction of the trunk. The Rouse chain bead friction was modified to incorporate the extra friction contributed by the loops based on the pom-pom picture using Rouse dynamics for the relaxation of loops instead of arm retraction.

For an unentangled ring in its melt, the scaling exponent of the radius of gyration with molecular weight from th Cates and Deutsch (1986) conjecture is expected to be $\nu = 0.4$. In this case the diffusion coefficient derived from the modified Rouse dynamics scales as $D \sim N^{-1.2}$ (see Table 3.2) and the Rouse relaxation time scales as $\sim N^2$. This appears to be in agreement with recent simulation studies on unentangled rings in melt (Müller *et al.*, 2000; Hur *et al.*, 2006). Note that for a swollen ring chain for which $R \sim N^{1/2}$, we recover the linear-like scaling for the various parameters in Table 3.2.

We find that the theoretical predictions of plateau modulus, relaxation times and ZSV by the PPR framework vary sharply with exponent ν (Table 3.3). Since there is some uncertainty

Quantity	Scaling from PPR
Number of trunk segments	$N_K^{2\nu}$
Number of loop segments	$N_K^{1-2\nu}$
Rouse bead friction/τ_e	$N_K^{2(1-2\nu)}$
Curvilinear diffusion coefficient	$N_K^{2\nu-2}$
Self diffusion coefficient	N_K^{-2}
Longest relaxation time	$N_K^{2\nu+2}$
Plateau modulus	$N_K^{2\nu-1}$
Viscosity	$N_K^{4\nu-2}$

Table 3.2: Scaling relationships for a ring with its $R_g \sim N^\nu$

regarding the exact value of ν for a melt of rings, we have attempted to compare the PPR predictions of linear viscoelastic variables with experimental data for various values of ν. In particular, we have chosen the rheological data of Roovers (1988) on polybutadiene (PBD) polymers. We specifically utilized the data of two samples: a linear PBD (sample KPBD34PC, $MW = 5.7 \times 10^4 g/mol$, $\eta_0 = 6.7 \times 10^5 P$) and a ring PBD (sample KPBD34B3, $MW = 6.0 \times 10^4 g/mol$, $\eta_0 = 6.3 \times 10^4 P$). This particular ring sample was free of linear contaminant that could potentially have substantially altered the rheology of ring melts (Roovers, 1988). The linear and the ring PBDs have similar molecular weight and polydispersity, however, the ZSV and the plateau modulus of the ring sample were lower than those for the linear sample (Roovers, 1988).

In order to compare PPR theory predictions with experimental data we need parameters concerning chain dimensions and entanglement spacing for PBD. The molecular parameters $a \approx 44.5$Å, $b \approx 11.3$Å, $M_0 = 175.9$ were obtained from Fetters *et al.* (1996) for the PBD-62 sample (see also Table II of Fetters *et al.* (2006)). This linear PBD contains 62% 1, 2 microstructure which is similar to the 63% 1, 2 microstructure in Roovers PBD sample. We obtained the concentration (c) of Kuhn segments per unit volume in the melt by using ($c = \rho_m N_A / M_0$) where ρ_m is the melt density tabulated for PBD-62 (Fetters *et al.*, 2006) and N_A is the Avogadro number. The ring is expected to have a collapsed structure as compared to the linear chain in a melt of rings (Müller *et al.*, 2000, 1996; Cates and Deutsch, 1986), which implies $\nu \leq 1/2$.

Quantity	Experiments	PPR $a_r = a_l$	PPR $a_r = 0.7a_l$
		($\nu = 0.25$)	($\nu = 0.25$)
Ratio of plateau modulus $\left(\frac{G^0_{Nr}}{G^0_{Nl}}\right)$	0.15	0.21	0.3
Ratio of relaxation times $\left(\frac{\tau_{dr}}{\tau_{dl}}\right)$	0.63	0.21	0.3
Ratio of ZSV $\left(\frac{\eta_{0r}}{\eta_{0l}}\right)$	0.094	0.044	0.09
		($\nu = 0.33$)	($\nu = 0.33$)
Ratio of plateau modulus $\left(\frac{G^0_{Nr}}{G^0_{Nl}}\right)$	0.15	0.33	0.53
Ratio of relaxation times $\left(\frac{\tau_{dr}}{\tau_{dl}}\right)$	0.63	0.33	0.53
Ratio of ZSV $\left(\frac{\eta_{0r}}{\eta_{0l}}\right)$	0.094	0.11	0.53
		($\nu = 0.4$)	($\nu = 0.4$)
Ratio of plateau modulus $\left(\frac{G^0_{Nr}}{G^0_{Nl}}\right)$	0.15	0.54	0.95
Ratio of relaxation times $\left(\frac{\tau_{dr}}{\tau_{dl}}\right)$	0.63	0.54	0.95
Ratio of ZSV $\left(\frac{\eta_{0r}}{\eta_{0l}}\right)$	0.094	0.29	0.9

Table 3.3: Comparison between PPR formulation based ratios for different ν and scenarios (a) $a_r = a_l$ (b) $a_r = 0.7a_l$ with ratios from Roovers (1988) PBD experiments.

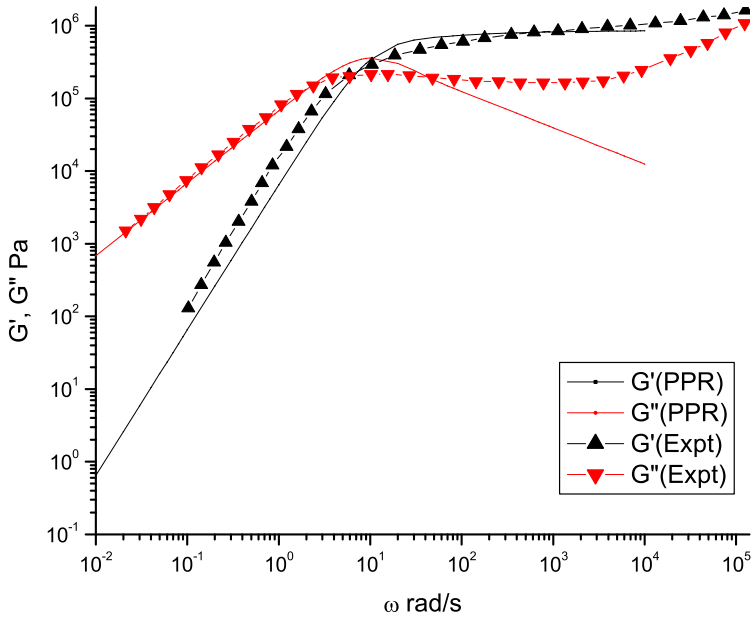

Figure 3.3: Fit of DE theory to linear PBD sample KPBD34PC (Roovers, 1988)

Also, experiments on plasmid DNA indicate that the tube size associated with the ring chain is smaller than that of linear chain (Robertson and Smith, 2007a). This leads us to consider two distinct scenarios for prediction of viscoelastic response of rings – (a) the entanglement spacing $a_r < a_l$ and (b) the entanglement spacing same as that of linear polymers $a_r = a_l$. In addition to parameters concerning chain dimension and entanglement spacing we need friction coefficient, ζ, of the Rouse bead. This was obtained by fitting the predictions of Doi and Edwards (1986) theory to experimental data of Roovers (1988) linear sample KPBD34PC for the viscosity (see Fig. 3.3). The bead friction coefficient $\zeta = 1.4 \times 10^{-9} Nsm^{-1}$ obtained from the fit was used in PPR framework based calculations for ring PBD. It is seen that the crossover predictions for linear chains is approximately twice that of experiment with this friction coefficient. Thus, the longest relaxation time (taken as the inverse of the crossover frequency in the experimental data) is under-predicted an indication that the friction value obtained may be lower than the actual value.

We find that the predictions of the ZSV ratios are in close agreement with the experimental data for $\nu = 0.25$ for modified entanglement spacing scenario and $\nu = 0.33$ without modification of entanglement spacing. The experimental ring-linear ratios of the plateau mod-

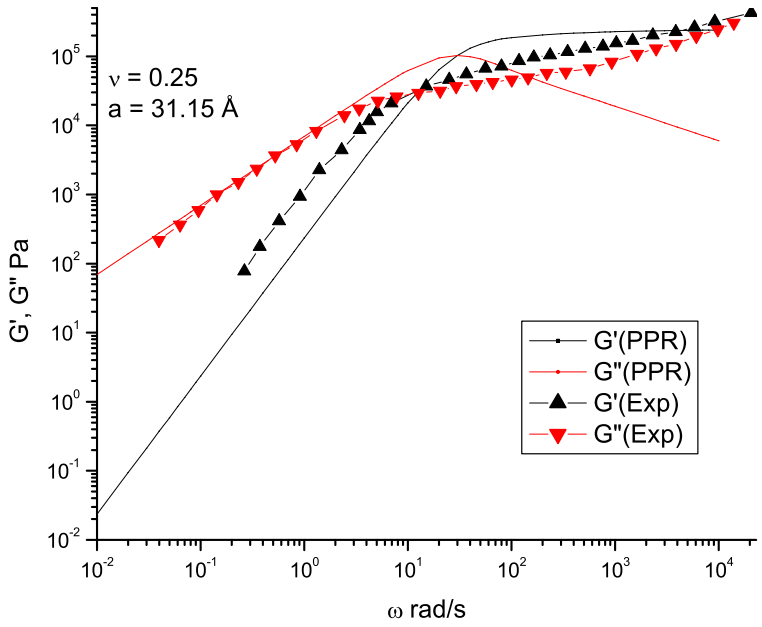

Figure 3.4: Comparison of PPR formulation based viscoelastic response predictions ($\nu = 0.25$ and $a = 31.15$Å) to ring PBD sample KPBD34B3 (Roovers, 1988)

ulus are overpredicted by the PPR model predictions. It is seen that the crossover predictions for ring chains is approximately thrice that of experiment with the friction coefficient obtained from Doi and Edwards (1986) theory. The longest relaxation time (taken as the inverse of the crossover frequency in the experimental data) is under-predicted similar to the case of linear chain predictions using the Doi and Edwards (1986) model. Figure 3.4 and Figure 3.5 show the comparison between the experimental frequency data and the PPR predictions for the two scenarios, modified entanglement spacing ($\nu = 0.25$) and without modification of entanglement spacing ($\nu = 0.33$), respectively. The predictions of the PPR model in the terminal regime are encouragingly close to the experimental data for both cases.The PPR model predictions are seen to increase with decrease in a as shown in Figure 3.6 for $\nu = 0.33$ and $a = 31.15$Å. The PPR model predictions are seen to increase with increase in ν as shown in Figure 3.7 for $\nu = 0.4$ and $a = 44.5$Å. The PPR model predictions are expected to approach linear chain predictions for $\nu = 1/2$ and $a = 44.5$Å.

We have compared our predictions with only one experimental rheological data set of Roovers (1988) that is believed to be obtained for a melt of pure rings having no linear con-

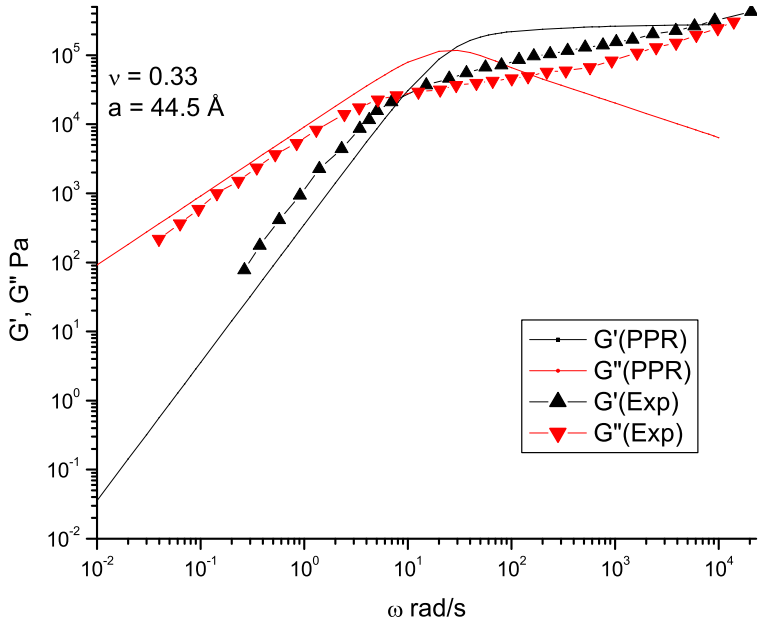

Figure 3.5: Comparison of PPR formulation based viscoelastic response predictions ($\nu = 0.33$ and $a = 44.5$Å) to ring PBD sample KPBD34B3 (Roovers, 1988)

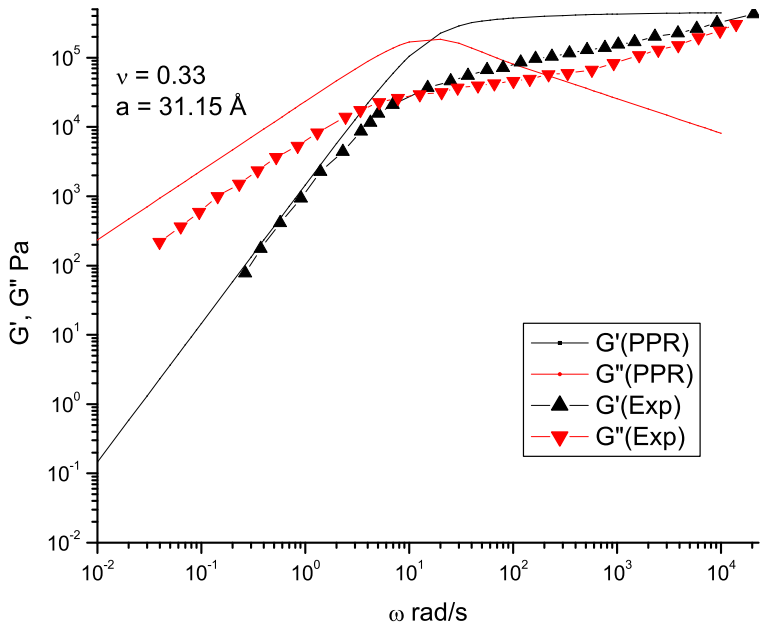

Figure 3.6: Comparison of PPR formulation based viscoelastic response predictions ($\nu = 0.33$ and $a = 31.15$Å) to ring PBD sample KPBD34B3 (Roovers, 1988)

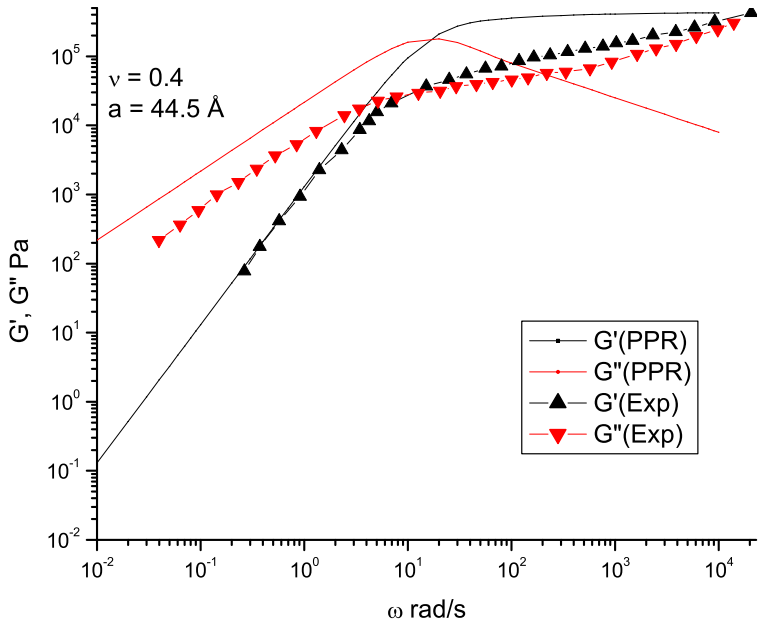

Figure 3.7: Comparison of PPR formulation based viscoelastic response predictions ($\nu = 0.4$ and $a = 44.5$Å) to ring PBD sample KPBD34B3 (Roovers, 1988)

taminants that could otherwise dramatically affect the rheological behavior. The comparison indicates that depending on the scenario adopted, with respect to the modification of entanglement spacing, the PPR framework gives reasonable predictions of the ZSV ratio and frequency sweep experimental data but for different values of the static scaling exponent ν. The use of Cates and Deutsch (1986) conjecture, supported by the results of early simulations by Müller *et al.* (1996), exponent $\nu = 2/5$ over-predicts the viscoelastic response. In a more recent work of Müller *et al.* (2000) it is argued that use of a general exponent ν lying between $1/4$ and $1/2$ is more appropriate. Such a general exponent ν will be compatible with both the scenarios.

In the PPR framework the chain is considered to remain a Gaussian at the length scale of entanglement. This requires that the number of Kuhn segments between entanglements N_e for rings decreases with decrease in entanglement spacing a_r. Experiments on DNA indicate that the a_r for ring macromolecule are smaller than that of the linear (Robertson and Smith, 2007a). This implies N_e is smaller for the ring chain and hence there are more entanglements for a ring chain than a linear chain with the same degree of polymerization. There is an apparent contradiction that although the ring chain takes a collapsed structure it has more entanglements

than that of a linear chain. For the ring chain in the melt this anomaly can be understood in light of the Müller *et al.* (2000) simulations on the influence of length of rings on its structure which indicate that long rings are in fact both compact and at the same time have more neighbors in their correlation hole resulting in a tightly double folded Cayley tree structure.

The Cayley tree structure of a ring is a fractal self-similar structure and it is expected to have self-similar dynamics at all length scales. However, in the PPR formulation we consistently consider hierarchical relaxation and break down the dynamics to fast relaxing loops and slow relaxing trunk. The loops intrinsically are considered to be unentangled and consequently relaxing through Rouse dynamics while the trunk waits till the loops relax before relaxing via a 1-D diffusional motion. Invoking such a hierarchical relaxation mechanism does not address the simultaneous relaxation of all the substructures and consequently the PPR formulation does not predict dynamic self-similarity. Thus, the predictions of dynamics obtained from this formulation are valid only in the terminal regime of a ring chain which has an entangled primary trunk and unentangled loops as is the case of Roovers (1988) PBD sample. It is observed that the Roovers (1988) PBD sample and in the more recent experiments on PS by Kapnistos *et al.* (2008) there is an absence of plateau modulus and there is a power-law dependence of relaxation modulus which can be considered as a signature of dynamic self-similarity. The PPR framework is inadequate to predict the power-law dependence of the visoelastic response in the intermediate frequency regime.

Chapter 4

Blob-Spring Model: Fluctuations Approach to Ring Dynamics

4.1 DOR Scaling: Fluctuation Interpretation

In chapter 3 section 3.1 we discussed the DOR scaling (Obukhov *et al.*, 1994) and used the reptation interpretation of the scaling arguments to build the PPR framework. An alternative fluctuation interpretation of the DOR scaling arguments is presented in this section. In the DOR scaling the authors proposed that the perpetual evolution of perimeter through motion of kinks drives the dynamics of a ring. The Cayley tree-like structure of the ring polymer in the array of obstacles was broken down into trunk, branch and leaf substructures. It was argued that kink rearrangements in the branches and leaves occur much more rapidly than fluctuations kink rearrangements along the trunk and the long time dynamics of the ring polymer was considered to be governed by slow relaxation of the trunk. Thus in the DOR model, dynamical parameters for a ring are estimated from examining the kink rearrangements in the Cayley-tree structure.

In the fluctuation interpretation of DOR scaling arguments we consider such rearrangements of the kinks as corresponding to fluctuations of the Cayley tree polymeric fractal. Thus, the perpetual evolution of the perimeter of the polymeric fractal happens through fluctuations of the fractal object and causes the diffusion of the ring chain. The fluctuations in the leaves and branches can be considered to be dissipative and non-contributing to the center of mass motion. The fluctuations of the trunk of the ring chain can be considered to govern the long time dynamics and center of mass diffusion of the ring chain. In order to work out the consequences of fluctuations of the Cayley tree polymeric fractal it is illustrative to start with a brief idea of

fluctuations in the Gaussian chain model.

The Gaussian chain model of a polymer is known to be a fractal object, *i.e.*, it exhibits statistical-similarity of structure at different length scales. In structure-property relationships, from a reductionist viewpoint, we consider the structure of the object as governing its dynamic response. Based on this viewpoint the self-similarity of structure implies self-similarity of dynamics. In the case of the Gaussian chain it is known to have a fractal dimensionality $d_f = 2$ (see section 2.2.3). The Gaussian chain is often represented by a mechanical model of beads connected by harmonic springs. The fluctuation dynamics of such a bead-spring chain without hydrodynamic interactions is explored through the Rouse (1953) formulation. The relaxation spectrum in the Rouse formulation is given by (Doi and Edwards, 1986):

$$\tau_p = \frac{1}{3}\frac{b^2}{\pi^2}\frac{\zeta}{k_B T}\left(\frac{N_K}{p}\right)^2 \tag{4.1}$$

where, the relaxation time τ_p corresponds to the relaxation of the N_K/p section of the chain. The relaxation time of any such section of the chain according to expression (4.1) is seen to scale as the square of the number of segments in the section $(N_K/p)^2$. This is indicative of the dynamic self-similarity of the Gaussian chain at different length scales.

The effect of the dynamic self-similarity on the viscoelastic response of the Gaussian chain can be understood based on the scaling arguments of Rubinstein and Colby (2003). According to this argument the Gaussian chain is considered to relax through $p = 1, 2, ...$ independent relaxation modes; the p^{th} mode corresponds to relaxation of N/p blobs and has a relaxation time given by $\tau_p \sim \tau_0(N/p)^2$. A simple rearrangement of the relaxation time scaling yields:

$$\frac{p}{N} \sim \left(\frac{\tau_0}{\tau_p}\right)^{1/2} \tag{4.2}$$

The stress relaxation modulus at time τ_p is expected to be proportional the number density of stress storing structures, $(c_b/N)p$, and to the thermal energy, $k_B T$,:

$$G(\tau_p) \sim \frac{c_b}{N} p\, k_B T \tag{4.3}$$

The substitution for p/N from expression (4.2) into equation (4.3) gives $G(\tau_p) \sim (\tau_0/\tau_p)^{1/2}$. This suggests that for any time $t < \tau_1$ the relaxation modulus would scale as $G(t) \sim t^{-1/2}$. Including the exponential decay term representing the stress decay due to relaxation above the time scale $t > \tau_1$, we obtain:

$$G(t) \sim c_b\, k_B T \left(\frac{\tau_0}{t}\right)^{1/2} \exp\left(-\frac{t}{\tau_1}\right) \tag{4.4}$$

The relaxation modulus expression (4.4) suggests that a power law decay of stress is expected at time scales $t < \tau_1$ for a system composed of Gaussian chains.

The Cayley tree structure of the ring chain, in an array of fixed obstacles, is a fractal structure with fractal dimensionality $d_f = 4$. Analogous to the Gaussian chain the self-similarity of the Cayley tree ring chain structure implies self-similarity of dynamics at different length scales. According to the DOR scaling longest relaxation time of the ring chain in an array of fixed obstacles is given by $\tau_N \sim N^{5/2}$. Dynamics self-similarity implies any section of the chain composed of n segments has a longest relaxation time given by $\tau_n \sim n^{5/2}$. Simulations by Obukhov *et al.* (1994) show that the mean square length of chain that has passed through a pore in an array of obstacles at any given time t is given by $\langle l^2 \rangle \sim t^{4/5}$ – a result indicating dynamic self-similarity. Scaling arguments analogous to that presented for the relaxation modulus of system of Gaussian chains is expected to yield a power law decay of stress for $t < \tau_N$ for a system composed of Cayley tree ring chains (see section 2.2.2). We show in this chapter that based on the Blob-Spring (BS) framework a relaxation modulus with a power law decay of stress at times $t < \tau_N$ and exponential decay of stress for long times can be obtained. In the following section we develop the BS framework for the dynamics of a Cayley tree ring based on the fluctuation iterpretation of DOR scaling.

4.2 Blob-Spring Model

We start by proposing that the $N = N_K/N_e$ blobs of a ring polymer are connected to each other on a fractal polymeric skeleton by springs as shown schematically in Figure 4.1. The springs are considered to be Gaussian and the spring constant associated with the springs between blobs is $k = 3k_BT/a^2$. The skeleton has a fractal dimensionality $d_f = 4$, when $R \approx N^{1/4}$. The dynamics of the skeleton can be modeled using the theory developed by Muthukumar (1985) for unentangled fractal polymers (branched polymers). According to the theory the generalized Rouse equation for a fractal polymer can be written as (see section 2.2.3):

$$\zeta^p_{eff} \frac{\partial \mathbf{R_n}}{\partial t} = k \nabla_s^2 \mathbf{R_n} + \mathbf{f_n} \tag{4.5}$$

where, ∇_s^2 denotes the generalized Laplacian in the spectral dimension.

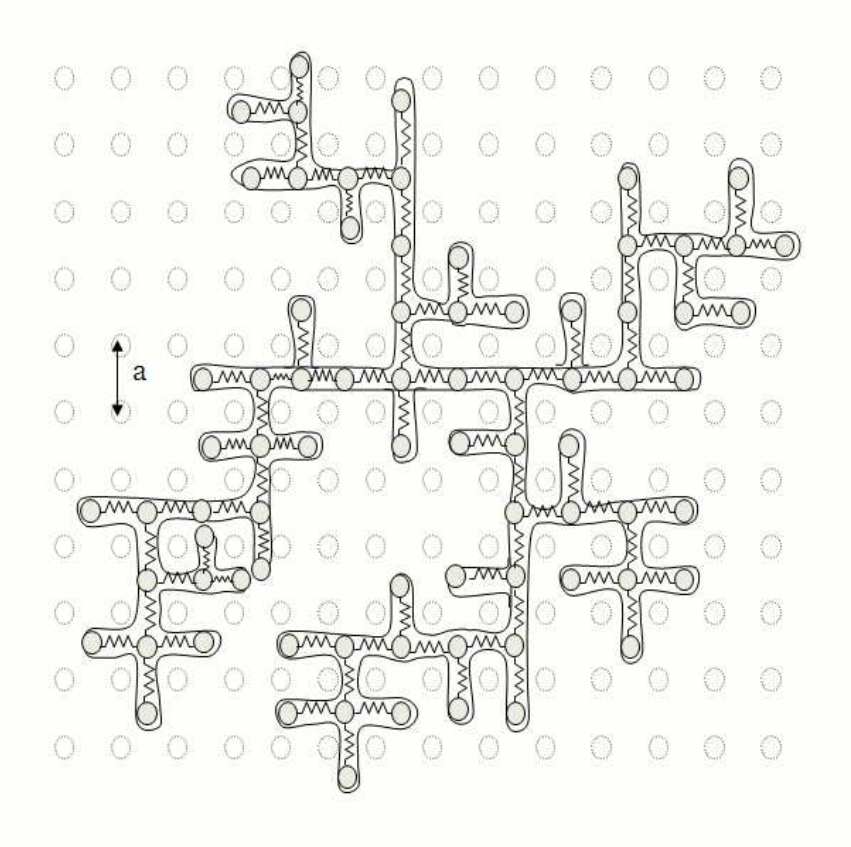

Figure 4.1: Schematic of Blob-Spring represenation for a flxible ring polymer in an array of fixed obstacles

If the normal coordinates are defined in the spectral dimension by:

$$\mathbf{R_n} = \mathbf{X_0} + 2\sum_{p_s} \mathbf{X_p} \cos\left(\frac{p_s \pi n}{N}\right) \tag{4.6}$$

$$\mathbf{f_n} = \frac{\mathbf{f_0}}{N} + \frac{1}{N}\sum_{p_s} \mathbf{f_p} \cos\left(\frac{p_s \pi n}{N}\right) \tag{4.7}$$

$$\mathbf{X_p} = \frac{1}{N}\int_0^N dn \cos\left(\frac{p_s \pi n}{N}\right)\mathbf{R_n} \tag{4.8}$$

$$\mathbf{f_p} = 2\int_0^N dn \cos\left(\frac{p_s \pi n}{N}\right)\mathbf{f_n} \tag{4.9}$$

then the Langevin equation in the conjugate space for the fractal polymer is given by:

$$\zeta_0 \frac{d\mathbf{X_0}}{dt} = \mathbf{f_0} \tag{4.10}$$

$$\zeta_p \frac{d\mathbf{X_p}}{dt} = -k_p \mathbf{X_p} + \mathbf{f_p} \tag{4.11}$$

where, $\zeta_0 = N\zeta^0_{eff}$, $\zeta_p = 2N\zeta^p_{eff}$ and $k_p = 2Nk^p_{eff}$. In the expression ζ^0_{eff} indicates the effective friction coefficient associated with the blob functioning as a part of the entire ring chain and ζ^p_{eff} indicates the effective friction coefficient associated with the blob functioning as part of N/p section chain. The constant k^p_{eff} reflects the fractal structure of the ring chain in the array of obstacles.

The friction coefficients are determined by the blob rearrangement dynamics in the fractal structure. The dynamics of the ring polymer in the array of obstacles happens through random fluctuations which causes a shape evolution like that of amoeba (McLeish, 2002a). Of the random fluctuations some fluctuations cause only local rearrangements that do not contribute to the center of mass motion of the section under consideration. The number of fluctuations that do not contribute to the center of mass motion is expected to be proportional to the size of the section, *i.e.*, the larger the section under consideration more the number of local rearrangements that do not contribute to the motion of the chain section. Based on this physical idea the effective friction for a blob in a section of the ring chain is given by:

$$\zeta^0_{eff} = N\zeta_{blob} \tag{4.12}$$

$$\zeta^p_{eff} = \frac{N}{p}\,\zeta_{blob} \tag{4.13}$$

where, ζ_{blob} is given by expression (3.3) as discussed in section 3.2 of chapter 3.

The constant k_{eff}^{p} associated with the fractal skeleton is obtained from the conjugate Langevin of Muthukumar (1985) and is given by:

$$k_{eff}^{p} = k\left(\frac{p_s\pi}{N}\right)^2 = k\left(\frac{p\pi}{N}\right)^{3/2} \tag{4.14}$$

The fluctuation-dissipation theorem requires that the stochastic forces in equations (4.10) and (4.11) satisfy:

$$\langle(f_{0\alpha}(t_1)f_{0\beta}(t_2))\rangle = 2\zeta_0 k_B T\delta_{\alpha\beta}\delta(t_1-t_2) \tag{4.15}$$

$$\langle(f_{p\alpha}(t_1)f_{q\beta}(t_2))\rangle = 2\zeta_p k_B T\delta_{pq}\delta_{\alpha\beta}\delta(t_1-t_2) \tag{4.16}$$

4.3 Trunk Fluctuations in Blob-Spring Model

Consider the rearrangement of the conjugate Langevin equation (4.11) as follows:

$$\frac{N}{p}\zeta_{eff}^{p}\frac{d\mathbf{X_p}}{dt} = -k\pi\left(\frac{p\pi}{N}\right)^{1/2}\mathbf{X_p} + \frac{\mathbf{f_p}}{p} \tag{4.17}$$

The Langevin equation in the form (4.17) can be considered as the intra-chain force balance equation on the N/p section chain. The left hand side of the equation is the friction force on the chain. The first term on the right hand side is the spring force and the second term is the stochastic force on the section of the chain. The spring force term in the equation (4.17) is related to the statistics of the primitive path (trunk) of the Cayley tree structure of the ring chain and allows for the BS model to be viewed alternatively as a description of the fluctuations of the trunk of the ring chain. In order to understand the relation we view the Cayley tree structure of the ring polymer in an array of fixed obstacles in the light of Nechaev (1998) statistics.

The conditional probability that two sub-chains C_1 and C_2 with m and $N-m$ segments have a common primitive path $\Bbbk$ in the Cayley tree is given by (Nechaev, 1998):

$$P(\Bbbk, m|N) \simeq \left(\frac{N}{2m(N-m)}\right)^{3/2}\Bbbk^2\exp\left(-\frac{\Bbbk^2 N}{N(N-m)}\right) \tag{4.18}$$

Using expression (4.18) the mean length of the primitive path $\langle\Bbbk(m)\rangle$ can be determined to be:

$$\langle\Bbbk(m)\rangle = \sum_{\Bbbk=0}^{N}\Bbbk P(\Bbbk, m|N) \simeq \frac{2}{\sqrt{\pi}}\sqrt{\frac{2m(N-m)}{N}} \tag{4.19}$$

The size distribution for the chain with a primitive path $\Bbbk$ is given by the Gaussian distribution:

$$P(R, \Bbbk) = \left(\frac{3}{2\Bbbk a^2}\right)^{3/2}\exp\left(-\frac{3R^2}{2\Bbbk a^2}\right) \tag{4.20}$$

In case C_1 and C_2 have the same number of segments, $N/2$, then from expression (4.19) $\langle \Bbbk(m) \rangle \sim N^{1/2}$. Replacing $\Bbbk$ by $\langle \Bbbk(m) \rangle$ in the equation (4.20) we have:

$$P(R, \langle \Bbbk \rangle) \simeq \left(\frac{3}{2N^{1/2}a^2} \right)^{3/2} \exp\left(-\frac{3R^2}{2N^{1/2}a^2} \right) \tag{4.21}$$

We can extend this argument for a N/p section chain and the size distribution of the trunk of a N/p section chain is given by:

$$P(R_{N/p}, \langle \Bbbk(N/p) \rangle) = \left(\frac{3}{2(N/p)^{1/2}a^2} \right)^{3/2} \exp\left(-\frac{3R_{N/p}^2}{2(N/p)^{1/2}a^2} \right) \tag{4.22}$$

The Gaussian distribution allows for a mechanical representation of the primitive paths as beads connected by harmonic springs (Doi and Edwards, 1986) whose potential energy is given by:

$$U(\mathbf{R}_{N/p}) = \frac{3}{2(N/p)^{1/2}a^2} k_B T R_{N/p}^2 \tag{4.23}$$

The spring constant associated with the harmonic springs connecting two ends of the primitive path of a N/p section can be deduced from expression (4.23) as:

$$k_{N/p} = \frac{3k_B T}{a^2} \left(\frac{p}{N} \right)^{1/2} = k \left(\frac{p}{N} \right)^{1/2} \tag{4.24}$$

A comparison of the form of spring constant term in the expression (4.24) to that in the equation (4.17) shows that they are similar. Thus, the BS model can indeed be viewed as a description of the fluctuations of the trunk of the ring chain.

4.4 Diffusion Coefficient and Relaxation Spectrum

Using the BS framework we can determine the diffusion coefficient and relaxation spectrum of the ring chain by considering the dynamics of the blobs connected in the fractal skeleton by springs. Equation (4.10) is the center of mass motion governing equation. It is a first order linear ordinary differential equation whose solution is given by:

$$\mathbf{X_0} = \frac{1}{\zeta_0} \int_{-\infty}^{t} dt_1 \mathbf{f_0}(t_1) \tag{4.25}$$

The center of mass diffusion coefficient of the ring polymer is given by:

$$D = \lim_{t \to \infty} \frac{1}{6t} \left\langle (\mathbf{X_0}(t) - \mathbf{X_0}(0))^2 \right\rangle \tag{4.26}$$

From the solution (4.25) and the fluctuation-dissipation equation (4.15) the correlation at the right hand side of the equation (4.26) is given by:

$$\left\langle (\mathbf{X_0}(t) - \mathbf{X_0}(0))^2 \right\rangle = \frac{k_B T}{\zeta_0} t \tag{4.27}$$

Using the correlation expression (4.27), the effective friction expression (4.13) and blob friction coefficient expression (3.3) in the diffusion coefficient expression (4.26):

$$D = \frac{k_B T}{N^2 \zeta_{blob}} = \frac{a^2}{b^2} \frac{k_B T}{N_K^2 \zeta} \tag{4.28}$$

In arriving at expressions (4.28) we have used $N = N_k/N_e$ and $a^2 = N_e b^2$.

The dynamics of the intra chain sections of the blob chain is governed by the mode equation (4.11). The solution to mode equation is given by:

$$\mathbf{X_p} = \frac{1}{\zeta_p} \int_{-\infty}^{t} dt_1 \exp\left(-\frac{(t - t_1)}{\tau_p} \right) \mathbf{f_p}(t_1) \tag{4.29}$$

where, τ_p is the relaxation time associated with the N/p section ring chain. The expression for relaxation time τ_p can be arrived at using equations (4.13), (3.3), (4.14) and the Gaussian statistics $a^2 = N_e b^2$:

$$\tau_p = \frac{\zeta_p}{k_p} = \frac{\pi}{3} \frac{a^4}{b^2} \frac{\zeta}{k_B T} \left(\frac{N}{p\pi} \right)^{5/2} \tag{4.30}$$

The longest relaxation time corresponds to the relaxation of the entire ring chain, *i.e.*, $p = 1$ and is given by:

$$\tau_1 = \frac{\pi}{3} \frac{a^4}{b^2} \frac{\zeta}{k_B T} \left(\frac{N}{\pi} \right)^{5/2} \tag{4.31}$$

The smallest relaxation time corresponds to the relaxation of a single section of the ring chain, *i.e.*, $p = N$ and is given by:

$$\tau_N = \frac{\pi}{3} \frac{a^4}{b^2} \frac{\zeta}{k_B T} \left(\frac{1}{\pi} \right)^{5/2} \tag{4.32}$$

The scaling exponents of N in self-diffusion coefficient and the relaxation times obtained from the BS model are the same as that of DOR model. Expression (4.30) indicates that the dynamics is self-similar in terms of the relaxation time as it depends on the number of sections for any given section of the chain in the same way.

4.5 Constitutive Relation

The microscopic expression for the stress tensor is given by (Doi and Edwards, 1986):

$$\sigma_{\alpha\beta} = \frac{c_b}{N} \sum_n \left\langle \frac{\partial U}{\partial R_{n\alpha}} R_{n\beta} \right\rangle \tag{4.33}$$

It can be inferred from Muthukumar arguments (Muthukumar, 1985) that for polymeric fractals U is given by:

$$U = \frac{k}{2}\sum_{n=2}^{N}(\mathbf{R_n} - \mathbf{R_{n-1}})^2 \tag{4.34}$$

in the spectral dimension. Combining the insights from equations (4.33) and (4.34) the microscopic expression for the stress tensor according to the BS model can be written as:

$$\sigma_{\alpha\beta} = \frac{c_b}{N}k\int_0^N dn\,\langle \nabla_s R_{n\alpha}\nabla_s R_{n\beta}\rangle \tag{4.35}$$

where, ∇_s denotes gradient in the spectral dimension of the fractal network and c_b is the number density of the blobs that make up the ring polymer and is given by $c_b = c/N_e$.

Using the normal coordinate transformation (4.6)-(4.9) the stress tensor expression is given by:

$$\sigma_{\alpha\beta} = \frac{c_b}{N}\sum_{p_s} k_{ps}\,\langle X_{p\alpha}X_{p\beta}\rangle \tag{4.36}$$

where, $k_{ps} = 2Nk(p_s\pi/N)^2$. Equation (4.36) is appropriately modified in the conjugate space and the stress tensor expression is given by:

$$\sigma_{\alpha\beta} = \frac{c_b}{N}\sum_{p} k_{p}\,\langle X_{p\alpha}X_{p\beta}\rangle \tag{4.37}$$

We now impose a homogeneous deformation gradient $\bar{v}(\mathbf{r},t) = \bar{\bar{\kappa}}(t).\mathbf{r}$. During such a deformation the Langevin equation for the p^{th} normal coordinate, $\mathbf{X}_p$, becomes:

$$\frac{\partial \mathbf{X}_p}{\partial t} = -\frac{k_p}{\zeta_p}\mathbf{X}_p + \frac{1}{\zeta_p}\mathbf{f_p} + \bar{\bar{\kappa}}(t).\mathbf{X}_p \tag{4.38}$$

From the Langevin equation (3.31) we obtain the equation for the correlation $\langle X_{p\alpha}X_{p\beta}\rangle$ as:

$$\frac{\partial}{\partial t}\langle X_{p\alpha}X_{p\beta}\rangle = -2\frac{k_p}{\zeta_p}\langle X_{p\alpha}X_{p\beta}\rangle + 4\frac{k_BT}{\zeta_p}\delta_{\alpha\beta} + \kappa_{\alpha\mu}\langle X_{p\mu}X_{p\beta}\rangle + \kappa_{\beta\mu}\langle X_{p\alpha}X_{p\mu}\rangle \tag{4.39}$$

Equation (4.39) can be solved to obtain $\langle X_{p\alpha}X_{p\beta}\rangle$ for any given homogeneous deformation gradient. For homogeneous shear where $\bar{\bar{\kappa}}(t)$ is given by:

$$\begin{bmatrix} 0 & \kappa(t) & 0 \\ 0 & 0 & 0 \\ 0 & 0 & 0 \end{bmatrix}$$

we have the equation for the xy component of the correlation given by:

$$\frac{\partial}{\partial t}\langle X_{px}X_{py}\rangle = -2\frac{k_p}{\zeta_p}\langle X_{px}X_{py}\rangle + \kappa(t)\langle X_{py}^2\rangle \tag{4.40}$$

Considering the system to be close to equilibrium we have $\left\langle X_{py}^2 \right\rangle = k_B T/k_p$, using which the solution to equation (4.40) is obtained as:

$$\langle X_{px} X_{py} \rangle = \frac{k_B T}{k_p} \int_{-\infty}^{t} dt_1 \exp\left(-2\frac{(t-t_1)}{\tau_p}\right) \kappa(t_1) \tag{4.41}$$

Substituting equation (4.41) in equation (4.37) we obtain:

$$\sigma_{xy} = \frac{c_b}{N} k_B T \sum_p \int_{-\infty}^{t} dt_1 \exp\left(-2\frac{(t-t_1)}{\tau_p}\right) \kappa(t_1) \tag{4.42}$$

The phenomenological expression for stress tensor in terms of the relaxation modulus is given by:

$$\sigma_{xy}(t) = \int_{-\infty}^{t} dt_1 G(t-t_1)\kappa(t_1) \tag{4.43}$$

Comparing equation (3.35) with equation (3.36) we obtain:

$$G(t) = \frac{c_b}{N} k_B T \sum_p \exp\left(-2\frac{t}{\tau_p}\right) \tag{4.44}$$

Continuous form of expression (4.44) can be written as:

$$G(t) = \frac{c_b}{N} k_B T \int_0^{\infty} dp \ \exp\left(-2p^{5/2}\frac{t}{\tau_1}\right) \tag{4.45}$$

By the variable transformation $x = 2(t\tau_1)p^{5/2}$ equation (4.45) becomes:

$$G(t) = \frac{2}{5}\frac{c_b}{N} k_B T \left(\frac{1}{2}\right)^{2/5} \left(\frac{\tau_1}{t}\right)^{2/5} \int_0^{\infty} dx \ x^{-3/5} \exp(-x) \tag{4.46}$$

The integral in expression (4.46) is a gamma function $\Gamma[2/5]$ which takes a constant value. For $t < \tau_1$ the relaxation modulus can thus be considered to have a power law scaling $G(t) \sim t^{-2/5}$. The expression (4.44) can also be expanded in the form:

$$G(t) = \frac{c_b}{N} k_B T \exp\left(-2\frac{t}{\tau_1}\right) \left[1 + \exp\left(-9.3\frac{t}{\tau_1}\right) + \exp\left(-29.2\frac{t}{\tau_1}\right) + ...\right] \tag{4.47}$$

The higher order exponential decays in the expression (4.47) can be neglected for $t > \tau_1$. Thus, the relaxation modulus can be approximated as:

$$G(t) \approx \frac{2}{5}\frac{c_b}{N} k_B T \left(\frac{1}{2}\right)^{2/5} \left(\frac{\tau_1}{t}\right)^{2/5} \Gamma\left[\frac{2}{5}\right] \exp\left(-2\frac{t}{\tau_1}\right) \tag{4.48}$$

4.6 Melt of Ring Polymers

The assumptions implicit to the DOR model for a ring in a fixed array of obstacles are (i) excluded volume and hydrodynamic interactions are neglected, (ii) the ring follows the tree-like statistics indicated above with a trunk of length $L_p \approx aN^{\rho}$, where $\rho = 1/2$ (Gutin *et al.*, 1993), and (iii) different parts of a ring do not interpenetrate. The fluctuation approach to dynamics of ring polymers in an array of fixed obstacles can be extended to the case of melt of rings. We assume that:

- The ring polymer in its melt still has a lattice animal (self-similar) structure with its fractal dimension d_f between 2 and 4, *i.e.*, the size exponent in $R \sim N^{\nu}$ lies between 1/4 and 1/2.
- Hydrodynamic interactions are screened.
- Excluded volume interactions are neglected.
- For small ring polymers, *i.e.*, in the absence of excluded volume interactions, the mean length of the primitive path scales as $\langle \mathbb{k} \rangle \sim N^{2\nu}$. For large ring polymers excluded volume interactions due to increased possibility of segmental overlap causes the trunk to stretch, and the mean length of the primitive path scales as $\langle \mathbb{k} \rangle \sim N^{\rho}$, where, $\rho = (2\nu + 1)/3$ (Gutin *et al.*, 1993).
- The dynamics of the fractal structure can be described by dynamics of independent modes.

Simulations of Müller *et al.* (1996) supports the first assumption. The second assumption is natural in dense systems like melt. The excluded volume interactions can be neglected under the condition $N < (b^2/ar)^{1/(2-3\nu)}$, where r is the cross sectional area of the polymer chain (Obukhov *et al.*, 1994). This assumption can be accounted for by considering the stretching of the trunk as mentioned in section (4.1). This leads to substituting ρ in place of the exponent 2ν in all equations of the BS model, where $\rho = (2\nu + 1)/3$ (Gutin *et al.*, 1993). The assumption of independent modes is the weakest assumption in a melt of ring polymers.

In a melt constant k^p_{eff} associated with the fractal skeleton is obtained from the conjugate Langevin of Muthukumar (1985) and is given by:

$$k^p_{eff} = k \left(\frac{p_s \pi}{N} \right)^2 = k \left(\frac{p\pi}{N} \right)^{2\nu+1} \tag{4.49}$$

where, ν lies between 1/2 and 1/4. The relaxation time associated with the N/p section chain is given by:

$$\tau_p = \frac{\zeta_p}{k_p} = \frac{\pi}{3}\frac{a^4}{b^2}\frac{\zeta}{k_B T}\left(\frac{N}{p\pi}\right)^{2\nu+2} \tag{4.50}$$

The expression for the relaxation modulus remains identical to equation (4.44) except that expression for τ_p in it is given by expression (4.50).

4.7 Results and Discussion

The implicit assumptions of the blob-spring model described above are the same as those made for the DOR theory namely, (a) excluded volume and hydrodynamic interactions are neglected, (b) excluded volume interactions arising from self avoiding structure of a lattice animal is neglected, and (c) there are independent modes of relaxation. Of these assumptions, the first is reasonable for a melt of rings. The second assumption holds when,$N < (b^2/ar)^{1/(2-3\nu)}$ where r is the cross-sectional area of a polymer chain (Obukhov *et al.*, 1994). However, this assumption can be easily corrected by accounting for the stretching of the trunk. This implies substituting ρ in place of ν in all equations of the blob-spring model, and then calculating ρ as $\rho = (2\nu+1)/3$ (Gutin *et al.*, 1993). The third assumption is possibly the weakest when applied to the case of a melt of rings.

We will however proceed to compare the predictions of the blob-spring model with experimental data on the linear viscoelastic response of melt of Roovers PBD rings (Roovers, 1988). Large deviations from predictions, if observed, could then suggest the importance of loop interpenetration for these samples. An additional relaxation mode that may be of importance in case of a melt of rings is that caused by release of constraints as the surrounding chains relax. This can be expected to be important because of the wide spectrum of relaxation times expected from equation (4.50).

The various molecular parameters of PBD used in our calculations are listed in chapter (3) section (3.8). We have assumed a, the obstacle length scale, and ν, the inverse of the fractal dimension to be variable parameters of the model. One of the values assumed for parameter a is equal to the tube diameter of the linear polymers in melt state. Assuming $r = 1nm$, the criteria $N < (b^2/ar)^{1/(2-3\nu)}$ was not satisfied for the PBD ring sample. This suggests that excluded volume interactions from self avoiding structure of the rings might be important. The excluded volume interactions are expected to change the exponent ν and they are taken into consideration

as ν is an adjustable parameter in the model. The relaxation modulus was calculated from equation (4.44), while the dynamic moduli were calculated from Fourier transform of equation (4.44), which gives:

$$G'(\omega) = \frac{c_b}{N} k_B T \sum_{p=1}^{N} \frac{\omega^2 \tau_p^2}{4 + \omega^2 \tau_p^2} \tag{4.51}$$

$$G''(\omega) = 2\frac{c_b}{N} k_B T \sum_{p=1}^{N} \frac{\omega \tau_p}{4 + \omega^2 \tau_p^2} \tag{4.52}$$

The model predictions based on equations (3.3), (4.51) and (4.52) for ring PBD melt of molecular weight $6.0 \times 10^4 g/mol$ are shown in figures 4.2-4.4. We have considered the same two scenarios as were considered for the PPR framework predictions *viz.* with modification entanglement spacing ($a \approx 31.1$Å) and without modification of entanglement spacing ($a \approx 44.5$Å). The comparison of BS model predictions for $\nu = 0.25$ for the modified entanglement spacing with the experimental data for the ring melt KPBD34B3 (Roovers, 1988) is shown in figure 4.2. In figures 4.3-4.5 the comparison with ring melt KPBD34B3 (Roovers, 1988) experiments is done for different ν and a as in the PPR framework. It is seen from these predictions that BS model predicts the power-law relaxation modulus at higher frequencies. However, there is severe under- prediction of the viscoeleastic response in the terminal regime. It is clear that the viscosity, which corresponds to the loss modulus in the terminal regime, of a melt of ring PBD as predicted by the BS model is much lower than the observed values. Such an under prediction also indicates a strong under prediction of the relaxation times. This can be considered as the effect of loop interpenetration or slowing down of the fluctuation rearrangements of sections of the ring chain by confinement effects. The BS model based on mode independent fluctuation dynamics is seen to be severely limited in capturing such slowing down of dynamics. However, it can be shown that if the slowing down is considered to increase the friction coefficient by a factor of N_e the BS model gives quantitatively comparable predictions for both the terminal and high frequency regimes (see Figure 4.6).

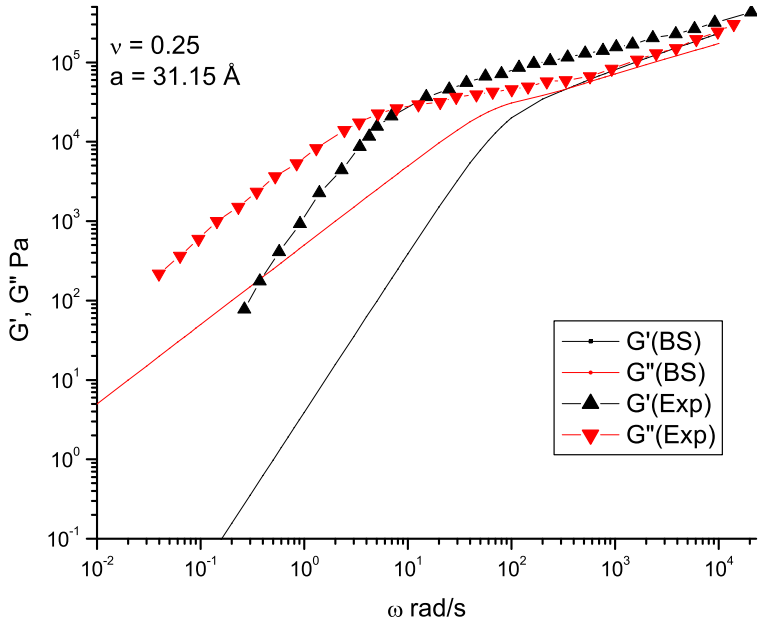

Figure 4.2: Comparison of Blob-Spring model based viscoelastic response predictions ($\nu = 0.25$ and $a = 31.15$Å) to ring PBD sample KPBD34B3 (Roovers, 1988)

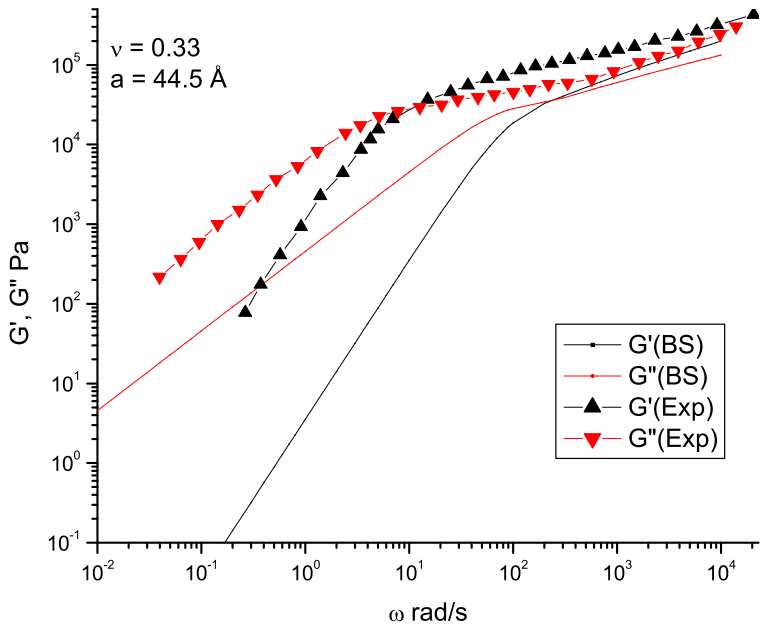

Figure 4.3: Comparison of Blob-Spring model based viscoelastic response predictions ($\nu = 0.33$ and $a = 44.5$Å) to ring PBD sample KPBD34B3 (Roovers, 1988)

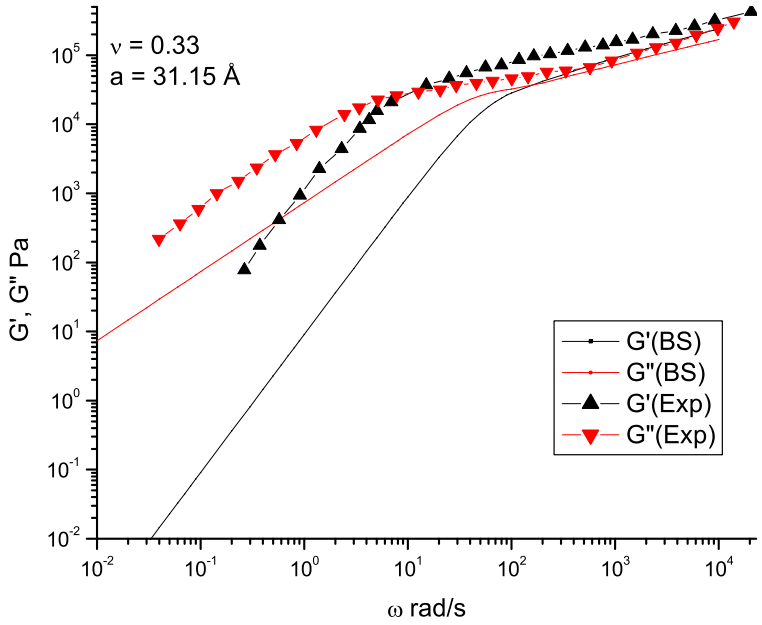

Figure 4.4: Comparison of Blob-Spring model based viscoelastic response predictions ($\nu = 0.33$ and $a = 31.15$Å) to ring PBD sample KPBD34B3 (Roovers, 1988)

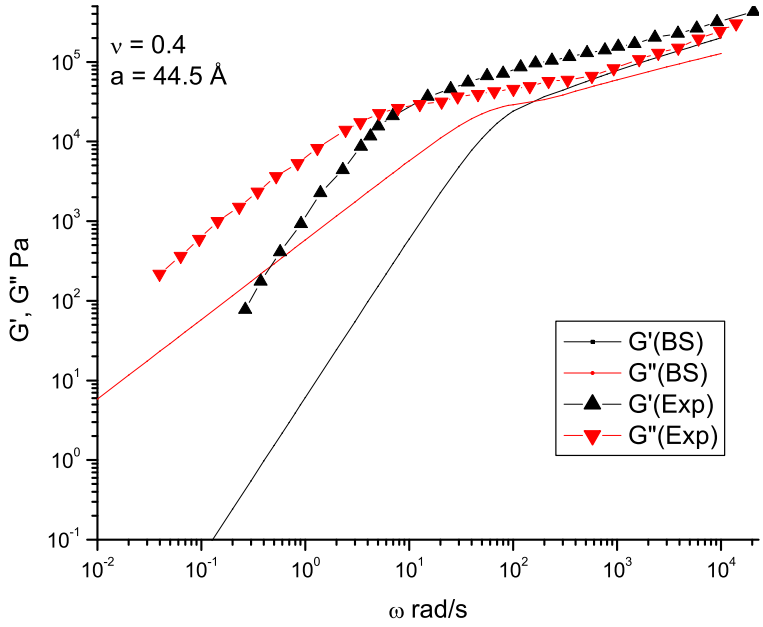

Figure 4.5: Comparison of Blob-Spring model based viscoelastic response predictions ($\nu = 0.4$ and $a = 44.5$Å) to ring PBD sample KPBD34B3 (Roovers, 1988)

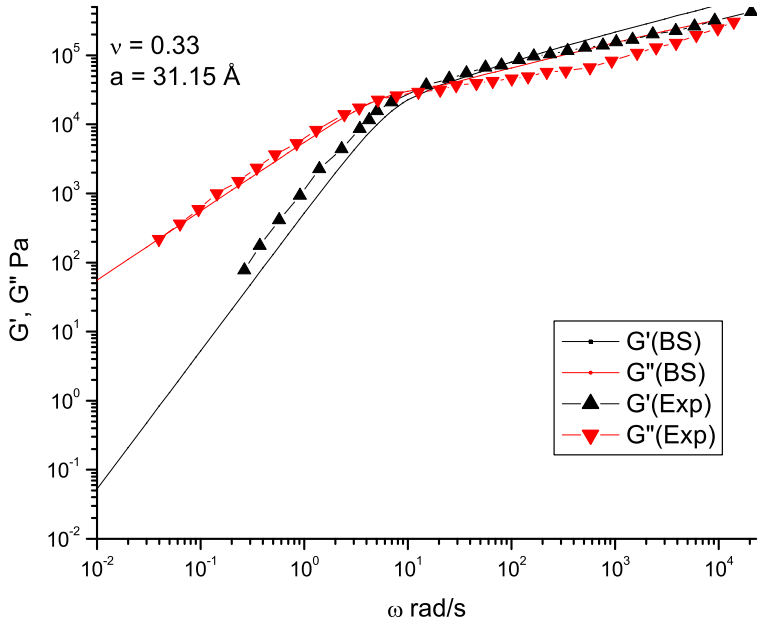

Figure 4.6: Comparison of Blob-Spring model with increased friction based viscoelastic response predictions ($\nu = 0.33$ and $a = 31.15$Å) to ring PBD sample KPBD34B3 (Roovers, 1988)

Chapter 5

Fractal Gate Model: Fluctuations and Mean Field Approach to Ring Dynamics

5.1 Fluctuations and Mean-Field in Ring Dynamics

In the DOR scaling arguments it was argued that over a time scale $\tau_0 \sim N_e^2\zeta/k_BT$, which is the Rouse relaxation time of an unconstrained blob, each loop would release one kink into the trunk. The statistics of the tree-like structure dictates that in a fixed array of obstacles there are on an average $N^{1/2}$ loops attached to a trunk which has a length of $L_P \approx aN^{1/2}$. The frequency of release of kinks into the trunk is therefore equal to $N^{1/2}/\tau_0$. In the time τ_0 a kink diffuses along the trunk over a length equal to the blob size, but the center of mass diffuses over a length a/N. Hence the curvilinear diffusion coefficient of the center of mass along the trunk due to motion of all kinks is estimated as $D_P \sim (a/N)^2(N^{1/2}/\tau_0)$. The longest relaxation time, τ_1, is then calculated as the time required for the center of mass to diffuse over the entire trunk length with the curvilinear diffusion coefficient estimated above. Thus, $\tau_1 \sim L_P^2/D_P \approx \tau_0 N^{5/2}$ and the center of mass diffusion coefficient in 3-D is given by $D \sim R^2/\tau_1 \approx (a^2/\tau_0)N^{-2}$.

Recent rheology experiments on high molecular weight ring polystyrene melts show a power-law stress relaxation (Kapnistos *et al.*, 2008). According to Kapnistos *et al.* (2008) argument all the loops in the system composed of m segments in the melt rearrange simultaneously and loose their memory of their original conformation in a time scale $\tau_m \sim \tau_0\, m^{5/2}$. The remaining stress in the melt is k_BT per segment composed of m segments. This corresponds to the stress relaxation modulus of $G(\tau_m) \sim k_BT/(\vartheta m)$, where ϑ is the volume of a segment. By substituting the time dependence of the the number of relaxing segments $m \sim (\tau_m/\tau_0)^{2/5}$ into

the scaling expression for stress relaxation it is seen that $G(\tau_m) \sim (\tau_0/\tau_m)^{2/5}$. The self-similar process continues till the whole ring chain has relaxed at the time scale of $\tau_N \sim \tau_0\ N^{5/2}$. At longer times, $t > \tau_N$, the relaxation modulus decreases exponentially with time and thus the overall stress relaxation of melt is given by:

$$G(t) \sim G^0 \left(\frac{\tau_0}{t}\right)^{2/5} \exp\left(-\frac{t}{\tau_N}\right) \tag{5.1}$$

It is important to note that the argument here looks similar to the derivation of the relaxation modulus for the Gaussian chain undergoing Rouse dynamics (see section 4.1).

According to Kapnistos *et al.* (2008) the expression (5.1) implicitly takes into account the many-chain effects in the relaxation of the ring melt. This implies that constraint release in the ring melt is accounted for implicitly in the expression for stress relaxation. In the same article they suggested that for an ideal ring constrained in an array of fixed obstacles the relaxation modulus would decay as $G(t) \sim t^{-1/5}$. Their argument was based on the concept of 'gates' which are pairs of obstacles that define the relative posisitons of loops on a trunk (see Figure 5.1) and the rarrangement of such relative positions of the loops causes the center of mass diffusion of parts of the ring. It is important to note that the dynamics of inherent constraint release put forth by Kapnistos *et al.* (2008) is different from that of Rouse dynamics. This may be considered illustrative of the fact that self-similarity in dynamics exhibited by two different structures may not necessarily imply similarity of dynamics of the structures. We have already seen the successes and limitations of the Pom-Pom Ring and the Blob-Spring approach in the chapters 3 and 4 respectively. In this chapter we propose a judicious combination of fluctuations and mean-field approach which incorporates into it the physical ideas of DOR scaling in order to arrive at rigorous framework for understanding dynamics of rings in an obstacle environment.

Following Kapnistos *et al.* (2008), we assume that the relaxation of a non-concatenated flexible ring chain in an array of fixed obstacles occur by the simultaneous relaxation of all possible sections of a ring chain in a self similar manner. Relaxation of any given section is modeled as a one dimensional diffusion of its center of mass along the contour of the trunk of that section; the curvilinear diffusion coefficient is derived in a very specific and formal way through the fractal Rouse dynamics. Relaxation of the section is deemed complete when the centre of mass diffuses over the entire length of the trunk whereby it escapes from the gate where it is attached to the rest of the ring chain. The net relaxation modulus is therefore written as the superposition of relaxations of all sections weighted by the number fraction of each section. There are thus three key steps in the derivation:

- Derivation of the curvilinear diffusion coefficient by fluctuations of fractal Rouse chain.
- Derivation of the confinement memory of the trunk by diffusion in a mean-field.
- Estimation of the number fraction of any given section of the ring chain using the concept of 'gates' of entanglement.

The next three sections provide the necessary derivations of quantities indicated above. We end this contribution with a brief discussion about extending the model to the case of melt of rings.

5.2 Fractal Rouse Model

We start by proposing that any arbitrary closed section composed of $m = m_K/N_e$ blobs of a ring polymer are connected to each other on a (hypothetical) fractal polymeric skeleton by (hypothetical) springs as shown schematically in 4.1. The springs are considered to be Gaussian and the spring constant associated with the springs between blobs is $k = 3k_BT/a^2$. The dynamics of the skeleton can be modeled using the theory developed by Muthukumar (1985) for unentangled fractal polymers (branched polymers) as in BS model. The generalized Rouse equation governing the dynamics of such section of the chain is still given by equation (4.5).

If the normal coordinates for any arbitrary closed section of the ring chain are defined in the spectral dimension by:

$$\mathbf{R}_n = \mathbf{X}_0 + 2\sum_{p_s} \mathbf{X}_p \cos\left(\frac{p_s\pi n}{m}\right) \tag{5.2}$$

$$\mathbf{f}_n = \frac{\mathbf{f}_0}{m} + \frac{1}{m}\sum_{p_s} \mathbf{f}_p \cos\left(\frac{p_s\pi n}{m}\right) \tag{5.3}$$

$$\mathbf{X}_p = \frac{1}{m}\int_0^m dn \cos\left(\frac{p_s\pi n}{m}\right)\mathbf{R}_n \tag{5.4}$$

$$\mathbf{f}_p = 2\int_0^m dn \cos\left(\frac{p_s\pi n}{m}\right)\mathbf{f}_n \tag{5.5}$$

then the Langevin equation in the conjugate space for the fractal polymer is given by:

$$\zeta_0\frac{d\mathbf{X}_0}{dt} = \mathbf{f}_0 \tag{5.6}$$

$$\zeta_p\frac{d\mathbf{X}_p}{dt} = -k_p\mathbf{X}_p + \mathbf{f}_p \tag{5.7}$$

where, $\zeta_0 = m\zeta^0_{eff}$, $\zeta_p = 2m\zeta^p_{eff}$ and $k_p = 2mk^p_{eff}$. In the expression ζ^0_{eff} indicates the effective friction coefficient associated with the blob functioning as a part of the entire ring chain and ζ^p_{eff} indicates the effective friction coefficient associated with the blob functioning as part of N/p section chain. The constant k^p_{eff} reflects the fractal structure of the ring chain in the array of obstacles.

The friction coefficients are determined by the blob rearrangement dynamics in the fractal structure. In the BS model we argued that of the random fluctuations in chain some fluctuations cause local rearrangements that do not contribute to the motion of the section under consideration and consequently increase the friction experienced by a blob of the chain section. However, we also argued that the number of such fluctuations is proportional to the section of the chain under consideration. According to the DOR sclaing the fast relaxing loops do not contribute to the center of mass motion and the size of such fast relaxing loops in section composed of m segments scales as $\sim m^{1/2}$. Based on this physical idea and considering that instead of the friction being proportional to the size of the section m/p it is proportional to the size of fast relaxing structures in the section, *i.e.*, $\sim (m/p)^{1/2}$, the effective friction for a blob in a section of the chain is given by:

$$\zeta^0_{eff} = m^{1/2}\zeta_{blob} \tag{5.8}$$

$$\zeta^p_{eff} = \left(\frac{m}{p}\right)^{1/2}\zeta_{blob} \tag{5.9}$$

The friction coefficient of a blob, ζ_{blob}, can be derived from the understanding that it consists of N_e unentangled Kuhn segments (beads), which are undergoing the usual Rouse or Zimm dynamics depending on the environment in the pore of the array of obstacles. The Rouse diffusion coefficient of a N_e segment Gaussian chain is given by (Doi and Edwards, 1986):

$$D_{blob} = \frac{k_B T}{N_e \zeta} \tag{5.10}$$

From the Einstein argument the blob friction coefficient can be obtained as:

$$\zeta_{blob} = \frac{k_B T}{D_{blob}} = N_e \zeta \tag{5.11}$$

The constant k^p_{eff} associated with the fractal skeleton is obtained from the conjugate Langevin of Muthukumar (1985) and is given by:

$$k^p_{eff} = k\left(\frac{p_s \pi}{m}\right)^2 = k\left(\frac{p\pi}{m}\right)^{3/2} \tag{5.12}$$

The fluctuation-dissipation theorem requires that the stochastic forces in equations (5.6) and (5.7) satisfy:

$$\langle (f_{0\alpha}(t_1) f_{0\beta}(t_2)) \rangle = 2\zeta_0 k_B T \delta_{\alpha\beta} \delta(t_1 - t_2) \tag{5.13}$$

$$\langle (f_{p\alpha}(t_1) f_{q\beta}(t_2)) \rangle = 2\zeta_p k_B T \delta_{pq} \delta_{\alpha\beta} \delta(t_1 - t_2) \tag{5.14}$$

Using the fractal Rouse framework we can determine the diffusion coefficient and relaxation spectrum of the m section of the ring chain by considering the dynamics of the blobs connected in the fractal skeleton by springs. Equation (5.6) is the m section center of mass motion governing equation the solution to which is given by:

$$\mathbf{X_0} = \frac{1}{\zeta_0} \int_{-\infty}^{t} dt_1 \mathbf{f_0}(t_1) \tag{5.15}$$

The center of mass diffusion coefficient of the m segment section is given by:

$$D_{mR} = \lim_{t \to \infty} \frac{1}{6t} \left\langle (\mathbf{X_0}(t) - \mathbf{X_0}(0))^2 \right\rangle \tag{5.16}$$

From the solution (5.15) and the fluctuation-dissipation relation (5.13) the correlation at the right hand side of the equation (5.16) is given by:

$$\left\langle (\mathbf{X_0}(t) - \mathbf{X_0}(0))^2 \right\rangle = \frac{k_B T}{\zeta_0} t \tag{5.17}$$

Using the correlation expression (5.17), the effective friction expression (5.9) and blob friction coefficient expression (5.11) in the diffusion coefficient expression (5.16):

$$D_{mR} = \frac{k_B T}{m^{3/2} \zeta_{blob}} = \frac{a}{b} \frac{k_B T}{m_K^{3/2} \zeta} \tag{5.18}$$

In arriving at expression (5.18) we have used expression (5.11) for ζ_{blob}, $m = m_k/N_e$ and $a^2 = N_e b^2$. The molecular weight scaling of the curvilinear diffusion coefficient in equation (5.18) is in agreement with the DOR scaling for curvilinear diffusion coefficient for the center of mass of an m section of the chain.

The dynamics of the intra chain sections of the blob chain is governed by the mode equation (5.7). The solution to mode equation is given by:

$$\mathbf{X_p} = \frac{1}{\zeta_p} \int_{-\infty}^{t} dt_1 \exp\left(-\frac{(t - t_1)}{\tau_p} \right) \mathbf{f_p}(t_1) \tag{5.19}$$

where, τ_p is the relaxation time associated with the m/p section of the ring chain. The expression for relaxation time τ_p can be arrived at using equations (5.9), (5.11), (5.12) and the Gaussian statistics $a^2 = N_e b^2$ and is given by:

$$\tau_p = \frac{\zeta_p}{k_p} = \frac{1}{p^2} \pi^{1/2} \frac{1}{3\pi^2} \frac{a^4}{b^2} \frac{\zeta}{k_B T} m^2 \tag{5.20}$$

The longest relaxation time corresponds to the relaxation of the entire m section, *i.e.*, $p = 1$ and is given by:

$$\tau_1 = \pi^{1/2} \frac{1}{3\pi^2} \frac{a^4}{b^2} \frac{\zeta}{k_B T} m^2 \tag{5.21}$$

The shortest relaxation time corresponds to the relaxation of a single section of the ring chain, *i.e.*, $p = m$ and is given by:

$$\tau_m = \pi^{1/2} \frac{1}{3\pi^2} \frac{a^4}{b^2} \frac{\zeta}{k_B T} = \pi^{1/2} \frac{1}{3} \frac{b^2}{\pi^2} \frac{\zeta}{k_B T} N_e^2 \tag{5.22}$$

It scales as $\sim N_e^2$ and corresponds to the relaxation time of an unentangled blob of N_e Kuhn segments.

It is also straightforward to show that due to dynamic self-similarity the center of mass curvilinear diffusion coefficient and the longest relaxation time of the entire ring chain containing N blobs (or equivalently, N_k Kuhn segments) are given by:

$$D_N = \frac{k_B T}{N^{3/2} \zeta_{blob}} = \frac{a}{b} \frac{k_B T}{N_K^{3/2} \zeta} \tag{5.23}$$

$$\tau_N = \frac{1}{p^2} \pi^{1/2} \frac{1}{3\pi^2} \frac{a^4}{b^2} \frac{\zeta}{k_B T} N^2 \tag{5.24}$$

The scaling exponent of diffusion coefficient obtained from the fractal Rouse model is the same as that of curvilinear diffusion coefficient corresponding to the center of mass of the ring chain in the DOR scaling model and is different from the scaling for a linear Gaussian chain. Expression (5.24) indicates that the relaxation time in fractal ring chain is similar to that of the Rouse relaxation time of a linear chain.

5.3 One Dimensional Diffusion

So far we have considered the influence of the array of fixed obstacles on the structure of the ring chain and thereby on its dynamics. However, we can also expect the fixed obstacles to form topological constraints akin to a tube and restrict the centre of mass motion of the ring chain. We consider a section of the ring chain made of m blobs which is connected to the rest of the chain through a pair of gates (Figure 5.1). The gates define the relative position of the m section with respect to the rest of the ring. The m section is characterized by its fractal structure, *i.e.*, a trunk and attached loops. The center of mass of the m section is not free to undergo random fluctuations due to topological constraints, but is confined within a tube of length equal to the

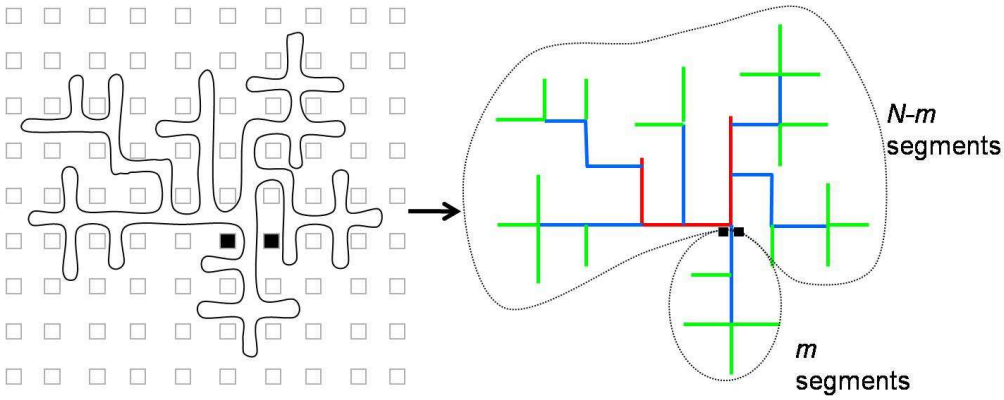

Figure 5.1: Gate of entanglement of a ring chain in an array of fixed obstacles

length of the trunk. The center of mass diffuses within the tube with a diffusion coefficient given by equation (5.18) and when it travels a mean square distance equal to the square of the length of the tube it 'escapes' the confinement and also the pair of gates thereby changing it relative position with respect to the other sections of the ring chain. While the trunk of the m section as in Figure 5.2 might appear at first instance like the branch of a branched polymer, it is actually different in two aspects. First, it is not covalently pinned to the ring and second, the diffusive motion of its center of mass within the tube does not occur against a free energy barrier since the ring has already paid an entropic penalty when forced to double fold and meander through the array of obstacles.

We can formulate the diffusion of the trunk along its contour analogous to the Doi-Edwards formulation of reptation of a linear chain (Doi and Edwards, 1986). Let $\Psi(\xi, t; s)$ be the probability that the trunk moves a distance ξ while its ends have not reached the segment s of the original trunk contour point. The probability satisfies the one dimensional diffusion equation given by:

$$\frac{\partial \Psi}{\partial t} = D_{mR} \frac{\partial^2 \Psi}{\partial \xi^2} \tag{5.25}$$

with the initial condition

$$\Psi(\xi, 0; s) = \delta(\xi) \tag{5.26}$$

When $\xi = s$, the segment s is reached by the trunk and $\Psi(\xi, t; s)$ vanishes. Similarly when $\xi = s - L_m$, the tube segment s is reached by the other end of the trunk and $\Psi(\xi, t; s)$ vanishes. Here, $L_m = am^{1/2}$ is the length of the trunk of the m section. This yields boundary conditions:

$$\Psi(\xi, t; s) = 0 \ \text{ at } \ \xi = s \ \text{ and } \ \xi = s - L_m \tag{5.27}$$

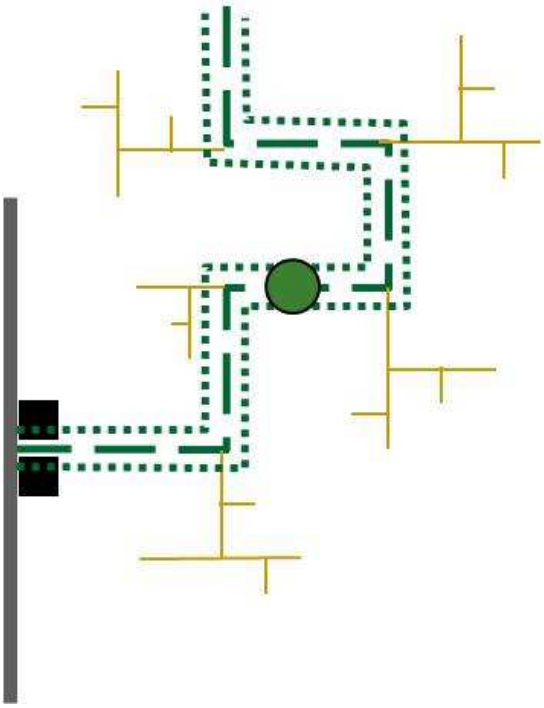

Figure 5.2: An m section of a ring chain is connected to the rest of the ring (grey) through a pair of gates (black filled squares), which define its position relative to the other parts of the ring chain. The m section is characterized by its trunk (thick dashed green line) and attached loops (thin yellow lines). The center of mass of the m section (filled green circle) undergoes one dimensional diffusion along the contour of its trunk due to the confining effect of the tube (dotted lines).

The solution to the one dimensional diffusion equation (5.25) subject to conditions (5.26) and (5.27) is given by (Doi and Edwards, 1986):

$$\Psi(\xi,t;s)=\sum_{p}\frac{2}{L}\sin\left(\frac{p\pi s}{L}\right)\sin\left(\frac{p\pi(s-\xi)}{L}\right)\exp\left(-p^2\frac{t}{\tau_d}\right) \tag{5.28}$$

where,

$$\tau_d^m=\frac{L_m^2}{D_{mR}\pi^2}=\frac{1}{\pi^2}\frac{a^4}{b^2}\frac{\zeta}{k_BT}m^{5/2} \tag{5.29}$$

The time scale τ_d^m is the time taken for the center of mass of the m section to diffuse out of the confinement. Note that for $m=1$

$$\tau_d^1=\tau_0=\frac{1}{\pi^2}\frac{a^4}{b^2}\frac{\zeta}{k_BT}=\frac{3}{\pi^{1/2}}\tau_m \tag{5.30}$$

where, the last equality is derived from equation (5.22) and for $m=N$:

$$\tau_d^N=\tau_{ring}=\frac{1}{\pi^2}\frac{a^4}{b^2}\frac{\zeta}{k_BT}N^{5/2} \tag{5.31}$$

where, τ_d^N is the longest relaxation time for the entire ring and its scaling with molecular weight is in agreement with the DOR model.

The memory of the confinement of the m section trunk is lost over the time scale τ_d^m. For the memory of the original segment s to remain, ξ can be anywhere between $s-L_m$ and s, so that:

$$\psi_m(s,t)=\int_{s-L_m}^{s}d\xi\Psi(\xi,t;s)=\sum_{p;odd}\frac{4}{p\pi}\sin\left(\frac{p\pi s}{L_m}\right)\exp\left(-p^2\frac{t}{\tau_d^m}\right) \tag{5.32}$$

The fraction of the confinement memory available at any given time t is given by:

$$\psi_m(t)=\frac{1}{L_m}\int_0^{L_m}ds\psi(s,t)=\sum_{p;odd}\frac{8}{p^2\pi^2}\exp\left(-p^2\frac{t}{\tau_d^m}\right) \tag{5.33}$$

5.4 Constitutive Relation

The contribution of a m section to the relaxation modulus of the ring chain is related to the fraction of confinement memory equation (5.33) and is given by:

$$G_m(t)=G^0\psi_m(t) \tag{5.34}$$

In equation (5.34) G^0 is the modulus at time $t=\tau_e(\tau_e<\tau_1)$, which is the time required for a blob to move a distance of order of its size a, and at which time $\psi_m(\tau_e)=1$. τ_e is obtained from

the relationship between time and average mean-square displacement of a blob in an m section and is given by (see Appendix B.2):

$$\tau_e = \frac{\pi^{9/2}}{3 \times 4^4} \left(\Gamma \left[\frac{3}{4} \right] \right)^{-4} \frac{a^4}{b^2} \frac{\zeta}{k_B T} \approxeq 1.7 \tau_m \tag{5.35}$$

The relaxation modulus expression of fractal Rouse chain at τ_e can be shown to be (see equation (B.33)):

$$G(\tau_e) = \frac{c_b}{m} k_B T \sum_p \exp\left(-2 \frac{t}{\tau_p} \right) \tag{5.36}$$

Moving from discrete to continuous expression:

$$G(\tau_e) = \frac{c_b}{m} k_B T \int_0^\infty dp \, \exp\left(-2 \frac{t}{\tau_p} \right) = \frac{c_b}{m} k_B T \sqrt{\frac{\pi}{8}} \sqrt{\frac{\tau_1}{\tau_e}} \tag{5.37}$$

Using equation (5.35) and (5.21) in equation (5.37) we obtain:

$$G^0 = G(\tau_e) = \frac{8}{\sqrt{2}\pi^{5/2}} \left(\Gamma \left[\frac{3}{4} \right] \right)^2 c_b k_B T \approxeq 0.5 c_b k_B T \tag{5.38}$$

Dynamic self similarity, as indicated by the simulations of Obukhov et al (Obukhov *et al.*, 1994), suggests that all sections of the ring chain $m = 1, 2, ..N$ relax in a manner described in the previous section 5.3. Unlike covalently connected branched polymers in which different sections of the polymer relax in a hierarchical manner with the relaxation of larger structures occurring only after smaller substructures attached to them have relaxed, the different sections of a ring chain relax simultaneously since they are not pinned. Thus, the overall relaxation modulus of the ring chain is given by the superposition of the relaxation moduli of all sections weighted by the number fraction of such sections:

$$G(t) = \sum_m n_m G_m(t) \tag{5.39}$$

n_m in equation (5.39) is the number fraction of m sections of the ring chain trapped in a pair of gates. Another interpretation of equation (5.39) is that the stress in the system of a ring in fixed obstacles is supported by gates. In a double-folded Cayley tree conformation of a ring chain the positions of obstacles that divides the chain in to two closed loops having a common origin can be considered as gates (Figure 5.1). If the double folded ring chain is collapsed to a single line of highest density then the gate corresponds to an entanglement which divides the ring in to two parts. The collapsed structure is similar to that of hyperbranched polymer and the gate can be considered to be a bond that divides it into two parts (Figure 5.3). Withdrawal of sections of the ring from their gates causes relaxation of the stress.

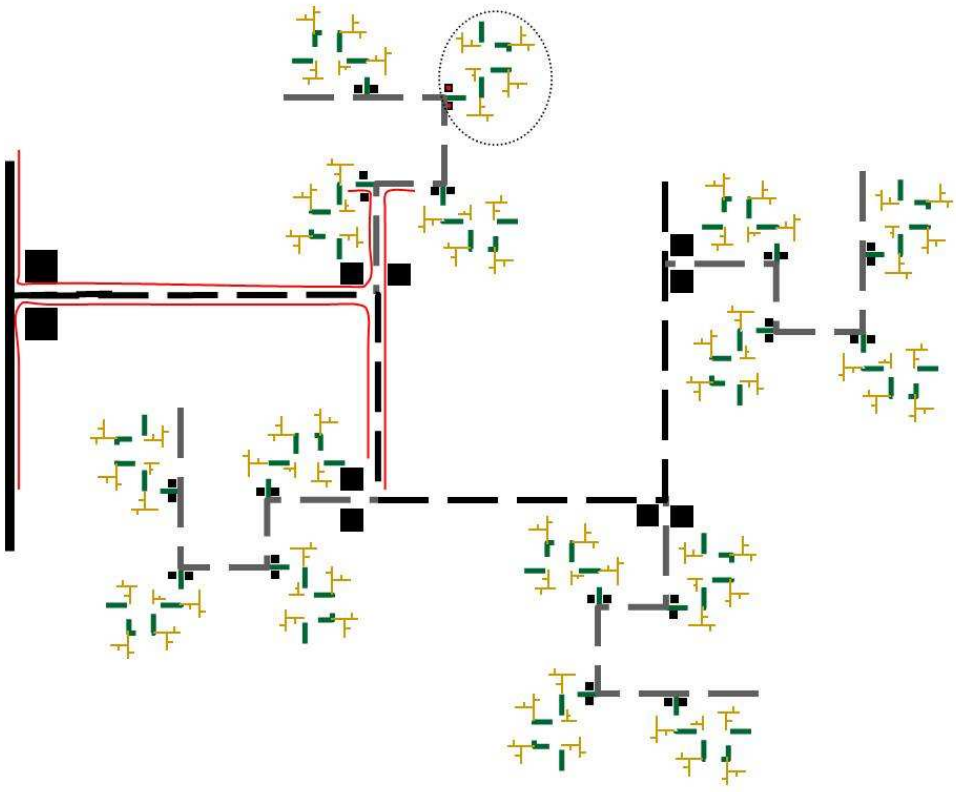

Figure 5.3: Shown is a part of the double folded ring chain (in red) collapsed into lines so that the structure resembles a hyperbranched polymer. An m section of the ring chain is shown in dotted circle and is confined by the gates shown in red. The gate is equivalent to a bond of the hyperbranched polymer that divides it into two parts of m and $N - m$ segments.

It now remains to calculate the number fraction of m sections of the ring chain entrapped by a pair of gates. The fraction of such gates can be determined from the probability of finding bonds in a hyperbranched polymer of segments that divides the polymer into two parts of m and $N-m$ segments (see Appendix B.4). The Cayley tree structure of the ring can be thought of as formed by condensation polymerization of A_z monomers, where z is the coordination number of the Cayley tree lattice. In this case since the polymer molecules are composed of only A groups the probability of finding an unreacted A group as a part of a m-mer is the same as that of number fraction of m-mers associated with AB_{z-1} condensation polymerization and is given by (see Appendix B.4):

$$u_m(\epsilon) = \frac{1}{\sqrt{2\pi}}\sqrt{\frac{z-1}{z-2}}m^{-3/2}\exp(-\epsilon^2 m) \tag{5.40}$$

for $m >> 1$. ϵ in equation (5.40) is the relative extent of reaction given by $\epsilon = (\varphi - \varphi_c)/\varphi_c$, where φ and φ_c are respectively the conversion and critical conversion for gelation; ϵ takes values between 0 and -1. The probability of forming a hyperbranched N-mer that was formed by reaction of two hyperbranched polymers composed of m and $N-m$ segments respectively is given by the product of the probability of finding an unreacted A group as part of an m-mer and the probability of finding an unreacted A group as part of $(N-m)$-mer:

$$\begin{aligned} u_{m|N-m}(\epsilon) &= u_m(\epsilon) \times u_{N-m}(\epsilon) \\ &= \frac{1}{2\pi}\frac{z-1}{z-2}m^{-3/2}(N-m)^{-3/2}\exp(-\epsilon^2 N) \end{aligned} \tag{5.41}$$

for $m >> 1$ and $N - m >> 1$. Thus, the number fraction of gates associated with a ring chain made up of loops of m segments is given by normalizing the probability:

$$n_m = \frac{u_{m|N-m}}{\sum_m u_{m|N-m}} \approxeq \frac{1}{4}\, m^{-3/2} \tag{5.42}$$

The constitutive equation for rings in an array of fixed obstacles is given by the combination of eqs. (5.34-5.39) and eq (5.42) and may be written as:

$$G(t) \approxeq \frac{1}{4}\sum_m m^{-3/2}G_m(t) = \frac{16}{\sqrt{2}\pi^{9/2}}\left(\Gamma\left[\frac{3}{4}\right]\right)^2 c_b k_B T \int_1^N dm\, m^{-3/2}\exp\left(-\frac{t}{\tau_d^m}\right) \tag{5.43}$$

In writing equation (5.43) we have assumed that since the right hand side of equation (5.33) is a rapidly converging series therefore only the first dominant term may be considered. Also, the summation over m has been replaced by an integral over m and can be justified for large N using the Taylor-Maclaurin approximation. It is worth noting that although the summation over

m is assumed to be from $m = 1$ to N the expression for n_m given in equation (5.42) cannot really be used over the entire range $m = 1, N$. Considering $\tau_d^m = \tau_0\ m^{5/2}$ and substituting $x = (t/\tau_0)m^{-5/2}$ equation (5.43) can be written as:

$$G(t) \approxeq \frac{32}{5\sqrt{2}} \frac{1}{\pi^{9/2}} \left(\Gamma\left[\frac{3}{4}\right]\right)^2 c_b k_B T \left(\frac{\tau_0}{t}\right)^{1/5} \int_{t/\tau_{ring}}^{t/\tau_0} dx\ x^{(1/5)-1} \exp(-x) \tag{5.44}$$

The integral is an incomplete gamma function $-\Gamma\left[\frac{1}{5}, \frac{t}{\tau_{ring}}\right]$ and for times $\frac{t}{\tau_{ring}} > 10$ can be approximated by $0.1 \exp\left(-\frac{t}{\tau_{ring}}\right)$ which shows that the relaxation modulus is dictated by exponential decay of the stress memory of the largest length scale (primary trunk) of the ring chain. The relaxation modulus expression can thus be approximated as:

$$\begin{aligned} G(t) &\approxeq \frac{32}{50\sqrt{2}} \frac{1}{\pi^{9/2}} \left(\Gamma\left[\frac{3}{4}\right]\right)^2 c_b k_B T \left(\frac{\tau_0}{t}\right)^{1/5} \exp\left(-\frac{t}{\tau_{ring}}\right) \\ &\approxeq 0.004 c_b k_B T \left(\frac{\tau_0}{t}\right)^{1/5} \exp\left(-\frac{t}{\tau_{ring}}\right) \end{aligned} \tag{5.45}$$

The relaxation modulus expression is in agreement with the scaling proposed by Kapnistos *et al.* (2008).

5.5 Comments on Melt of Rings

The following things are expected to change in going from rings in an array of fixed obstacles to a melt of rings:

1. While large rings are expected to retain a lattice animal configuration in melt, their fractal dimension can be anywhere between $2 < d_f < 4$; the Cates and Deutsch argument gives $d_f = 5/2$ and the same has been indicated by various simulations as described in section 2.1.2. Thus, the equations derived in sections 5.2–5.4 will have to be derived for a more general fractal structure.

2. The value of N_e will be governed by the flexibility of the polymer, and need not be the same as that for a linear chain.

3. Constraint release, which was irrelevant for the case of fixed obstacles, will become an important relaxation mechanism since faster modes of neighboring chains will dynamically relax the topological constraints of slower modes of any given chain.

There are various theoretical treatments to account for constraint release in the case of entangled linear chains (Marrucci, 1985; Tsenoglou, 1991; des Cloizeaux, 1990a,b). Following the tube dilation approach of Marrucci (1985) the constitutive relation for a melt of ring may be written as:

$$G(t) = G_0 \left(\sum_m n_m \psi_m(t) \right)^2 \tag{5.46}$$

In equation (5.46) the expression for n_m is given by equation (5.42)) and the expression for $G_m(t)$ is given by equations (5.33)–(5.38) with:

$$G(\tau_e) = G_0 = \frac{1}{2\sqrt{2}} \frac{1}{\nu^{\frac{1}{2\nu}}} \frac{1}{\pi^{\frac{\nu+1}{2\nu}}} \left(\Gamma[1-\nu]\right)^{\frac{1}{2\nu}} c_b k_B T \tag{5.47}$$

and τ_d^m is given by:

$$\tau_d^m = \frac{L_m^2}{D_{mR}\pi^2} = \frac{1}{\pi^2} \frac{a^4}{b^2} \frac{\zeta}{k_B T} m^{2\nu+2} \tag{5.48}$$

The expression for $G(\tau_e)$ is obtained by a procedure similar to that elaborated in section 5.4 using the expression (B.20) for τ_e and expression (B.6) for τ_1. The expression for τ_d^m is obtained using $L_m = m^{2\nu} a$ and expression (B.4) for D_{mR}.

In equation (5.48) $\nu = 1/d_f$. Substituting in equation (5.46) and solving yields:

$$G(t) = \varpi \left(\frac{\tau_0}{t}\right)^{1/(2\nu+2)} \left[\int_{(t/\tau_{ring})}^{(t/\tau_0)} x^{(1/2(2\nu+2))-1} \exp(-x) \right]^2 \tag{5.49}$$

where ϖ is given by:

$$\varpi = G_0 \frac{4}{\pi^4} \left(\frac{1}{2\nu+2} \right)^2 \tag{5.50}$$

The integral in the expression (5.49) is an incomplete gamma function $-\Gamma\left[\frac{1}{4\nu+4}, \frac{t}{\tau_{ring}}\right]$ and for $\frac{t}{\tau_{ring}} > 10$ can be approximated by an exponential decay $0.1 \exp\left(-\frac{t}{\tau_{ring}}\right)$. The long time response can thus be shown to be an exponential decay so that an approximate constitutive equation can be written in an asymptotic form as:

$$G(t) \approxeq \frac{\varpi}{10} \left(\frac{\tau_0}{t}\right)^{1/(2\nu+2)} \exp\left(-\frac{t}{\tau_{ring}}\right) \tag{5.51}$$

For $d_f = 4$ we obtain:

$$G(t) \approxeq 3.2 \times 10^{-5} c_b k_B T \left(\frac{\tau_0}{t}\right)^{2/5} \exp\left(-\frac{t}{\tau_{ring}}\right) \tag{5.52}$$

This equation is in agreement with that proposed by Kapnistos *et al.* (2008) except for the prefactor.

The gain and loss modulus can be obtained from the expression (5.51) through the transform:

$$G'(\omega) = \omega \int_0^\infty dt\, G(t)\, \sin(\omega t) \tag{5.53}$$

$$G''(\omega) = \omega \int_0^\infty dt\, G(t)\, \cos(\omega t) \tag{5.54}$$

The exponential decay in the relaxation modulus is expected to yield $G'(\omega) \sim \omega^2$ and $G''(\omega) \sim \omega$ at low frequencies $\omega << 1/\tau_{ring}$. At small times, *i.e.*, frequencies above the crossover frequency $\omega_c = 1/\tau_{ring}$ the power law decay is expected to be stronger than the exponential decay and hence we consider only the transform of the power law decay given by:

$$G'(\omega) \sim G''(\omega) \sim (\omega\tau_0)^{1/(2\nu+2)} \tag{5.55}$$

The equations (5.55) suggest that for higher than the crossover frequency the gain and loss moduli follow a power law frequency dependence. For $d_f = 4$ we have $G', G'' \sim \omega^{2/5}$. Thus, the high frequency behavior of rings is unlike linear entangled chains which show a constant gain modulus (the so called plateau modulus) and a decreasing loss modulus after the crossover frequency.

Chapter 6

Scaling Arguments in Semi-Dilute Solution

6.1 Concentration Dependence of Size

It is known that a flexible ring polymer takes a collapsed conformation in a topologically constraining environment such as in a gel (Khokhlov and Nechaev, 1985; Obukhov *et al.*, 1994) or a melt of ring polymers (Cates and Deutsch, 1986; Müller *et al.*, 1996; Brown and Szamel, 1998; Müller *et al.*, 2000; Arrighi *et al.*, 2004; Gagliardi *et al.*, 2005; Hur *et al.*, 2006; Kawaguchi *et al.*, 2006; Suzuki *et al.*, 2008). The collapse of a ring polymer in a melt environment is triggered by the non-concatenation topological constraint (Fig 6.1). In a semi-dilute solution we may expect the non-concatenation topological constraint to be activated at a concentration where the ring 'sees' other rings. Consequently, the non-concatenation constraint can be expected to change the concentration dependence of size of a ring chain from that of a linear chain.

We will define C^* as the threshold concentration where transition from dilute to semi-dilute regime happens, and $C^\#$ as the overlap concentration above which topological constraints are activated. In the semi-dilute regime, we may consider two cases:

- An unconstrained state between the threshold and the overlap concentrations, $C^* < C < C^\#$, where lack of sufficient ring chain neighbors prevents the collapse of ring chain.
- A topologically constrained state at higher concentrations $C > C^\#$ where a given ring chain is surrounded by many ring chain neighbors which causes the ring chain to take up collapsed lattice-animal conformation due to the non-concatenation constraint (Cates and Deutsch, 1986; Müller *et al.*, 2000).

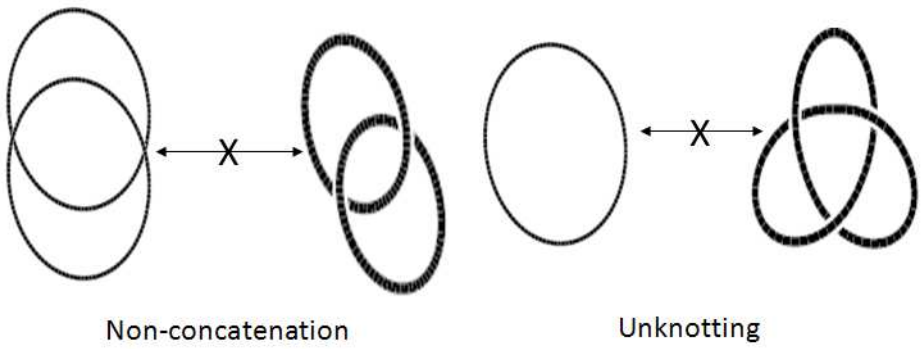

Figure 6.1: Schematic of topological constraints associated with ring polymers

Since the segment density of a lattice-tree increases with mass, large ring polymers at high concentration will experience interactions in order to avoid segment overlap events (Obukhov *et al.*, 1994). Therefore we also consider the cases of small and large ring polymers in the high concentration range.

6.1.1 Θ-Solvent

The size of a ring polymer in a Θ-solvent under dilute conditions is given by (Zimm and Stockmayer, 1949):

$$R_{dil}^2 = \frac{N_K b^2}{12} \tag{6.1}$$

As more ring polymers are dissolved in the solution a threshold is reached when the concentration of ring polymers in solution C^* becomes nearly equal to the segment density of a single chain. Thus,

$$C^* \sim \frac{N_K}{R_{dil}^3} \sim N_K^{-1/2} b^{-3} \tag{6.2}$$

At the overlap concentration C^* the correlation length ξ, *i.e.*, the mean distance between Kuhn segments on neighboring ring chains, is of the order of the ring size R_{dil}. Beyond the overlap concentration the solution enters the semi-dilute regime and ξ becomes smaller than R_{dil}. We may then expect ξ to be independent of the number of Kuhn segments N_K in a chain. The concentration dependence of the correlation length is then given by:

$$\xi \sim R_{dil} \left(\frac{C^*}{C} \right)^m \sim N_K^0 \tag{6.3}$$

Substituting from equations (6.1) and (6.2) into equation (6.3) we obtain $m = 1$. Thus, the correlation length depends inversely on the concentration:

$$\xi \sim R_{dil} \left(\frac{C^*}{C} \right) \tag{6.4}$$

Considering the ring chain to be composed of blobs of size ξ each made of N_b Kuhn segments the structure of the ring can be examined at length scales $< \xi$ and $> \xi$. Below the correlation length the chain segments behave as if they are under dilute Θ-solvent condition so that $\xi \sim N_b^{1/2} b$. From equation (6.4) we have:

$$N_b \sim N_K \left(\frac{C^*}{C} \right)^2 \tag{6.5}$$

Above the correlation length scale a ring polymer on an average sees only ring neighbors. For solution concentrations in the range $C^* < C < C^{\#}$ the non-concatenation constraints are weak and consequently the size of ring polymers is given by:

$$R \sim \xi \left(\frac{N_K}{N_b} \right)^{1/2} \tag{6.6}$$

Substituting from equations (6.4) and (6.5) into equation(6.6) we get:

$$R \sim R_{dil} \tag{6.7}$$

i.e., the size of the ring is independent of the solution concentration. At higher concentrations in the range $C > C^{\#}$ the non-concatenation constraints become effective at length scale of the order ξ. Ring polymers now take a lattice animal conformation at this length scale. We may then consider a ring to be composed of $N = N_K/N_b$ blobs each of size ξ and having only ring neighbors. The size of such a ring would be given by:

$$R \sim \xi \left(\frac{N_K}{N_b} \right)^{\nu} \tag{6.8}$$

Here, ν is a general exponent lying between 1/4 and 1/2 (Müller *et al.*, 2000). Substituting from equations (6.4) and (6.5) into equation (6.8) we get:

$$R \sim R_{dil} \left(\frac{C^*}{C} \right)^{1-2\nu} \tag{6.9}$$

6.1.2 Good Solvent

The scaling relations for ring size in good solvent can be derived using the same arguments presented in section 6.1.1. Thus, the ring size in dilute solution and the overlap concentration

are given by:

$$R_{dil} \sim N_K^{3/5} b \tag{6.10}$$

$$C^* \sim \frac{N_K}{R_{dil}^3} \sim N_K^{-4/5} b^{-3} \tag{6.11}$$

The correlation length is given by:

$$\xi \sim R_{dil} \left(\frac{C^*}{C} \right)^{3/4} \tag{6.12}$$

and the number of Kuhn segments in a blob of size ξ is given by:

$$N_b \sim N_K \left(\frac{C^*}{C} \right)^{5/4} \tag{6.13}$$

At concentrations above the overlap concentration and at length scale of the order ξ the ring chain can be considered as being surrounded by only ring neighbors and therefore all excluded volume interactions can be considered to be screened. For solution concentrations in the range $C^* < C < C^{\#}$ the non-concatenation constraint are weak and the size of the ring is given by:

$$R \sim \xi \left(\frac{N_K}{N_b} \right)^{1/2} \tag{6.14}$$

Substituting from relations (6.12) and (6.13) into equation (6.14) we get:

$$R \sim R_{dil} \left(\frac{C^*}{C} \right)^{1/8} \tag{6.15}$$

At higher concentrations in the range $C > C^{\#}$ the non-concatenation constraint becomes effective and hence the size of the ring is given by:

$$R \sim \xi \left(\frac{N_K}{N_b} \right)^{\nu} \tag{6.16}$$

Substituting from relations (6.12) and (6.13) into relation (6.16) gives:

$$R \sim \xi \left(\frac{C^*}{C} \right)^{(3-5\nu)/4} \tag{6.17}$$

6.2 Concentration Dependence of Relaxation Time

In the chapters 3, 4 and 5 we saw that dynamics of non-concatenated ring polymers in a topologically constraining environment is different from that of linear polymers. In going from a dilute solution to a semi-dilute solution we already saw the influence of topological constraints

playing a role in altering the structure and consequently the size of the ring chain. Further, on activation of the topological constraints the dynamics is expected to change from Zimm to Rouse and at higher concentrations to the Cayley tree structure dynamics discussed in detail in the previous chapters. It is useful to explore the concentration dependence of the longest relaxation time as an aid to understand the influence of concentration on the dynamic response of the ring polymer. Due to the difference in dynamic response of the ring polymer from that of the linear polymer the concentration dependence of longest relaxation time of a ring chain in semi-dilute solution is expected to be different from that of a linear chain.

6.2.1 Θ-Solvent

We start by looking at the dynamic response of a ring polymer in dilute regime. The relaxation time as per Zimm dynamics is given by (Doi and Edwards, 1986; Liu and Öttinger, 1987):

$$\tau_{dil} \simeq \frac{\eta_s b^3 N_K^{3/2}}{\sqrt{3\pi} k_B T} \tag{6.18}$$

In the semi-dilute regime it is known that the hydrodynamic screening length, ξ_H, is of the same order as the correlation length ξ (Rubinstein and Colby, 2003). As the concentration increases beyond the overlap concentration both the correlation length and the hydrodynamic screening length decrease. The latter causes an alteration of the dynamic response and hence we expect the relaxation time to show concentration dependence. In the semi-dilute regime the dynamics of a ring chain is different at different length scales. Below a length scale of ξ the chain sees dilute solution and hence hydrodynamic interactions are active. Above the length scale of ξ a coarse grained chain sees only ring neighbors and hence the hydrodynamic interactions are screened. For solution concentrations in the range $C^* < C < C^{\#}$ the relaxation time of a coarse grained ring chain is given by:

$$\tau \sim \tau_\xi \left(\frac{N_K}{N_b}\right)^2 \tag{6.19}$$

Here τ_ξ is the Zimm relaxation time of a blob of size ξ containing N_b Kuhn segments and is given by:

$$\tau_\xi \simeq \frac{\eta_s b^3 N_b^{3/2}}{\sqrt{3\pi} k_B T} \simeq \frac{\eta_s}{\sqrt{3\pi}} \xi^3 \tag{6.20}$$

where we have made use of the relation $\xi \sim N_b^{1/2} b$. Substituting from relation (6.20) into equation (6.19) and using relations (6.4) and (6.5) we get:

$$\tau \sim \tau_{dil} \left(\frac{C^*}{C}\right)^{-1} \tag{6.21}$$

At higher concentrations in the range $C > C^{\#}$ coarse grained ring chains assume lattice-tree conformation and their dynamics are governed by rearrangement of this structure as discussed in the previous chapters. If the ring chains are small such that excluded volume interactions due to segment overlap can be neglected then the longest relaxation time of such chains is given by:

$$\tau \sim \tau_{\xi} \left(\frac{N_K}{N_b} \right)^{2\nu+2} \tag{6.22}$$

The assumptions made in determining the longest relaxation time for the case of melt of ring polymers are implicit in using equation (6.22) for estimating the longest relaxation time in semi-dilute solution. Substituting $N_b \sim (\xi/b)^2$ and τ_{ξ} from relation (6.20) into relation (6.22), and using relations (6.4) and (6.5) we obtain:

$$\tau \sim \tau_{dil} \left(\frac{C^*}{C} \right)^{-(4\nu+1)} \tag{6.23}$$

Large ring chains would assume a self avoiding lattice-tree conformation for which the molecular weight dependence of the size of the chain remains unchanged; however, the trunk is stretched in a way similar to that in annealed branched polymers (Gutin *et al.*, 1993) (see section 2.1.2). The concentration and molecular weight at which stretching effects might become relevant can be estimated by considering that stretching is activated when the ratio of excluded volume of Kuhn segment pairs to the pervaded volume is greater than unity, *i.e.*, when $N_K^2(b^2 r)/R^3 > 1$ (Obukhov *et al.*, 1994). Here, r is the cross-sectional radius of the chain and $b^2 r$ is the excluded volume of a Kuhn segment. Using relation (6.9) for R and relation (6.1) for R_{dil} it can be shown that the stretching effects cannot be neglected when:

$$\sqrt{N_K} \left(\frac{C}{C^*} \right)^{3(1-2\nu)} > \frac{b}{r} \tag{6.24}$$

In a melt of ring polymers the concentration can be written as $C_{melt} \sim N_e/a^3$, where, a is the correlation length and N_e is the number of Kuhn segment in a blob of size a. Equation (6.24) is then equivalent to the condition $N > (b^2/ar)^{1/(2-3\nu)}$.

The longest relaxation time of a self avoiding lattice-tree is given by:

$$\tau \sim \tau_{\xi} \left(\frac{N_K}{N_b} \right)^{2+\rho} \tag{6.25}$$

where $\rho = (2\nu + 1)/3$ (Gutin *et al.*, 1993) (see section 2.1.2). Substituting $N_b \sim (\xi/b)^2$ and τ_{ξ} from relation (6.20) into relation (6.23) and using relations (6.4) and (6.5) we obtain:

$$\tau \sim \tau_{dil} \left(\frac{C^*}{C} \right)^{-(4\nu+5)/3} \tag{6.26}$$

6.2.2 Good Solvent

The scaling relations for the longest relaxation time of a ring chain dissolved in a good solvent in semi-dilute regime can be derived using the same arguments presented in section 6.2.1. The relaxation time of a ring chain in a dilute solution of a good solvent is given by:

$$\tau_{dil} \simeq \frac{\eta_s (b N_K^{3/5})^3}{\sqrt{3\pi} k_B T} \tag{6.27}$$

For solution concentrations in the range $C^* < C < C^{\#}$ the relaxation time of a coarse grained ring chain is given by equation (6.20) where:

$$\tau_\xi \simeq \frac{\eta_s (b N_b^{3/5})^3}{\sqrt{3\pi} k_B T} \simeq \frac{\eta_s}{\sqrt{3\pi}} \xi^3 \tag{6.28}$$

Here we have made use of the relation $\xi \sim N_b^{3/5} b$. Substituting τ_ξ from relation (6.28) into relation (6.19), and using relations (6.12) and (6.11) we get:

$$\tau \sim \tau_{dil} \left(\frac{C^*}{C} \right)^{-(1/4)} \tag{6.29}$$

At higher concentrations in the range $C > C^{\#}$ the relaxation time of a small ring chain is given by equation (6.22). Substituting $N_b \sim (\xi/b)^{5/3}$ and τ_ξ from relation (6.28) into equation (6.22), and using relations (6.11) and (6.10) we get:

$$\tau \sim \tau_{dil} \left(\frac{C^*}{C} \right)^{-(10\nu+1)/4} \tag{6.30}$$

Large ring polymers will experience excluded volume interactions due to segment overlap when $N_K^2 (b^2 r)/R^3 > 1$. Using equations (6.17) and (6.10) it can be shown that the excluded volume interactions become important when:

$$N_K^{1/5} \left(\frac{C}{C^*} \right)^{3(3-5\nu)/4} > \frac{b}{r} \tag{6.31}$$

The longest relaxation time of such a chain is given by equation (6.25). Substituting $N_b \sim (\xi/b)^{5/3}$ and τ_ξ from relation (6.28) into equation (6.25), and using relations (6.12) and (6.10) we get:

$$\tau \sim \tau_{dil} \left(\frac{C^*}{C} \right)^{-(5\nu+4)/6} \tag{6.32}$$

6.3 Diffusion Coefficient

Diffusion studies on ring polymers aimed at understanding the effect of absence of chain ends on polymer dynamics has been a subject of recent interest (Klein, 1986; Mills *et al.*, 1987; Cosgrove *et al.*, 1992, 1996; Müller *et al.*, 1996; Brown and Szamel, 1998; Müller *et al.*, 2000; Hur *et al.*, 2006; Kawaguchi *et al.*, 2006; Kanaeda and Deguchi, 2008). Diffusion of flexible ring chains through a gel/cross-linked network can be considered as a model system for providing insights into diffusion of plasmid DNA in gel-electrophoresis and controlled drug delivery systems. The diffusion coefficient of a ring polymer is given by:

$$D \sim \frac{R^2}{\tau} \tag{6.33}$$

where, R^2 is the mean size of the ring chain and τ is its longest relaxation time. The concentration dependence of size and relaxation time for a ring chain in semi-dilute solution, derived in the previous sections, can be used in expression (6.33) to obtain the concentration dependence of diffusion coefficient.

6.3.1 Θ-Solvent

We have used the relevant equations from sections (6.1.1) and (6.2.1) in expression (6.33) to obtain the scaling relations for the diffusion coefficient shown in Table (6.1). In Table (6.1) we have used $\rho = (2\nu + 1)/3$ and:

$$D_{dil} \sim \frac{R^2_{dil}}{\tau_{dil}} \simeq \frac{\sqrt{3\pi} k_B T}{\eta_s b N_K^{1/2}} \tag{6.34}$$

6.3.2 Good Solvent

We have used the relevant equations from sections (6.1.2) and (6.2.2) in expression (6.33) to obtain the scaling relations for the diffusion coefficient shown in Table (6.2). In Table (6.2) we have used $\rho = (2\nu + 1)/3$ and:

$$D_{dil} \sim \frac{R^2_{dil}}{\tau_{dil}} \simeq \frac{\sqrt{3\pi} k_B T}{\eta_s b N_K^{3/5}} \tag{6.35}$$

Regime	R	τ	$D \sim R^2/\tau$
Dilute $(C < C^*)$	$R_{dil} \sim N_K^{1/2} b$	$\tau_{dil} \sim \frac{\eta_s b^3 N_K^{3/2}}{\sqrt{3\pi} k_B T}$	$\frac{\sqrt{3\pi} k_B T}{\eta_s b N_K^{1/2}} \left(\frac{C^*}{C}\right)^0$
Semi-dilute $(C^* < C < C^\#)$	R_{dil}	$\tau_{dil} \left(\frac{C^*}{C}\right)^{-1}$	$D_{dil} \left(\frac{C^*}{C}\right)$
Small Ring Chain Semi-dilute $(C > C^\#)$	$R_{dil} \left(\frac{C^*}{C}\right)^{1-2\nu}$	$\tau_{dil} \left(\frac{C^*}{C}\right)^{-(4\nu+1)}$	$D_{dil} \left(\frac{C^*}{C}\right)^3$
Large Ring Chain Semi-dilute $(C > C^\#)$ $\sqrt{N_K} \left(\frac{C^*}{C}\right)^{3(1-2\nu)} > \frac{b}{r}$	$R_{dil} \left(\frac{C^*}{C}\right)^{1-2\nu}$	$\tau_{dil} \left(\frac{C^*}{C}\right)^{-(4\nu+5)/3}$	$D_{dil} \left(\frac{C^*}{C}\right)^{(11-8\nu)/3}$

Table 6.1: Scaling relationships for ring polymers in Θ-solvent semi-dilute solution

Regime	R	τ	$D \sim R^2/\tau$
Dilute $(C < C^*)$	$R_{dil} \sim N_K^{3/5} b$	$\tau_{dil} \sim \frac{\eta_s (b N_K^{3/5})^3}{\sqrt{3\pi} k_B T}$	$\frac{\sqrt{3\pi} k_B T}{\eta_s b N_K^{3/5}} \left(\frac{C^*}{C} \right)^0$
Semi-dilute $(C^* < C < C^\#)$	$R_{dil} \left(\frac{C^*}{C} \right)^{1/8}$	$\tau_{dil} \left(\frac{C^*}{C} \right)^{-1/4}$	$D_{dil} \left(\frac{C^*}{C} \right)^{1/2}$
Small Ring Chain Semi-dilute $(C > C^\#)$	$R_{dil} \left(\frac{C^*}{C} \right)^{(3-5\nu)/4}$	$\tau_{dil} \left(\frac{C^*}{C} \right)^{-(10\nu+1)/4}$	$D_{dil} \left(\frac{C^*}{C} \right)^{7/4}$
Large Ring Chain Semi-dilute $(C > C^\#)$ $N_K^{1/5} \left(\frac{C^*}{C} \right)^{(13-10\nu)/6} > \frac{b}{r}$	$R_{dil} \left(\frac{C^*}{C} \right)^{(3-5\nu)/4}$	$\tau_{dil} \left(\frac{C^*}{C} \right)^{-(5\nu+4)/12}$	$D_{dil} \left(\frac{C^*}{C} \right)^{(11-8\nu)/3}$

Table 6.2: Scaling relationships for ring polymers in good solvent semi-dilute solution

6.4 Ring-Linear Blends

A simple Flory-like free energy argument was used by Cates and Deutsch (Cates and Deutsch, 1986) to show the effect of the non-concatenation constraint on the size of a ring polymer (see section 2.1.2). According to this argument the free energy of a ring polymer can be written as:

$$F(R) = \frac{R^3}{N_K} + \frac{N_K}{R^2} \tag{6.36}$$

It is argued that one degree of freedom is lost due to presence of a ring neighbor contributing to the non-concatenation constraint. The number of ring neighbors scales as R^3/N_K in pure melt and hence degrees of freedom lost scales as R^3/N_K. The non-concatenation constraint being compressive is balanced by the Gaussian free energy penalty against compression N_K/R^2. The free energy minimization $dF/dR = 0$ yields $R \sim N_K^{2/5}$.

In a melt of ring chain addition of a linear chain is expected to dilute the non-concatenation constraint and consequently swell the ring chain. For determining the size dependence of a ring chain on its concentration in a ring-linear blend we start the scaling arguments from the case of small amount of ring chains in a melt of linear chains. A ring-linear blend at low concentration of rings in a linear melt can be thought of as dilute solution of rings. Since the ring polymer does not experience excluded volume interactions in a sea of linear chains its conformation is identical to that in a Θ-solvent. At the threshold concentration C_r^* the concentration in the solution is the same as the concentration of Kuhn segments within a single ring chain. This concentration is given by the ratio of number of Kuhn segments in a single ring chain, N_K, to the pervaded volume of the ring chain in dilute solution,$(R_{dil})^3 \sim N_K^{3/2}$:

$$C_r^* = \frac{N_K}{(R_{dil})^3} \sim \frac{N_K}{N_K^{3/2}} \sim N_K^{-1/2} \tag{6.37}$$

At the threshold concentration, C_r^*, the correlation length, ξ, *i.e.*, the mean distance between Kuhn segments on neighboring ring chains is of the order of the size of the ring chain, R_{dil}. Beyond the threshold concentration C_r^* the ring-linear blend enters the semi-dilute regime and the correlation length ξ becomes lower than that of the radius of gyration, R_{dil}. Further we expect the correlation length to be independent of number of Kuhn segments in the chain, N_K, beyond the overlap threshold concentration. The correlation length dependence on the concentration is then given by:

$$\xi = R_{dil} \left(\frac{C_r^*}{C_r} \right)^m \sim N_K^0 \tag{6.38}$$

Using $R_{dil} \sim N_K^{1/2}$, the scaling relationship for C_r^* given by equation(6.37) and noting that C_r is independent of N we obtain $m = 1$. Thus, the correlation length scales inversely as the concentration in the semi-dilute regime, $\xi(C_r) \sim (C_r/C_r^*)^{-1}$.

Considering the ring chain to be composed of blobs of size ξ made of say, N_b, Kuhn segments, the ring chain can be examined at length scales $< \xi$ and of the order of $\sim \xi$. Below the correlation length scale, ξ, we argue that the ring encounters on an average only linear neighbors and the chain section in a blob of size ξ behaves as if it is under Θ-conditions. This gives the correlation length ξ scaling as $N_b^{1/2}$. Given that $\xi(C_r) \sim (C_r/C_r^*)^{-1}$ we have $N_b \sim (C_r/C_r^*)^{-2}$. For a coarse grained picture on length scales of the order of ξ we argue that ring on an average only sees ring chain neighbors. The non-concatenation constraint becomes operational at this length scale and hence the ring would appear to have a lattice-tree structure (Cates and Deutsch, 1986). As per the arguments in section 6.1.1 the non-concatenation constraints become active at a concentration $C_r > C_r^{\#}$

At the length scale ξ we consider the ring to be composed of N_K/N_b segments of length ξ with only ring neighbors. Such a structure would have a size scaling as $(N_K/N_b)^{\nu}\xi$, where ν is a general exponent lying between 1/4 and 1/2 (Khokhlov and Nechaev, 1985; Müller *et al.*, 2000). Noting that N_K is independent of concentration, $N_b \sim (C_r/C_r^*)^{-2}$ and $\xi \sim (C_r/C_r^*)^{-1}$ we have (identical to relation (6.9)):

$$R_r \sim \left(\frac{C_r^0}{(C_r/C_r^*)^{-2}}\right)^{\nu} \left(\frac{C_r}{C_r^*}\right)^{-1} \sim \left(\frac{C_r}{C_r^*}\right)^{2\nu-1} \tag{6.39}$$

In the case we use $\nu = 2/5$, as indicated by the Cates and Deutsch argument (Cates and Deutsch, 1986), we obtain that in the semi-dilute regime the radius of gyration of a ring chain scales with concentration of ring as $(C_r/C_r^*)^{-1/5}$.

We can follow a similar line of reasoning for the case of linear chains in a melt of ring chains starting from a small fraction of linear chains up to the semi-dilute regime. In the semi-dilute regime the linear chains can also be considered to be composed of blobs of size ξ. Due to the absence of non-concatenation constraint the linear chain has the same scaling of the size at length scales $< \xi$ and of the order of ξ. This yields a size of the linear in the semi-dilute regime scaling as $(N_K/N_b)^{1/2}\xi$. Noting that N_K is independent of concentration, $N_b \sim C_l^{-2}$ and $\xi \sim C_l^{-1}$ we have:

$$R_l \sim \left(\frac{C_l^0}{C_l^{-2}}\right)^{1/2} C_l^{-1} \sim C_l^0 \tag{6.40}$$

It is observed from relation (6.40) that in the case of linear chains the radius of gyration is

independent of concentration C_l. This is expected as the linear chains do not have a constraint imposed with change of its neighbors unlike the ring chains.

A simple extension of relation (6.36) to the case of ring-linear blend in the limit of $C_r > C_r^*$ in the semi-dilute regime can be written as:

$$\frac{F(R)}{k_BT} = \Phi\frac{R^3}{N_K} + \frac{N_K}{R^2} \tag{6.41}$$

where, Φ is the fraction of ring neighbors of any given ring in a ring-linear blend. In a mean field sense this is expected to be the same as the number fraction of rings in the system. We have assumed in relation (6.41) that the entropic penalty scales linearly with the number fraction of rings in the semi-dilute regime. The minimization of free energy relation (6.41) with respect to R yields:

$$R \sim N^{2/5}\Phi^{-1/5}. \tag{6.42}$$

The number fraction Φ is given by :

$$\Phi = \frac{n_r}{n_r + n_l} \tag{6.43}$$

where, n_r and n_l are the number of ring and linear chains in the system respectively. The density of a ring-linear blend made of ring and linear polymers of identical repeat units remains unaltered with amount of ring and linear chains in the system. Considering density of system remains constant we have the number density of the system a constant and hence $n_r + n_l$ can be considered constant for a given volume of the blend.

If $n_r + n_l$ remains constant in the system, then we have from relation (6.43) $(\Phi/\Phi^*) \sim (n_r/n_r^*) \sim (C_r/C_r^*)$, where, Φ^* is the number fraction at threshold concentration. Using this in relation (6.39) we have:

$$R_r \sim \left(\frac{\Phi}{\Phi^*}\right)^{2\nu-1} \tag{6.44}$$

Comparing the scaling results in relation (6.44) for $\nu = 2/5$ with the free energy based scaling results in relation (6.42) we see that the results of free energy minimization corroborate with the concentration scaling arguments.

6.5 Results and Discussion

Concentration dependence of the self diffusion coefficients of a ring polymer are shown schematically in figures 6.2 and 6.3, respectively, for the Θ-solvent and good-solvent cases. In these

Regime	R	τ	$D \sim R^2/\tau$
Dilute $(C < C^*)$	$R \sim N_K^{1/2} b$	$\tau \sim \frac{\eta_s (b N_K^{1/2})^3}{\sqrt{3\pi} k_B T}$	$\frac{\sqrt{3\pi} k_B T}{\eta_s b N_K^{1/2}} \left(\frac{C^*}{C}\right)^0$
Semi-dilute $(C < C < C^\#)$	$bN_K^{1/2}$	$\tau_{dil} \left(\frac{C^*}{C}\right)^{-1}$	$D_{dil} \left(\frac{C^*}{C}\right)$
Semi-dilute $(C > C^\#)$	$bN_K^{1/2}$	$\tau_{dil} \left(\frac{C^*}{C}\right)^{-3}$	$D_{dil} \left(\frac{C^*}{C}\right)^3$

Table 6.3: Scaling relationships for linear polymers in Θ-solvent semi-dilute solution

figures C^{ex} indicates the threshold concentration above which excluded volume interactions due to ring segment overlap are active. The concentration dependence of the diffusion coefficient of a linear polymer in Θ-solvent and good-solvent cases are given in Table 6.3 and Table 6.4, respectively, for comparative purpose. We observe that in the regimes $C^* < C < C^\#$ and $C > C^\#$ the concentration dependence of diffusion coefficients for ring polymers are identical to those for linear polymers. However, the presence of excluded volume interactions for large ring polymers at high concentration causes the diffusion coefficient to decrease relatively weakly with concentration for all $\nu > 1/4$. We also note that by combining the equations for C^* [relations (6.2) and (6.11)] and D_{dil} [relations (6.34) and (6.35)] for small ring polymers we obtain the molecular weight dependence of diffusion coefficient namely, $D \sim N_K^{-1}$ in the concentration range $C^* < C < C^\#$ and $D \sim N_K^{-2}$ in the concentration range $C > C^\#$ for both θ-solvent and good solvent cases, which is similar to that for linear polymers. For large ring polymers at high concentrations where excluded volume interactions can become relevant we get $N_K^{(7-4\nu)/3}$ for both Θ-solvent and good solvent cases, which is a slightly weaker dependence than for small ring polymers for all $\nu > 1/4$. In figures 6.3 and 6.4, respectively, the comparison of scaled self-diffusion coefficients and scaled radii of gyration of a ring in good solvent obtained from MC simulations are shown to be in good agreement with the scaling relationships.

We compare the relations summarized in Table 6.2 with the experimental data of Robert-

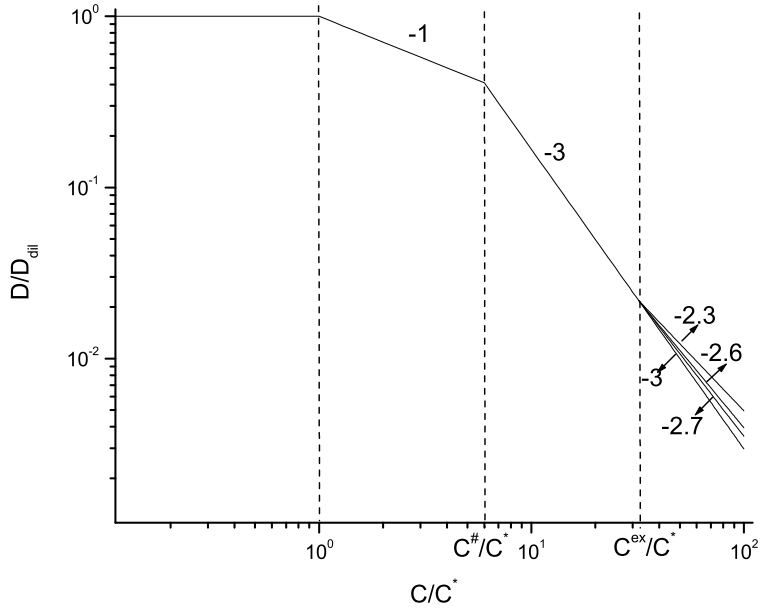

Figure 6.2: Concentration dependence of diffusion coefficient for Θ-solvent

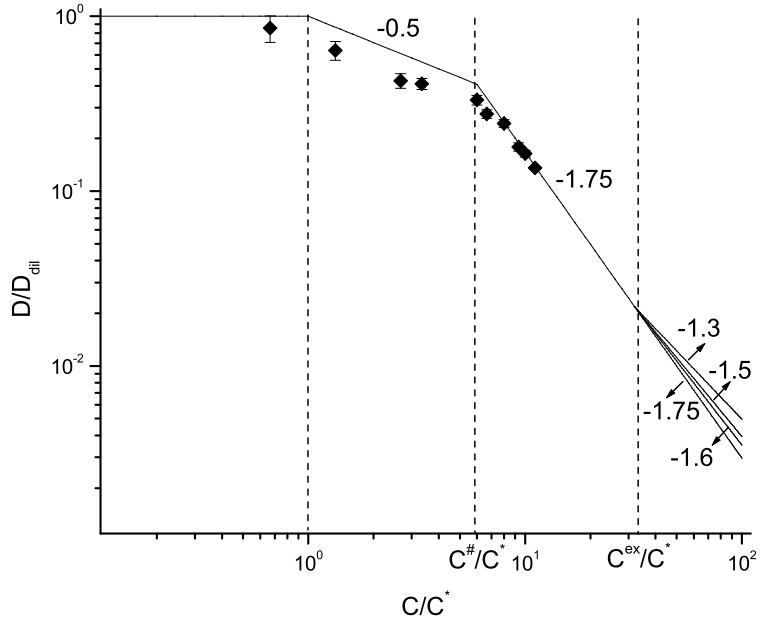

Figure 6.3: Concentration dependence of diffusion coefficient in good-solvent. Points obtained from MC simulations by Sachin Shanbhag.

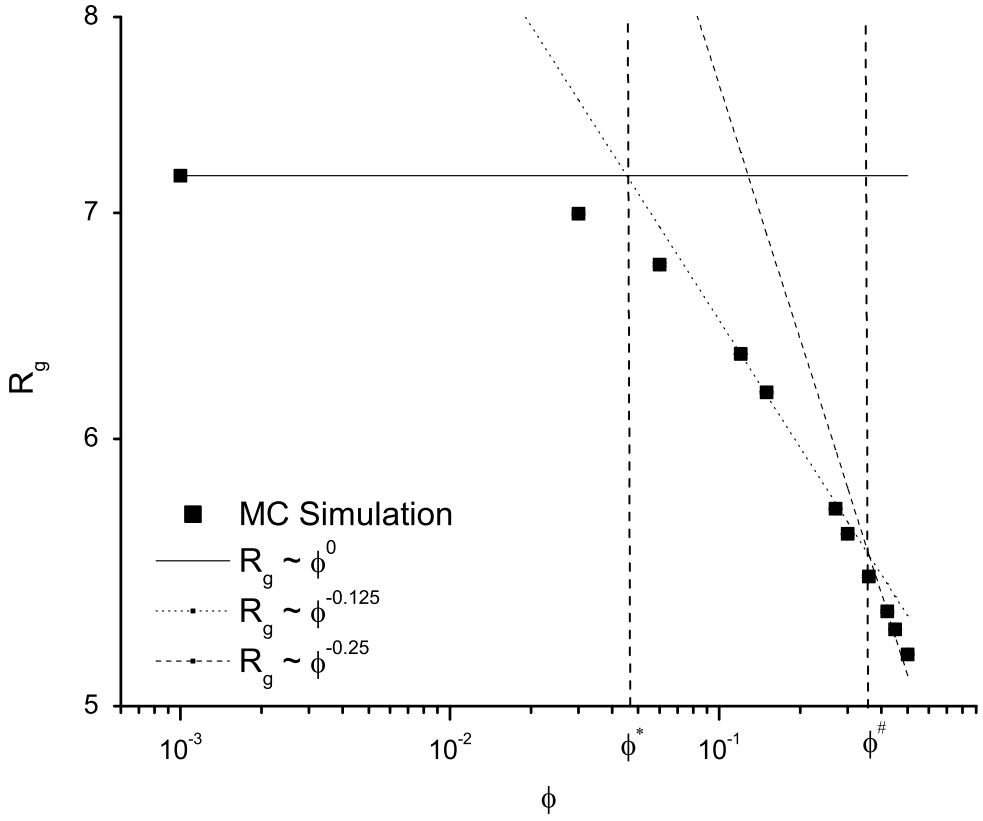

Figure 6.4: Comparison of the concentration dependence of size of a ring polymer in good-solvent obtained from MC simulations by Sachin Shanbhag (points) and scaling arguments (lines obtained using $\nu = 2/5$ in Table 6.2).

Regime	R	τ	$D \sim R^2/\tau$
Dilute $(C < C^*)$	$R \sim N_K^{3/5} b$	$\tau \sim \frac{\eta_s (b N_K^{3/5})^3}{\sqrt{3\pi} k_B T}$	$\frac{\sqrt{3\pi} k_B T}{\eta_s b N_K^{3/5}} \left(\frac{C^*}{C}\right)^0$
Semi-dilute $(C < C < C^{\#})$	$R_{dil} \left(\frac{C^*}{C}\right)^{1/8}$	$\tau_{dil} \left(\frac{C^*}{C}\right)^{-1/4}$	$D_{dil} \left(\frac{C^*}{C}\right)^{1/2}$
Semi-dilute $(C > C^{\#})$	$R_{dil} \left(\frac{C^*}{C}\right)^{1/8}$	$\tau_{dil} \left(\frac{C^*}{C}\right)^{-3/2}$	$D_{dil} \left(\frac{C^*}{C}\right)^{7/4}$

Table 6.4: Scaling relationships for linear polymers in Good solvent semi-dilute solution

son and Smith (2007b) on self diffusion coefficient of cyclic DNA of different chain lengths (5.9-45 kbp) dissolved in aqueous buffer solution in the semi-dilute regime. The data shows that the self diffusion coefficients of all cyclic DNAs scale as $D \sim L^{-n} C^{-0.5}$ at lower concentrations, where L and C are the contour length and the concentration, respectively, of cyclic DNA in the buffer solution and $n \sim 0.5 - 1$. The concentration dependence is in agreement with the prediction in the concentration range $C^* < C < C^{\#}$ reported in Table 6.2. Noting that the contour length is proportional to the number of Kuhn segments, the observed molecular weight scaling corresponds to either dilute or semi-dilute case. Above a concentration of approximately $C^{\#} \approx 4C^*$, being the overlap concentration, the diffusion coefficients for the 25 and 45 kbp cyclic DNAs scale as $D \sim L^{-m} C^{-1.75}$; the observed values for the exponent m are in the range 1-2. While the molecular weight dependence corresponds to somewhere between Rouse regime ($C^* < C < C^{\#}$) and topologically constrained regime ($C > C^{\#}$), the concentration dependence is in agreement with the prediction for a small ring in the concentration range $C > C^{\#}$.

Considering the DNA to be composed of blobs, with each blob containing N_ξ Kuhn segments, the diffusion coefficients of a linear chain under such conditions is given by Doi and Edwards (1986) model:

$$D_{linear} = \frac{1}{3} \frac{k_B T}{\zeta} \frac{N_\xi}{N_K^2} \tag{6.45}$$

where, ζ is the friction coefficient of a Kuhn segment. Different expressions for the diffusion

coefficient of ring chain can be got from the PPR model, BS model and FG model respectively given by:

$$D_{PPR} = \frac{1}{3} D_P \frac{a}{L_P} = \frac{1}{3} \frac{k_B T}{\zeta} \frac{N_\xi}{N_K^2} \tag{6.46}$$

$$D_{BD} = \frac{k_B T}{\zeta} \frac{N_\xi}{N_K^2} \tag{6.47}$$

$$D_{FG} = \frac{1}{3} D_N \frac{a}{L_N} = \frac{1}{3} \frac{k_B T}{\zeta} \frac{N_\xi^{4\nu-1}}{N_K^2} \tag{6.48}$$

Using expression (6.45) and expressions (6.46), (6.47) and (6.48) we calculate below the diffusion coefficients of linear and ring DNA of 45 kbp at $12C^*$ and compare it with Robertson and Smith (2007b) experimental data.

The maximum concentrations reached in DNA experiments of Robertson and Smith are $\approx 12C^*$. The molecular weight between entanglement and the correlation length at $31C^*$ are reported to be respectively,$1.45MDa$ and $0.4\mu m$ (Teixeira *et al.*, 2007). Using the reported data at $31C^*$ and the concentration dependence of ξ as given in relation (6.12) we can estimate that $N_\xi = \xi^2/b^2 \approx 30$ at $12C^*$. Here we have assumed that cyclic DNA has the same Kuhn length as that for linear DNA, which is reported by Teixeira *et al.* (2007) to be $b = 0.132\mu m$. The same authors also report a fast relaxation time of $2.0 \pm 0.5s$ for a λ-phage DNA molecule of $R_g = 0.73\mu m$ and $N_K = 167$ for various concentrations in the entangled regime. Equating the Doi and Edwards (1986) expression for the rotational Rouse relaxation time (which is one half of the Rouse relaxation time) to 2.0 s we can estimate the segmental friction coefficient of the DNA molecule to be $\zeta = 0.061s/\mu m^2 k_B T$.

Using the above estimated segmental friction coefficient the diffusion coefficient of a 45 kbp linear DNA at $12C^*$ can be calculated using equation (6.45) to be $\approx 7 \times 10^{-3}\mu m^2/s$. This prediction is found to be higher than the value measured experimentally by Robertson and Smith (2007b) of $\approx 3.5 \times 10^{-3}\mu m^2/s$ by a factor of ≈ 2. Therefore we correspondingly increase the segmental friction coefficient by this factor in order to match the predicted diffusion coefficient of linear polymers with the experimentally measured diffusion coefficient. Now assuming that the segmental friction coefficient for a cyclic DNA is the same as that for a linear DNA, the diffusion coefficient of the cyclic DNA can be calculated using equation (6.46) to be $\approx 3.5 \times 10^{-3}\mu m^2/s$ – a value lower by a factor of ≈ 8 from that measured experimentally. We can similarly calculate the cyclic DNA diffusion coefficient using equation (6.47) and (6.48) respectively to be $\approx 1 \times 10^{-2}\mu m^2/s$ – a value lower by a factor of ≈ 3 and $\approx 9 \times 10^{-4}\mu m^2/s$

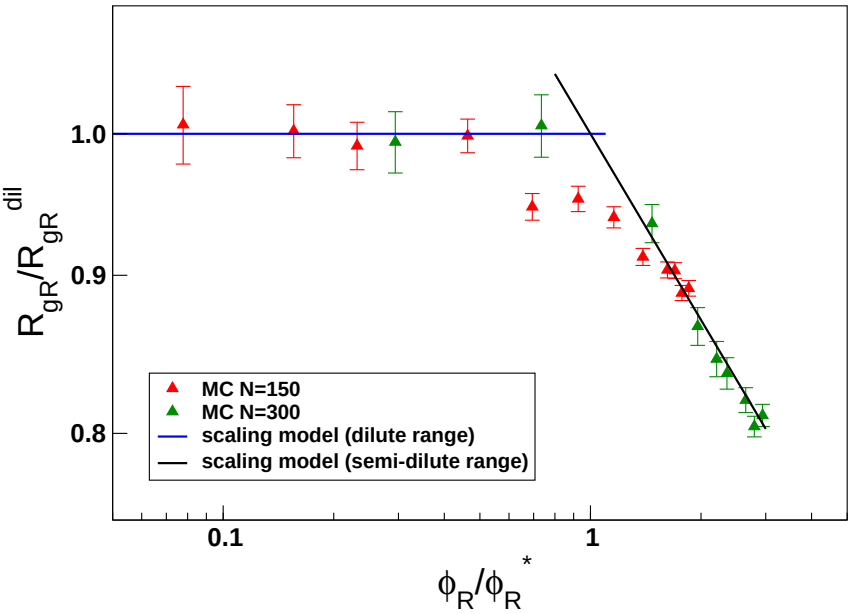

Figure 6.5: Comparison of concentration dependence of size in ring-linear blend scaling predictions with MC simulations by Sachin Shanbhag.

– a value lower by a factor of ≈ 30. It is observed that all the frameworks underpredict the diffusion coefficient of cyclic DNA as measured in the experiments of Robertson and Smith (2007b) at $12C^*$.

Note: 45 kbp cyclic DNA is large enough to experience excluded volume interactions in a strongly topologically constrained state (Obukhov *et al.*, 1994). However, for a 45 kbp cyclic DNA the predicted concentration at which excluded volume interactions could become relevant in a semi-dilute solution is estimated from relation (6.31) to be $C \approx 32C^*$, whereas the maximum concentration used in the experiments is $C \approx 12C^*$.

In Figure 6.5 we compare the scaling predictions of concentration dependence of ring size in a ring-linear blend for system with two different N with MC simulations by Sachin Shanbhag. In the ring-linear blend both the ring and the linear chain are of the same degree of polymerization. The ring and linear chains with degree of polymerization $N = 150$ and $N = 300$ are considered. For generating the master curve the ring size is scaled with dilute solution size and the concentration is scaled with the threshold concentration.

Appendix A

Pom-Pom Ring Framework

A.1 Normal Coordinates for $\mathbf{d_f = 1/\nu}$

Normal coordinates are defined by:

$$\mathbf{R}_n = \mathbf{X}_0 + 2\sum_p \mathbf{X}_p \cos\left(\frac{p\pi n}{N^{2\nu}}\right) \tag{A.1}$$

$$\mathbf{f}_n = \frac{\mathbf{f}_0}{N^{2\nu}} + \frac{1}{N^{2\nu}}\sum_p \mathbf{f}_p \cos\left(\frac{p\pi n}{N^{2\nu}}\right) \tag{A.2}$$

$$\mathbf{X}_p = \frac{1}{N^{2\nu}}\int_0^{N^{2\nu}} dn\ \cos\left(\frac{p\pi n}{N^{2\nu}}\right)\mathbf{R}_n \tag{A.3}$$

$$\mathbf{f}_p = 2\int_0^{N^{2\nu}} dn\ \cos\left(\frac{p\pi n}{N^{2\nu}}\right)\mathbf{f}_n \tag{A.4}$$

In the above equations ν is related to the fractal dimension of the Cayley-tree ring by $d_f = 1/\nu$. Thus, for an ideal ring in FO environment $\nu = 1/4$ and for a melt of rings ν can lie between $1/4$ and $1/2$.

The transformation of left hand side and the first term of the right hand side of equation (3.4) using normal coordinates (A.1) yields respectively:

$$\frac{\partial \mathbf{R}_n}{\partial t} = \frac{\partial \mathbf{X}_0}{\partial t} + 2\sum_p \frac{\partial \mathbf{X}_p}{\partial t}\cos\left(\frac{p\pi n}{N^{2\nu}}\right) \tag{A.5}$$

$$\frac{\partial^2 \mathbf{R}_n}{\partial n^2} = -2\sum_p \mathbf{X}_p \frac{p^2\pi^2}{N^{4\nu}}\cos\left(\frac{p\pi n}{N^{2\nu}}\right) \tag{A.6}$$

By equating coefficients of $\cos(p\pi n/N^{2\nu})$ in equation (3.4) we obtain:

$$\zeta_{eff}\frac{\partial \mathbf{X}_0}{\partial t} = \frac{\mathbf{f}_0}{N^{2\nu}} \tag{A.7}$$

$$2\zeta_{eff}\frac{\partial \mathbf{X}_p}{\partial t} = -2k_{eff}\frac{p^2\pi^2}{N^{4\nu}}\mathbf{X}_p + \frac{\mathbf{f}_p}{N^{2\nu}} \tag{A.8}$$

A.2 Zeroth and Higher Rouse Modes for $\mathrm{d_f} = 1/\nu$

The zeroth Rouse mode equation (A.7) can be written as:

$$\zeta_0\frac{\partial \mathbf{X}_0}{\partial t} = \mathbf{f}_0 \tag{A.9}$$

where $\zeta_0 = N^{2\nu}\zeta_{eff}$ and $\zeta_{eff} = \zeta_{loop}$ is the friction coefficient associated with the primary trunk segment. The solution of equation (A.9) gives the position of the center of mass of the chain and is given by:

$$\mathbf{X}_0 = \frac{1}{\zeta_0}\int_{-\infty}^{t} dt_1 \mathbf{f}_0(t_1) \tag{A.10}$$

In order to determine ζ_{loop} for Cayley tree chain with $d_f = 1/\nu$ and a trunk composed of $N^{2\nu}$ blobs we first determine that the loop is composed of $N^{1-2\nu}$ blobs using arguments similar to that in section 3.2. Using the pom-pom model analogy for loops composed of $N^{1-2\nu}$ blobs, the diffusion coefficient of a loop point, D_{loop}, is given by $D_{loop} \sim a^2/\tau_{loop}$, where $\tau_{loop} \sim a^2(N^{(1-2\nu)})^2\zeta_{blob}$ is the longest Rouse relaxation time of the loop attached to the loop point. Using the Einstein argument the drag on a loop point is given by:

$$\zeta_{loop} = \frac{k_BT}{D_{loop}} \approxeq N^{2(1-2\nu)}\zeta_{blob} \tag{A.11}$$

where ζ_{blob} is the friction coefficient of a single blob in the loop. Thus, the modified Rouse chain which constitutes the primitive chain has each of its beads having a friction coefficient of order $N^{2(1-2\nu)}\zeta_{blob}$ and hence ζ_{eff} is given by:

$$\zeta_{eff} = \zeta_{loop} \approxeq N^{2(1-2\nu)}\zeta_{blob} \tag{A.12}$$

Using the stochastic force correlation (3.10) and $\zeta_0 = N^{2\nu}\zeta_{eff}$ in equation (3.9) we obtain the mean square displacement of the center of mass:

$$\left\langle (X_{0\alpha}(t) - X_{0\alpha}(0))^2 \right\rangle = 2\frac{k_BT}{N^{2\nu}\zeta_{eff}}\delta_{\alpha\alpha}t \tag{A.13}$$

Using expression (A.13) in equation (3.8) the diffusion coefficient of the modified Rouse chain with an effective bead friction $N^{2(1-2\nu)}\zeta_{blob}$ is given by:

$$D_P = \frac{k_B T}{N^{2-2\nu}\zeta_{blob}} = \left(\frac{a}{b}\right)^{2(1-2\nu)} \frac{k_B T}{N_K^{2-2\nu}\zeta} \tag{A.14}$$

The decoupled equations for the higher normal modes are given by:

$$\zeta_p \frac{\partial \mathbf{X}_p}{\partial t} = -k_p \mathbf{X}_p + \mathbf{f}_p \tag{A.15}$$

where,

$$\zeta_p = 2N^{2\nu}\zeta_{eff} \tag{A.16a}$$

$$k_p = 2k_{eff}\frac{p^2\pi^2}{N^{2\nu}} \tag{A.16b}$$

The solution to equation (A.15) is given by:

$$\mathbf{X}_p(t) = \frac{1}{\zeta_p}\int_{-\infty}^{t} dt_1 \exp\left(-\frac{(t-t_1)}{\tau_p}\right)\mathbf{f}_p(t_1) \tag{A.17}$$

where, $\tau_p = \zeta_p/k_p$.

Substituting for ζ_p and k_p from equation (A.16) and using expression (A.12) for ζ_{eff} and $k_{eff} = 3k_BT/a^2$ we have:

$$\tau_p = \frac{1}{p^2}\frac{1}{3}\frac{a^2}{\pi^2}\frac{\zeta_{blob}}{k_B T}N^2 = \frac{1}{p^2}\frac{1}{3\pi^2}\frac{a^4}{b^2}\frac{\zeta}{k_B T}N^2 \tag{A.18}$$

where, we have used expression (3.3) for ζ_{blob} and the Gaussian statistics $a^2 = N_e b^2$. The longest relaxation time for Rouse like relaxation of the trunk corresponds to the first Rouse mode $p = 1$ and is given by:

$$\tau_1 = \frac{1}{3\pi^2}\frac{a^4}{b^2}\frac{\zeta}{k_B T}N^2 = \frac{1}{3}\frac{b^2}{\pi^2}\frac{\zeta}{k_B T}N_K^2 \tag{A.19}$$

where, we have used $N = N_K/N_e$. The shortest Rouse relaxation time of the trunk corresponds to that of the single blob of the trunk, *i.e.*, $p = N^{1/2}$ mode and is given by:

$$\tau_{N^{1/2}} = \frac{1}{3\pi^2}\frac{a^4}{b^2}\frac{\zeta}{k_B T}N = \frac{1}{3}\frac{a^2}{\pi^2}\frac{\zeta}{k_B T}N_K \tag{A.20}$$

The correlation of the Rouse modes $\langle X_{p\alpha}(t)X_{q\beta}(0)\rangle$ determines the stress in the system. In order to determine it we first obtain from equation (A.17):

$$\langle X_{p\alpha}(t)X_{q\beta}(0)\rangle = \frac{1}{\zeta_p^2}\int_{-\infty}^{t} dt_1 \int_{-\infty}^{0} dt_2 \exp\left(-\frac{(t-t_1)}{\tau_p}\right)\exp\left(\frac{t_2}{\tau_q}\right)\langle f_{p\alpha}(t_1)f_{q\beta}(t_2)\rangle \tag{A.21}$$

Using the fluctuation-dissipation theorem given by equation (3.5) and the normal coordinates transformation equation (A.2) we obtain:

$$\langle (f_{p\alpha}(t_1) f_{q\beta}(t_2)) \rangle = 2\zeta_p k_B T \delta_{pq} \delta_{\alpha\beta} \delta(t_1 - t_2) \tag{A.22}$$

Using equation (A.22) in equation (A.21), we obtain:

$$\langle (X_{p\alpha}(t) X_{q\beta}(0) \rangle = \frac{k_B T}{k_p} \delta_{pq} \delta_{\alpha\beta} \exp\left(-\frac{t}{\tau_p}\right) \tag{A.23}$$

A.3 Reptation of the trunk

The solution for equation (3.16) with the initial and boundary conditions, equations (3.17)-(3.19) is given by (Doi and Edwards, 1986):

$$\begin{aligned} \phi(s, s'; t) =& a|s - s'| + 2D_P \frac{a}{L_P} t \\ &+ 4\frac{L_P a}{\pi^2} \sum_p \frac{1}{p^2} \left[1 - \exp\left(-p^2 \frac{t}{\tau_d}\right)\right] \cos\left(\frac{p\pi s}{L_P}\right) \cos\left(\frac{p\pi s'}{L_P}\right) \end{aligned} \tag{A.24}$$

where,

$$\tau_d = \frac{L_P^2}{D_P \pi^2} = \frac{a^2}{\pi^2} \frac{\zeta_{blob}}{k_B T} N^{2\nu+2} = \frac{1}{\pi^2} \frac{b^{4\nu+1}}{a^{4\nu}} \frac{\zeta}{k_B T} N_K^{2\nu+2} \tag{A.25}$$

where we have used $L_P = N^{2\nu} a = N_K^{2\nu} b^{4\nu} / a^{4\nu-1}$ and D_P given by expression (A.14).

In the $\lim s' \to s$ we have $\phi(s, s; t) = \langle (\mathbf{R}(s,t) - \mathbf{R}(s,0))^2 \rangle$ the mean square displacement of the blob on the s^{th} position along the chain given by:

$$\left\langle (\mathbf{R}(s,t) - \mathbf{R}(s,0))^2 \right\rangle = 2D_P \frac{a}{L_P} t + 4\frac{L_P a}{\pi^2} \sum_p \frac{1}{p^2} \left[1 - \exp\left(-p^2 \frac{t}{\tau_d}\right)\right] \cos^2\left(\frac{p\pi s}{L_P}\right) \tag{A.26}$$

It can be seen from equation (A.26) for $t > \tau_d$ we get diffusive behavior with diffusion constant given by:

$$D = \lim_{t\to\infty} \frac{1}{6t} \phi(s, s; t) = \frac{1}{3} D_P \frac{a}{L_P} = \frac{1}{3} \frac{k_B T}{N^2 \zeta_{blob}} = \frac{1}{3} \frac{a^2}{b^2} \frac{k_B T}{N_K^2 \zeta} \tag{A.27}$$

In reptation the diffusive motion of the primitive chain determined by the evolution of correlation function $\phi(s, s; t)$ causes the chain to move out of the original tube of confinement. The original tube of confinement can be thought of as the orientational memory of the primitive chain. At long times, $t > \tau_d$, the diffusive motion causes the primitive chain to completely leave the original tube and loose its orientation completely. At intermediate times, $\tau_e < t < \tau_d$, a part of the primitive chain remains oriented within the original tube. The orientation of the primitive

chain is related to the time correlation function $G(s,s';t)$, of the tangent vectors, $\mathbf{u}(s,t)$, given by:

$$G(s,s';t) = \langle \mathbf{u}(s,t).\mathbf{u}(s',0) \rangle \tag{A.28}$$

The time correlation function of the tangent vector $G(s,s';t)$ is in turn related to the time correlation function $\phi(s,s';t)$ by (Doi and Edwards, 1986):

$$G(s,s';t) = \frac{1}{2}\frac{\partial^2}{\partial s \partial s'}\phi(s,s';t) \tag{A.29}$$

The correlation function $G(s,s';t)$ is non-zero when the tangent vectors $\mathbf{u}(s,t)$ and $\mathbf{u}(s',0)$ are correlated and zero when the tangent vectors are uncorrelated. All the tangent vectors of the primitive chain at time t, $\mathbf{u}(s,t)$, become uncorrelated with the original tube tangent vector at s', $\mathbf{u}(s',0)$, when any one end of the primitive chain passes the point s' along the original tube. The measure of correlation of all the tangent vectors at t, $\mathbf{u}(s,t)$, with the original tube tangent vector at s', $\mathbf{u}(s',0)$, is given by the integral of $G(s,s',t)$ over the contour of the primitive chain. This measure of correlation can be considered as the probability that the original tube segment s' remains at time t, $\psi(s',t)$, and is given by:

$$\psi(s',t) = \frac{1}{a}\int_0^{L_P} ds G(s,s';t) \tag{A.30}$$

The fraction of original tube/orientation of the primitive chain that remains at time t is then given by:

$$\begin{aligned}\psi(t) =& \frac{1}{L_P}\int_0^{L_P} ds'\psi(s',t) \\ =& \frac{8}{\pi^2}\sum_{p(odd)}\frac{1}{p^2}\exp\left(-p^2\frac{t}{\tau_d}\right)\end{aligned} \tag{A.31}$$

A.4 Mean square displacement of the blob

The mean-square displacement of a blob in terms of the normal coordinates is given by:

$$\begin{aligned}\left\langle (\mathbf{R}_n(t) - \mathbf{R}_n(0))^2 \right\rangle =& \left\langle (\mathbf{X}_0(t) - \mathbf{X}_0(0))^2 \right\rangle \\ &+ \left\langle \left[2\sum_p (\mathbf{X}_p(t) - \mathbf{X}_p(0)) \cos\left(\frac{p\pi n}{N^{2\nu}}\right)\right]^2 \right\rangle \\ &-4\left\langle (\mathbf{X}_0(t) - \mathbf{X}_0(0)) \sum_p (\mathbf{X}_p(t) - \mathbf{X}_p(0)) \cos\left(\frac{p\pi n}{N^{2\nu}}\right) \right\rangle\end{aligned} \tag{A.32}$$

The underlined term in expression (A.32) corresponds to the cross correlations between different modes in the modified Rouse chain and vanish due to the linear independence of the normal coordinates. Consequently, the mean square displacement of the modified Rouse blob is composed of two contributions, *viz.*, the center of mass contribution and the internal modes contribution. Substituting equation (3.11) for the center of mass contribution in equation (A.32) we obtain:

$$\left\langle (\mathbf{R}_n(t) - \mathbf{R}_n(0))^2 \right\rangle = 6D_P t + \underline{4 \sum_p \left\langle (\mathbf{X}_p(t) - \mathbf{X}_p(0))^2 \right\rangle \cos^2\left(\frac{p\pi n}{N^{2\nu}}\right)} \tag{A.33}$$

We expect that, the time taken by a modified Rouse blob to have a mean square displacement of order a^2, is much smaller than the longest modified Rouse relaxation time τ_1. For $t << \tau_1$ the contribution of the internal modes for the displacement of the modified Rouse blob dominates over the center of mass contribution. The underlined term of expression (A.33) corresponds to the internal modes contribution and can be expanded to obtain:

$$\begin{aligned} &4 \sum_p \left(\mathbf{X}_p(t) - \mathbf{X}_p(0)\right)^2 \cos^2\left(\frac{p\pi n}{N^{2\nu}}\right) \\ &\qquad = 4 \sum_p \left(\left\langle \mathbf{X}_p(t)^2 \right\rangle + \left\langle \mathbf{X}_p(0)^2 \right\rangle - 2 \left\langle \mathbf{X}_p(t).\mathbf{X}_p(0) \right\rangle \right) \cos^2\left(\frac{p\pi n}{N^{2\nu}}\right) \end{aligned} \tag{A.34}$$

From equation (A.17) we have:

$$\begin{aligned} &\langle X_{p\alpha}(t) X_{q\beta}(t) \rangle \\ &\qquad = \frac{1}{\zeta_p^2} \int_{-\infty}^{t} dt_1 \int_{-\infty}^{t} dt_2 \exp\left(-\frac{(t-t_1)}{\tau_p}\right) \exp\left(-\frac{(t-t_2)}{\tau_q}\right) \langle f_{p\alpha}(t_1) f_{q\beta}(t_2) \rangle \end{aligned} \tag{A.35}$$

Using expression (A.22) in equation (A.35) we obtain:

$$\begin{aligned} &\langle X_{p\alpha}(t) X_{q\beta}(t) \rangle \\ &\qquad = 2\frac{k_B T}{\zeta_p} \delta_{\alpha\beta} \delta_{pq} \int_{-\infty}^{t} dt_1 \int_{-\infty}^{t} dt_2 \exp\left(-\frac{(t-t_1)}{\tau_p}\right) \exp\left(-\frac{(t-t_2)}{\tau_q}\right) \delta(t_1 - t_2) \end{aligned} \tag{A.36}$$

Expression (A.36) yields $\left\langle (\mathbf{X}_p(t))^2 \right\rangle = 3k_B T/k_p$ for all t and $\left\langle \mathbf{X}_p(t).\mathbf{X}_p(0) \right\rangle = (3k_B T/k_p) \exp(-t/\tau_p)$. Substituting in equation (A.34) we obtain for $t << \tau_1$:

$$\left\langle (\mathbf{R}_n(t) - \mathbf{R}_n(0))^2 \right\rangle = 4N^{2\nu} \frac{a^2}{\pi^2} \sum_p \frac{1}{p^2} \left[1 - \exp\left(-p^2 \frac{t}{\tau_1}\right)\right] \cos^2\left(\frac{p\pi n}{N^{2\nu}}\right) \tag{A.37}$$

To obtain the average mean-square displacement of any segment of the chain we sum the displacement of all the beads and divide it by the number of beads:

$$\begin{aligned} AverageMSD =& \frac{1}{N^{2\nu}} \sum_{n=1}^{N^{2\nu}} \left\langle (\mathbf{R_n}(t) - \mathbf{R_n}(0))^2 \right\rangle \\ =& 4\frac{a^2}{\pi^2} \sum_p \frac{1}{p^2} \left[1 - \exp\left(-p^2 \frac{t}{\tau_1} \right) \right] \sum_{n=1}^{N^{2\nu}} \cos^2\left(\frac{p\pi n}{N^{2\nu}} \right) \end{aligned} \tag{A.38}$$

Moving from a discrete to continuous framework in n and p the summations are converted to integrals:

$$\sum_{n=1}^{N^{2\nu}} \cos^2\left(\frac{p\pi n}{N^{2\nu}} \right) = \int_0^{N^{2\nu}} dn \ \cos^2\left(\frac{p\pi n}{N^{2\nu}} \right) \tag{A.39}$$

$$\sum_p \frac{1}{p^2} \left[1 - \exp\left(-p^2 \frac{t}{\tau_1} \right) \right] = \int_0^{\infty} dp \ \frac{1}{p^2} \left[1 - \exp\left(-p^2 \frac{t}{\tau_1} \right) \right] \tag{A.40}$$

The average mean square displacement based on the continuous framework is given by:

$$AverageMSD = 2N^{2\nu} \frac{a^2}{\pi^2} \sqrt{\pi} \sqrt{\frac{t}{\tau_1}} \tag{A.41}$$

From equation (A.41) the time taken for a blob in the modified Rouse chain to have an average mean square displacement of a^2 is given by:

$$\tau_e = \frac{\pi}{12} \frac{a^4}{b^2} \frac{\zeta}{k_B T} N^{2(1-2\nu)} = \frac{\pi}{12} \frac{a^{8\nu}}{b^{8\nu-2}} \frac{\zeta}{k_B T} N_K^{2(1-2\nu)} \tag{A.42}$$

and is obtained based on the relaxation time expression (A.19).

A.5 Friction of the hierarchical trunk

Consider for example a three tier hierarchical structure of the lattice tree. Hierarchy level 1 consists of a primary trunk of $N^{1/2}$ blobs having as many primary loops attached to it, each of which contains on an average $N^{1/2}$ blobs. Hierarchical level 2 describes the fractal structure of a primary loop, *i.e.*, it consists of a secondary trunk of $N^{1/4}$ blobs having as many secondary loops attached to it, each of which contains on an average $N^{1/4}$ blobs. At the hierarchical level 3 each of the secondary loops is described as being composed of a tertiary trunk of $N^{1/8}$ segments having as many loops attached to it, each of which contains $N^{1/8}$ blobs. We will follow consistently the argument that at any hierarchical level a trunk segment can undergo

Brownian reorientational motions only after the loop attached to it has relaxed via its modified Rouse dynamics.

If the friction coefficient of an individual blob is ζ_{blob}, then longest Rouse relaxation time of the 3rd hierarchical level loops $\sim N^{1/4}\zeta_{blob}$. This will then manifest itself as the friction coefficient of the segment of the trunk of the 3rd hierarchical level, *i.e.*, $\zeta^{(3)} \sim N^{1/4}\zeta_{blob}$. Thus the modified Rouse chain at the 3rd hierarchical level would consist of a chain containing $N^{1/8}$ blobs each having a friction coefficient of order $N^{1/4}\zeta_{blob}$. Proceeding similarly to the next higher hierarchical level, the friction coefficient of a trunk blob of hierarchy 2 can be calculated from the longest relaxation time of the modified Rouse chain of hierarchy 3. Thus, $\zeta^{(2)} \sim (N^{1/8})^2\zeta^{(3)} \sim N^{1/2}\zeta_{blob}$. The trunk of the second hierarchy level contains $N^{1/4}$ blobs each having a friction coefficient given by $N^{1/2}\zeta_{blob}$. It is then straightforward to calculate the friction coefficient of a trunk blob on the 1st hierarchical level as being $\zeta^{(1)} \sim (N^{1/4})^2\zeta^{(2)} \sim N\zeta_{blob}$. Generalizing the above argument, it can be shown that for the i^{th} level of hierarchy, $i = 1$ being the primary trunk of $N^{1/2}$ blobs, the friction coefficient of a trunk segment at that hierarchical level is given by $\zeta^{(i)} \sim N^{(1/2)^{i-1}}\zeta_{blob}$.

Appendix B

Fractal Gate Framework

B.1 Fractal Rouse Model for $\mathbf{d_f = 1/\nu}$

The normal coordinates and the Langevin equation remain the same as that defined in section 5.1. However, the friction coefficients as determined by the blob rearrangement dynamics in the fractal structure is modified to be consistent with the fractal exponent $d_f = 1/\nu$. Considering that instead of the friction being proportional to the size of the section m/p it is proportional to the size of fast relaxing structures in the section, *i.e.*, $\sim (m/p)^{1-2\nu}$, the effective friction for a blob in a section of the chain is given by:

$$\zeta^0_{eff} = m^{1-2\nu}\zeta_{blob} \tag{B.1}$$

$$\zeta^p_{eff} = \left(\frac{m}{p}\right)^{1-2\nu}\zeta_{blob} \tag{B.2}$$

The constant k^p_{eff} associated with the fractal skeleton is obtained from the conjugate Langevin of Muthukumar (1985) and is given by:

$$k^p_{eff} = k\left(\frac{p_s\pi}{m}\right)^2 = k\left(\frac{p\pi}{m}\right)^{2\nu+1} \tag{B.3}$$

Using the correlation expression (5.17), the effective friction expression (B.2) and blob friction coefficient expressions (5.11) in the diffusion coefficient expression (5.16):

$$D_{mR} = \frac{k_BT}{m^{2-2\nu}\zeta_{blob}} = \left(\frac{a}{b}\right)^{4\nu-2}\frac{k_BT}{m_K^{3/2}\zeta} \tag{B.4}$$

In arriving at expression (B.4) we have used expression (5.11) for ζ_{blob}, $m = m_k/N_e$ and $a^2 = N_eb^2$.

The expression for relaxation time τ_p can be arrived at using equations (B.2), (5.11), (B.3) and the Gaussian statistics $a^2 = N_e b^2$ and is given by:

$$\tau_p = \frac{\zeta_p}{k_p} = \frac{1}{p^2}\pi^{1/2}\frac{1}{3\pi^2}\frac{a^4}{b^2}\frac{\zeta}{k_B T}m^2 \tag{B.5}$$

The longest relaxation time corresponds to the relaxation of the entire m section, *i.e.*, $p = 1$, and is given by:

$$\tau_1 = \pi^{1-2\nu}\frac{1}{3\pi^2}\frac{a^4}{b^2}\frac{\zeta}{k_B T}m^2 \tag{B.6}$$

The shortest relaxation time corresponds to the relaxation of a single section of the ring chain, *i.e.*, $p = m$ and is given by:

$$\tau_m = \pi^{1-2\nu}\frac{1}{3\pi^2}\frac{a^4}{b^2}\frac{\zeta}{k_B T} = \pi^{1/2}\frac{1}{3}\frac{b^2}{\pi^2}\frac{\zeta}{k_B T}N_e^2 \tag{B.7}$$

It scales as $\sim N_e^2$ and corresponds to the relaxation time of an unentangled blob of N_e Kuhn segments.

It is also straightforward to show that due to dynamic self-similarity the center of mass curvilinear diffusion coefficient and the longest relaxation time of the entire ring chain containing N blobs (or equivalently, N_K Kuhn segments) are given by:

$$D_N = \frac{k_B T}{N^{2-2\nu}\zeta_{blob}} = \left(\frac{a}{b}\right)^{4\nu-2}\frac{k_B T}{N_K^{2-2\nu}\zeta} \tag{B.8}$$

$$\tau_N = \frac{1}{p^2}\pi^{1-2\nu}\frac{1}{3\pi^2}\frac{a^4}{b^2}\frac{\zeta}{k_B T}N^2 \tag{B.9}$$

B.2 Mean square displacement of the blob

The mean-square displacement of a blob in terms of the normal coordinates (5.2–5.5) is given by:

$$\begin{aligned}\left\langle(\mathbf{R_n}(t) - \mathbf{R_n}(0))^2\right\rangle = &\left\langle(\mathbf{X_0}(t) - \mathbf{X_0}(0))^2\right\rangle \\ &+ \left\langle\left[2\sum_{p_s}(\mathbf{X_p}(t) - \mathbf{X_p}(0))\cos\left(\frac{p_s\pi n}{m}\right)\right]^2\right\rangle \\ &\underline{-4\left\langle(\mathbf{X_0}(t) - \mathbf{X_0}(0))\sum_{p_s}(\mathbf{X_p}(t) - \mathbf{X_p}(0))\cos\left(\frac{p_s\pi n}{m}\right)\right\rangle}\end{aligned} \tag{B.10}$$

The underlined term in expression (B.10) corresponds to the cross correlations between different modes in the fractal blob chain and vanish due to the linear independence of the normal

coordinates. Consequently, the mean square displacement of the fractal Rouse blob is composed of two contributions, *viz.*, the center of mass contribution and the internal modes contribution. Substituting equation (5.18) for the center of mass contribution in equation (B.10) we obtain:

$$\left\langle (\mathbf{R_n}(t) - \mathbf{R_n}(0))^2 \right\rangle = 6D_m t + \underline{4 \sum_p \left\langle (\mathbf{X_p}(t) - \mathbf{X_p}(0))^2 \right\rangle \cos^2 \left(\frac{f(p)\pi n}{m} \right)} \tag{B.11}$$

where we have tranformed variables from p_s to p as per expression (4.14) so that $f(p) = p_s = p^{(2\nu+1)/2}(m/\pi)^{(1-2\nu)/2}$ is a function of p which always takes integer values.

We expect that, the time taken by a blob to undergo a mean square displacement of order a^2, is much smaller than the longest fractal Rouse relaxation time τ_1. For $t << \tau_1$ the contribution of the internal modes for the displacement of the blob dominates over the center of mass contribution. The underlined term of expression (B.11) corresponds to the internal modes contribution and can be expanded to obtain:

$$\begin{aligned} & 4 \sum_p \left(\mathbf{X_p}(t) - \mathbf{X_p}(0) \right)^2 \cos^2 \left(\frac{f(p)\pi n}{m} \right) \\ & \quad = 4 \sum_p \left(\left\langle \mathbf{X_p}(t)^2 \right\rangle + \left\langle \mathbf{X_p}(0)^2 \right\rangle - 2 \left\langle \mathbf{X_p}(t).\mathbf{X_p}(0) \right\rangle \right) \cos^2 \left(\frac{f(p)\pi n}{m} \right) \end{aligned} \tag{B.12}$$

From equation (5.19) we have:

$$\begin{aligned} & \langle X_{p\alpha}(t) X_{q\beta}(t) \rangle \\ & \quad = \frac{1}{\zeta_p^2} \int_{-\infty}^{t} dt_1 \int_{-\infty}^{t} dt_2 \exp \left(-\frac{(t-t_1)}{\tau_p} \right) \exp \left(-\frac{(t-t_2)}{\tau_q} \right) \langle f_{p\alpha}(t_1) f_{q\beta}(t_2) \rangle \end{aligned} \tag{B.13}$$

Using expression (5.14) in equation (B.13) we obtain:

$$\begin{aligned} & \langle X_{p\alpha}(t) X_{q\beta}(t) \rangle \\ & \quad = 2 \frac{k_B T}{\zeta_p} \delta_{\alpha\beta} \delta_{pq} \int_{-\infty}^{t} dt_1 \int_{-\infty}^{t} dt_2 \exp \left(-\frac{(t-t_1)}{\tau_p} \right) \exp \left(-\frac{(t-t_2)}{\tau_q} \right) \delta(t_1 - t_2) \end{aligned} \tag{B.14}$$

Expression (B.14) yields $\left\langle (\mathbf{X_p}(t))^2 \right\rangle = 3k_B T/k_p$ for all t and $\left\langle \mathbf{X_p}(t).\mathbf{X_p}(0) \right\rangle = (3k_B T/k_p) \exp(-t/\tau_p)$. Substituting in equation (B.12) we obtain for $t << \tau_1$:

$$\left\langle (\mathbf{R_n}(t) - \mathbf{R_n}(0))^2 \right\rangle = 4m^{2\nu} \frac{a^2}{\pi^{2\nu+1}} \sum_p \frac{1}{p^{2\nu+1}} \left[1 - \exp \left(-p^2 \frac{t}{\tau_1} \right) \right] \cos^2 \left(\frac{f(p)\pi n}{m} \right) \tag{B.15}$$

To obtain the average mean-square displacement of any segment of the chain we sum the

displacement of all the blobs and divide it by the number of blobs:

$$\begin{aligned} AverageMSD =& \frac{1}{m}\sum_{n=1}^{m}\left\langle(\mathbf{R_n}(t)-\mathbf{R_n}(0))^2\right\rangle \\ =& \frac{4}{m^{2\nu}}\frac{a^2}{\pi^{2\nu+1}}\sum_{p}\frac{1}{p^{2\nu+1}}\left[1-\exp\left(-p^2\frac{t}{\tau_1}\right)\right]\sum_{n=1}^{m}\cos^2\left(\frac{f(p)\pi n}{m}\right) \end{aligned} \tag{B.16}$$

Moving from a discrete to continuous framework in n and p the summations are converted to integrals:

$$\sum_{n=1}^{m}\cos^2\left(\frac{f(p)\pi n}{m}\right) = \int_0^m dn\ \cos^2\left(\frac{f(p)\pi n}{m}\right) \tag{B.17}$$

$$\sum_{p}\frac{1}{p^{3/2}}\left[1-\exp\left(-p^2\frac{t}{\tau_1}\right)\right] = \int_0^\infty dp\ \frac{1}{p^{2\nu+1}}\left[1-\exp\left(-p^2\frac{t}{\tau_1}\right)\right] \tag{B.18}$$

The average mean square displacement based on the continuous framework is given by:

$$AverageMSD = m^{2\nu}\frac{a^2}{\pi^{2\nu+1}}\frac{1}{\nu}\Gamma\left[1-\nu\right]\left(\frac{t}{\tau_1}\right)^{\nu} \tag{B.19}$$

From equation (B.19) the time taken for a blob in the fractal blob chain to have an average mean square displacement of a^2 is given by:

$$\tau_e = \frac{1}{3}\pi^{\frac{(2\nu+1)(1-\nu)}{\nu}}\nu^{\frac{1}{\nu}}\ \left(\Gamma\left[1-\nu\right]\right)^{-\frac{1}{\nu}}\frac{a^4}{b^2}\frac{\zeta}{k_BT} \tag{B.20}$$

In arriving at the above result we have used the expression for τ_1 given by expression (B.6) and for the specific case of $d_f = 1/\nu = 4$ reduces to:

$$\tau_e = \frac{\pi^{9/2}}{3\times 4^4}\left(\Gamma\left[\frac{3}{4}\right]\right)^{-4}\frac{a^4}{b^2}\frac{\zeta}{k_BT} \tag{B.21}$$

.

B.3 Relaxation Modulus of the Fractal Rouse Chain

The microscopic expression for the stress tensor is given by (Doi and Edwards, 1986):

$$\sigma_{\alpha\beta} = \frac{c_b}{m}\sum_{n}\left\langle\frac{\partial U}{\partial R_{n\alpha}}R_{n\beta}\right\rangle \tag{B.22}$$

It can be inferred from Muthukumar (1985) arguments that for polymeric fractals U is given by:

$$U = \frac{k}{2}\sum_{n=2}^{m}(\mathbf{R_n}-\mathbf{R_{n-1}})^2 \tag{B.23}$$

in the spectral dimension. Combining the insights from equations (B.22) and (B.23) the microscopic expression for the stress tensor according to the Blob-Spring model can be written as:

$$\sigma_{\alpha\beta} = \frac{c_b}{m} k \int_0^N dn \left\langle \nabla_s R_{n\alpha} \nabla_s R_{n\beta} \right\rangle \tag{B.24}$$

where, ∇_s denotes gradient in the spectral dimension of the fractal network and c_b is the number density of the blobs that make up the ring polymer and is given by $c_b = c/N_e$.

Using the normal coordinate transformation (5.2)-(5.5) the stress tensor expression is given by:

$$\sigma_{\alpha\beta} = \frac{c_b}{m} \sum_{p_s} k_{ps} \left\langle X_{p\alpha} X_{p\beta} \right\rangle \tag{B.25}$$

where, $k_{ps} = 2mk(p_s\pi/m)^2$. Equation (B.25) is appropriately modified in the conjugate space and the stress tensor expression is given by:

$$\sigma_{\alpha\beta} = \frac{c_b}{m} \sum_{p} k_p \left\langle X_{p\alpha} X_{p\beta} \right\rangle \tag{B.26}$$

We now impose a homogeneous deformation gradient $\bar{v}(\mathbf{r}, t) = \bar{\bar{\kappa}}(t).\mathbf{r}$. During such a deformation the Langevin equation for the p^{th} normal coordinate, $\mathbf{X}_p$, becomes

$$\frac{\partial \mathbf{X}_p}{\partial t} = -\frac{k_p}{\zeta_p}\mathbf{X}_p + \frac{1}{\zeta_p}\mathbf{f_p} + \bar{\bar{\kappa}}(t).\mathbf{X}_p \tag{B.27}$$

From the Langevin equation (B.27) we obtain the equation for the correlation $\langle X_{p\alpha} X_{p\beta} \rangle$ as

$$\frac{\partial}{\partial t} \left\langle X_{p\alpha} X_{p\beta} \right\rangle = -2\frac{k_p}{\zeta_p} \left\langle X_{p\alpha} X_{p\beta} \right\rangle + 4\frac{k_B T}{\zeta_p}\delta_{\alpha\beta} + \kappa_{\alpha\mu} \left\langle X_{p\mu} X_{p\beta} \right\rangle + \kappa_{\beta\mu} \left\langle X_{p\alpha} X_{p\mu} \right\rangle \tag{B.28}$$

Equation (B.28) can be solved to obtain $\langle X_{p\alpha} X_{p\beta} \rangle$ for any given homogeneous deformation gradient. For homogeneous shear where $\bar{\bar{\kappa}}(t)$ is given by

$$\begin{bmatrix} 0 & \kappa(t) & 0 \\ 0 & 0 & 0 \\ 0 & 0 & 0 \end{bmatrix}$$

we have the equation for the xy component of the correlation given by

$$\frac{\partial}{\partial t} \left\langle X_{px} X_{py} \right\rangle = -2\frac{k_p}{\zeta_p} \left\langle X_{px} X_{py} \right\rangle + \kappa(t) \left\langle X_{py}^2 \right\rangle \tag{B.29}$$

Considering the system to be close to equilibrium we have $\left\langle X_{py}^2 \right\rangle = k_B T/k_p$, using which the solution to equation (B.29) is obtained as:

$$\left\langle X_{px} X_{py} \right\rangle = \frac{k_B T}{k_p} \int_{-\infty}^{t} dt_1 \exp\left(-2\frac{(t-t_1)}{\tau_p}\right) \kappa(t_1) \tag{B.30}$$

Substituting equation (B.30) in equation (B.26) we obtain:

$$\sigma_{xy} = \frac{c_b}{m} k_B T \sum_p \int_{-\infty}^{t} dt_1 \exp\left(-2\frac{(t-t_1)}{\tau_p}\right) \kappa(t_1) \tag{B.31}$$

The phenomenological expression for stress tensor in terms of the relaxation modulus is given by:

$$\sigma_{xy}(t) = \int_{-\infty}^{t} dt_1 G(t-t_1)\kappa(t_1) \tag{B.32}$$

Comparing equation (B.31) with equation (B.32) we obtain the contribution of the m section of the ring chain to the Blob-Spring relaxation modulus as:

$$G(t) = \frac{c_b}{m} k_B T \sum_p \exp\left(-2\frac{t}{\tau_p}\right) \tag{B.33}$$

B.4 Hyperbranched Polymers

We have seen that the ring polymer has a structure similar to that of randomly branched (hyperbranched) polymer. In this section the derivation of the results for hyperbranched polymers used in obtaining the expression for density of gates in a Cayley tree is presented. The derivations are based on the understanding of formation of hyperbranched structures in condensation polymerization of AB_{f-1} monomers which are composed of a single functional group of type A and $f-1$ functional groups of type B. In a condensation polymerization A reacts only with B and vice versa and hence for $f = 2$ a linear chain structure is obtained and for $f > 2$ an hyperbranched structure is obtained Rubinstein and Colby (2003). We derive the number fraction of N-mers in a system and present its relationship to probability of formation of specific structures.

B.4.1 Number Fraction of N-mers: $n_N(\varphi)$

In order to derive the number fraction of N-mers, $n_N(\varphi)$,as a function of fraction of reacted B groups φ we note that:

- There is only one unreacted A group per polymer molecule while there are several unreacted B groups per polymer molecule.
- The number of reacted A and B groups is the same and for a N-mer there are $N-1$ of these reacted groups.

- The number of unreacted B groups is given by $N(f-1)-(N-1) = N(f-2)+1$

The probability that a N-mer is formed in the process is thus given by:

$$P(N) = P_{RB}(N-1) \times P_{URB}(N(f-2)+1) \tag{B.34}$$

where $P_{RB}(N-1)$ is the probability of having $N-1$ reacted B groups and $P_{URB}(N(f-2)+1)$ is the probability of having $N(f-2)+1$ unreacted B groups. In terms of the fraction of reacted B groups $P_{RB} = \varphi^{N-1}$ and $P_{URB} = (1-\varphi)^{N(f-2)+1}$. The number fraction of N-mers in the system is thus given by:

$$n_N(p) = a_N \times \varphi^{N-1} \times (1-\varphi)^{N(f-2)+1} \tag{B.35}$$

where a_N is the number of ways the N monomers of the chain can be arranged to form a N-mer.

It is important to note that there exists a relationship between fractions of reacted B and A groups which sets a limit to the validity of expression (B.35). In order to understand this limit we consider the fractions of reacted A and B groups in a N-mer given by $(N-1)/N$ and $(N-1)/(N(f-1))$ respectively. This indicates a simple relationship between fractions of reacted A and B groups in the system given by $\varphi_A = \varphi(f-1)$. The fraction of unreacted A groups in the system is thus given by $1-\varphi(f-1)$. According to this expression at $\varphi_c = 1/(f-1)$ the fraction of unreacted A groups vanishes and hence the reaction can no longer proceed beyond this point. Thus, expression (B.35) is valid only for $\varphi < \varphi_c$, where φ_c is the critical fraction of reacted B groups beyond which there are no free A groups available for reaction.

B.4.2 Number Fraction of N-mers: $n_N(\epsilon)$

In order to explicitly account for the limit of validity it is useful to express the number fraction of N-mers as a function of relative extent of reaction ϵ defined as:

$$\epsilon = \frac{\varphi - \varphi_c}{\varphi_c} = \varphi(f-1) - 1 \tag{B.36}$$

The relative extent of reaction is the negative of the fraction of unreacted A groups and thus lies between $-1 \leq \epsilon < 0$. If the fractions of reacted and unreacted B are expressed in terms of the ϵ as:

$$\varphi = \frac{1+\epsilon}{f-1} \tag{B.37}$$

$$1-\varphi = \frac{f-2}{f-1}\left(1 - \frac{\epsilon}{f-2}\right) \tag{B.38}$$

then it can be shown that for sufficiently small negative values of ϵ the number fraction of $n_N(\epsilon)$ is given by:

$$n_N(\epsilon) = a_N \frac{(f-2)^{N(f-2)+1}}{(f-1)^{N(f-1)}} \exp(-\epsilon^2 N) \tag{B.39}$$

B.4.3 Derivation of a_N

In obtaining a_N we first note that there is a degeneracy of $N!$ arrangements in sequencing the N monomers as they are indistinguishable. However, formation of the N-mer involves reaction of the B groups and several ways of reacting the B groups. From the $N(f-1)$ such B groups there are as many number of ways of choosing the first B group. The number of ways of reacting the second B group is $(N(f-1)-1)$, the third B group is $(N(f-1)-2)$ and in general the number of ways of reacting the m^{th} B group is given by $(N(f-1)-(m-1))$. Thus, the number of ways of reacting $N-1$ such B groups in order to result in an N-mer is given by:

$$N_{RB} = N(f-1)(N(f-1)-1)...(N(f-1)-(N-2)) = \frac{[N(f-1)]!}{[N(f-1)-(N-1)]!} \tag{B.40}$$

The number of ways of arrangement a_N is obtained by the combination of degeneracy and the number of ways of reacting B groups and is given by:

$$a_N = N_{RB} \div N! = \frac{[N(f-1)]!}{N![N(f-1)-(N-1)]!} \tag{B.41}$$

For $N >> 1$ the factorial can be expressed using Stirling's approximation and can be written as:

$$\begin{aligned} N! &\approx \sqrt{2\pi N} N^N \exp(-N) \\ [N(f-1)]! &\approx \sqrt{2\pi N(f-1)} (N(f-1))^{N(f-1)} \exp(-N(f-1)) \\ [N(f-2)+1]! &\approx (N(f-2)+1)[N(f-2)]! \\ &\approx (N(f-2))\sqrt{2\pi N(f-2)} (N(f-2))^{N(f-2)} \exp(-N(f-2)) \end{aligned} \tag{B.42}$$

Using the Stirling's approximation for the factorial as written in set of expressions (B.42) in expression (B.41) we obtain:

$$a_N \approx \frac{1}{\sqrt{2\pi}} \sqrt{\frac{f-1}{f-2}} N^{-3/2} \frac{(f-1)^{N(f-1)}}{(f-2)^{N(f-2)+1}} \tag{B.43}$$

B.4.4 Probability of Structures

By combining expressions (B.35) and (B.43) we arrive at an approximate expression for number fraction of N-mers in AB_{f-1} condensation polymerization given by:

$$n_N(\epsilon) \approx \frac{1}{\sqrt{2\pi}}\sqrt{\frac{f-1}{f-2}}N^{-3/2}\exp(-\epsilon^2 N) \tag{B.44}$$

In the AB_{f-1} polymerization there is exactly one unreacted A group per molecule and thus the number fraction given by expression (B.44) corresponds to the probability of finding an unreacted A group that is part of an $N-mer$. In the condensation polymerization of A_f monomers since there are only A groups in the system the probability of finding an unreacted A group as a part of an N-mer is the same as the number fraction of N-mers in the AB_{f-1} condensation polymerization. Thus, the probability of finding an unreacted A group as a part of a m-mer in a system can be written as:

$$u_m(\epsilon) \approx \frac{1}{\sqrt{2\pi}}\sqrt{\frac{f-1}{f-2}}m^{-3/2}\exp(-\epsilon^2 m) \tag{B.45}$$

Based on the probability of unreacted A groups associated with different structures we can consider probability of formation of specific structures. For instance an N-mer can be formed by reacting a m-mer with an $(N-m)$-mer and we can calculate the probability of forming such a structure which was made starting from an m-mer and $(N-m)$-mer as:

$$\begin{aligned} u_{m|N-m}(\epsilon) &= u_m(\epsilon) \times u_{N-m}(\epsilon) \\ &= \frac{1}{2\pi}\frac{f-1}{f-2}m^{-3/2}(N-m)^{-3/2}\exp(-\epsilon^2 N) \end{aligned} \tag{B.46}$$

Bibliography

Alexander, S. and Orbach, R. (1982) Density of states on fractal :$\langle\langle fractons\rangle\rangle$. *J. Physique Lett.* **43**(17), 625–631.

Arrighi, V., Gagliardi, S., Dagger, A. C., Semlyen, J. A., Higgins, J. S. and Shenton, M. J. (2004) Conformation of Cyclics and Linear Chain Polymers in Bulk by SANS. *Macromolecules* **37**(8057-8065).

Barlow, M. T. and Kumagai, T. (2005) Random walk on the incipient infinite cluster on trees. arXiv:math/0503118v1 [math.PR].

Bloomfield, V. and Zimm, B. H. (1966) Viscosity, Sedimentation, et Cetera, of Ring- and Straight- Chain Polymers in Dilute Solution. *J. Chem. Phys.* **44**, 315–323.

Brown, S., Lenczycki, T. and Szamel, G. (2001) Influence of topological constraints on the statics and dynamics of ring polymers. *Physical Review E* **63**, 052801–1–4.

Brown, S. and Szamel, G. (1998) Computer simulation study of structure and dynamics of ring polymers. *J. Chem. Phys.* **109**, 6184–6192.

Carmesin, I. and Kremer, K. (1988) The bond fluctuation method: a new effective algorithm for the dynamics of polymers in all spatial dimensions. *Macromolecules* **21**, 2819–2823.

Cates, M. E. and Deutsch, J. M. (1986) Conjectures on the statistics of ring polymers. *J. Physique* **47**, 2121–2128.

Chandrasekhar, S. (1943) Stochastic Problems in Physics and Astronomy. *Reviews of Modern Physics* **15**(1), 1–89.

Chu, S. (1991) Laser Manipulation of Atoms and Particles. *Science* **253**, 861–866.

Cosgrove, T., Griffiths, P. C., Hollingshurst, J., Richards, R. D. C. and Semlyen, J. A. (1992) Self-Diffusion and Spin-Spin Relaxation in Cyclic and Linear Polydimethylsiloxane Melts. *Macromolecules* **25**, 6761–6764.

Cosgrove, T., Turner, M. J., Griffiths, P. C., Hollingshurst, J., Shempton, M. J. and Semlyen, J. A. (1996) Self-diffusion and spin-spin relaxation in blends of linear and cyclic polydimethylsiloxane melts. *Polymer* **37**(9), 1535–1540.

Daoud, M., Pincus, P., Stockmayer, W. H. and Jr., T. W. (1983) Phase separation in branched polymer solutions. *Macromolecules* **16**, 1833–1839.

de Gennes, P. G. (1971) Reptation of a polymer in a gel. *J. Chem. Phys.* **55**, 572–579.

de Gennes, P.-G. (1979) *Scaling Concepts in Polymer Physics*. Cornell University Press.

des Cloizeaux, J. (1981) Ring polymers in solution: topological effects. *J. Physique-Letters* **42**, L433–L436.

des Cloizeaux, J. (1990a) Relaxation and Viscosity Anomaly of Melts Made of Long Entangled Polymers. Time-Dependent Reptation. *Macromolecules* **23**(21), 4678–4687.

des Cloizeaux, J. (1990b) Relaxation of entangled polymer melts. *Macromolecules* **23**(17), 3992–4006.

Deutsch, J. M. (1999) Equilibrium size of large ring molecules. *Physical Review E* **59**, R2539–R2541.

Doi, M. (1983) Explanation for the 3.4-Power Law for Viscosity of Polymeric Liquids on the Basis of the Tube Model. *J. Polym. Sci. Polym. Phys.* **21**, 667–684.

Doi, M. and Edwards, S. F. (1978a) Dynamics of Concentrated Polymer Systems Part 1.-Brownian Motion in the Equilibrium State. *J. Chem. Soc. Faraday Trans.II* **74**, 1789–1801.

Doi, M. and Edwards, S. F. (1978b) Dynamics of Concentrated Polymer Systems Part 2.-Molecular Motions Under Flow. *J. Chem. Soc. Faraday Trans.II* **74**, 1802–1817.

Doi, M. and Edwards, S. F. (1978c) Dynamics of Concentrated Polymer Systems Part 3.-The Constitutive Equation. *J. Chem. Soc. Faraday Trans.II* **74**, 1818–1832.

Doi, M. and Edwards, S. F. (1979) Dynamics of Concentrated Polymer Systems Part 4.- Rheological Properties. *J. Chem. Soc. Faraday Trans.II* **75**, 38–54.

Doi, M. and Edwards, S. F. (1986) *The Theory of Polymer Dynamics*. Oxford University Press.

Duke, T. A. J. (1989) Tube Model of Field-Inversion Electrophoresis. *Phys. Rev. Lett.* **62**(24), 2877–2880.

Durhuus, B., Jonsson, T. and Wheater, J. F. (2007) The Spectral Dimension of Generic Trees. *J. Stat. Phys* **128**, 1237–1260.

Edwards, S. F. (1967a) Statistical mechanics of polymerized material. *Proc. Phys. Soc.* **92**, 9–16.

Edwards, S. F. (1967b) Statistical mechanics with topological constraints: I. *Proc. Phys. Soc.* **91**, 513–519.

Ferry, J. D. (1980) *Viscolelastic Properties of Polymers*. Wiley Publishers.

Fetters, L. J., Lohse, D. J. and Colby, R. H. (1996) *Physical Properties of Polymers Handbook*, chapter 24. Chain dimensions and entanglement spacings. AIP Press.

Fetters, L. J., Lohse, D. J. and Colby, R. H. (2006) *Physical Properties of Polymers Handbook*, chapter 25. Chain dimensions and entanglement spacings. AIP Press.

Fukatsu, M. and Kurata, M. (1966) Hydrodynamic Properties of Flexible-Ring Macromolecules. *J. Chem. Phys.* **44**(12), 4539–4545.

Gagliardi, S., Arrighi, V., Ferguson, R., Dagger, A. C., Semlyen, J. A. and Higgins, J. S. (2005) On the difference in scattering behavior of cyclic and linear polymers in bulk. *J. Chem. Phys.* **122**(064904-1:8).

Graessley, W. W. (1980) Some Phenomenological Consequences of the Doi-Edwards Theory of Viscoelasticity. *J. Polym. Sci. Polym. Phys.* **18**, 27–34.

Gutin, A. M., Grosberg, A. Y. and Shakhnovich, E. I. (1993) Polymers with Annealed and Quenched Branchings Belong to Different University Classes. *Macromolecules* **26**, 1293–1295.

Hermans, J. J. (1943) Theoretische Beschouwingen Over De Viskositeit En De Stromings-Dubblebreking In Oplossingen Van Mocromoleculaire Stoffen. *Physica* **10**(10), 777–789.

Higgins, J. S., Dodgson, K. and Semlyen, J. A. (1979) Studies of cyclic and linear poly(dimethyl siloxane): 3. Neutron scattering measurements of the dimensions of ring and chain polymer. *Polymer* **20**, 553–558.

Hur, K., Winkler, R. G. and Yoon, D. Y. (2006) Comparison of ring and linear polyethylene from molecular dynamics simulations. *Macromolecules* **39**, 3975–3977.

Isaacon, J. and Lubensky, T. C. (1980) Flory exponents of generalized polymer problems. *J. Physique Lett.* **41**, 469–471.

Kanaeda, N. and Deguchi, T. J. (2008) Diffusion of a ring polymer in good solution via the brownian dynamics with no bond crossing. *J. Phys.A: Math. Theor* **41**, 145004–1–145004–11.

Kapnistos, M., Lang, M., Vlassopoulous, D., Pyckour-Hintzen, W., Hitcher, D., Cho, D. and Rubinstein, M. (2008) Unexpected power-law stress relaxation of entangled ring polymers. *Nature Materials* **7**, 997–1002.

Karayiannis, N. C. and Mavrantzas, V. G. (2005) Hierarchical Modeling of the Dynamics of Polymers with a Nonlinear Molecular Architecture: Calculation of Branch Point Fraction and Chain Reptation Time of H-shaped Polethylene Melts from Long Molecular Dynamics Simulations. *Macromolecules* **38**, 8583–8596.

Kawaguchi, D., Masuoka, K., Takano, A., Tanaka, N., Torikai, N., Dalgliesh, R. M., Langridge, S. and Matsushita, Y. (2006) Comparison of interdiffusion behavior between cyclic and linear polystyrenes with high molecular weights. *Macromolecules* **39**, 5180–5182.

Khokhlov, A. R. and Nechaev, S. K. (1985) Polymer chain in an array of obstacles. *Phys. Lett.* **112A**, 156–160.

Klein, J. (1978) The Onset of Entanglement Behavior in Semidilute and Concentrated Polymer Solution. *Macromolecules* **11**(5), 852–858.

Klein, J. (1986) Dynamics of Entangled Linear, Branched and Cyclic Polymers. *Macromolecules* **19**, 105–118.

Kramer, H. A. (1944) Het getdrag van macromleculen in een stroomende vloeistof. *Physica* **11**(1), 1–19.

Kübel, C., González-Ronda, L., Drummy, L. F. and Martin, D. C. (2000) Defects-mediated twisting and curvature in polymer crystals. *J. Phys. Org. Chem.* **13**, 816–829.

Likhtman, A. E. and McLeish, T. C. B. (2002) Quantitative Theory of Linear Dynamics of Linear Entangled Polymers. *Macromolecules* **35**(16), 6332–6343.

Liu, T. W. and Öttinger, H. C. (1987) Bead-spring rings with hydrodynamic interactions. *J. Chem. Phys.* **87**, 3131–3136.

Lubensky, T. C. and Isaacson, J. (1979) Statistics of lattice animals and dilute branched polymers. *Physical Review A.* **20**(5), 2130–2146.

Marrucci, G. (1985) Relaxation by Reptation and Tube Enlargement: A Model for Polydisperse Polymers. *J. Poly. Sci. Polym. Phys.* **23**, 159–177.

McKenna, G. B., Hadziioannou, G., Lutz, P., G.Hild, Strazielle, C., C.Straupe, Rempp, P. and Kovacs, A. J. (1987) Dilute solution characteristics of cyclic polystyrene molecules and their zero-shear viscosity in the melt. *Macromolecules* **20**, 498–512.

McKenna, G. B., Hostetter, B. J., Hadjichristidia, N., Fetters, L. J. and Plazek, D. J. (1989) A Study of the Linear Viscoelastic Properties of Cyclic Polystyrenes Using Creep and Recovery Measurements. *Macromolecules* **22**, 1834–1852.

McLeish, T. C. B. (2002a) Polymers Without Begining or End. *Science* **297**, 2005–2006.

McLeish, T. C. B. (2002b) Tube theory of entangled polymer dynamics. *Advances in Physics* **51**(6), 1379–1527.

McLeish, T. C. B. (2003) Present puzzles of entangled polymeric systems. *Rheol. Rev.* pp. 197–232.

McLeish, T. C. B. and Larson, R. G. (1998) Molecular constitutive equations for a class of branched polymers: The pom-pom polymer. *J. Rheol* **42**(1), 81–110.

Meakin, P. and Stanley, H. E. (1983) Spectral Dimension for Diffusion-Limited Aggregation Model for Colloid Growth. *Phys. Rev. Lett* **51**(16), 1457–1460.

Mills, P. J., Mayer, J. M., Kramer, E. J., Hadziiannou, G., Lutz, P., Strazielle, C., Rempp, P. and Kovacs, A. J. (1987) Diffusion of polymer rings in linear polymer matrices. *Macromolecules* **20**, 513–518.

Milner, S. T. and McLeish, T. C. B. (1998) Reptation and Contour-Length Fluctuations of Melts of Linear Polymers. *Phys. Rev. Lett.* **81**(3), 725–728.

Müller, M., Wittmer, J. P. and Cates, M. E. (1996) Topological effects in ring polymers: A computer simulation study. *Phys. Rev. E.* **53**(5), 5063–5074.

Müller, M., Wittmer, J. P. and Cates, M. E. (2000) Topological effects in ring polymers: Influence of persistence length. *Phys. Rev. E.* **61**(4), 4078–4089.

Muthukumar, M. (1985) Dynamics of polymeric fractals. *J. Chem. Phys.* **83**(6), 3161–3168.

Nechaev, S. (1998) Statistics of knots and entangled random walks. arXiv:cond-mat/9812205.

Nechaev, S. K., Semenov, A. N. and Koleva, M. K. (1987) Dynamics of a polymer chain in an array of obstacles. *Physica* **140A**, 506–520.

Obukhov, S. P., Rubinstein, M. and T.Duke (1994) Dynamics of Ring Polymer in a Gel. *Phys. Rev. Lett.* **73**(9), 1263–1267.

Ohta, Y., Masuoka, K., Takano, A. and Matsushita, Y. (2006) Chain dimension of cyclic polymers in solution. *Physica B* **385-386**, 532–534.

Parisi, G. and Sourlas, N. (1981) Critical Behavior of Branched Polymers and the Lee-Yang Edge Singularity. *Phys. Rev. Lett.* **46**(14), 871–874.

Pathak, J. A., Kumar, S. K. and Colby, R. H. (2004) Miscible Polymer Blend Dynamics: Double Reptation Predicition of Linear Viscoelasticity in Model Blends of Polyisoprene and Poly(vinylethylene). *Macromolecules* **37**, 6994–7000.

Pearson, D. S. and Helfland, E. (1984) Viscoelastic Properties of Star-Shaped Polymers. *Macromolecules* **17**, 888–895.

Perkins, T. T., Smith, D. E. and Chu, S. (1994) Direct Observation of Tube-Like Motion of a Single Polymer Chain. *Science* **264**, 819–822.

Redner, S. (1979) Mean end-to-end distance of branched polymers. *J. Phys. A: Math. Gen.* **12**, L239–L244.

Robertson, R. M. and Smith, D. E. (2007a) Direct measurement of the confining forces imposed on a single molecule in a concentrated solution of ring polymers. *Macromolecules* **40**, 8737–8741.

Robertson, R. M. and Smith, D. E. (2007b) Self-diffusion of entangled linear and circular DNA molecules: Dependence on length and concentration. *Macromolecules* **40**, 3373–3377.

Robertson, R. M. and Smith, D. E. (2007c) Strong effects of molecular topology on diffusion of entangled DNA molecules. *PNAS* **104**(12), 4824–4827.

Roovers, J. (1985a) Dilute Solution Properties of Ring Polystyrenes. *J. Polym. Sci. Polym. Phys.* **23**, 1117–1126.

Roovers, J. (1985b) Melt properties of ring polysyrene. *Macromolecules* **18**, 1359–1361.

Roovers, J. (1988) Viscoelastic properties of polybutadiene rings. *Macromolecules* **21**, 1517–1521.

Roovers, J. and Toporowski, P. (1988) Synthesis and Characterization of Ring Polybutadiene. *J. Polym. Sci. Polym. Phys.* **26**, 1251–1259.

Roovers, J. and Toporowski, P. M. (1983) Synthesis of high molecular weight polystyrenes. *Macromolecules* **16**, 843–849.

Rouse, P. E. (1953) A Theory of the Viscoelastic Properties of the Dilute Solutions of Coiling Polymers. *J. Chem. Phys.* **21**, 1272–1280.

Rubinstein, M. (1986) Dynamics of Ring Polymers in Presence of Fixed Obstacles. *Phys. Rev. Lett.* **57**(24), 3023–3026.

Rubinstein, M. (1987) Discretized Model of Entangled-Polymer Dynamics. *Phys. Rev. Lett.* **59**(17), 1946–1949.

Rubinstein, M. and Colby, R. H. (1988) Self-consistent theory of polydisperse entangled polymers: Linear viscoelasticity of binary blends. *J. Chem. Phys* **89**, 5291.

Rubinstein, M. and Colby, R. H. (2003) *Polymer Physics*. Oxford University Press.

Rubinstein, M., Colby, R. H. and Gillmor, J. R. (1989) Dynamics Scaling for Polymer Gelation. In *Space-Time Organization in Macromolecular Fluids*, eds. Tanaka, F., Doi, M. and Ohta, T., pp. 67–74. Springer-Verlag Berlin, Hiedelberg.

Shaffer, J. S. (1994) Effect of polymer topology on polymer dynamics: Bulk melts. *J. Chem. Phys.* **101**(5), 4205.

Shaffer, J. S. (1995) Effect of polymer topology on polymer dynamics: Configurational relaxation in polymer melts. *J. Chem. Phys.* **103**(2), 761.

Suneel, Buzza, D. M. A., Groves, D. J., McLeish, T. C. B., Parker, D., Keemey, A. J. and Feast, W. J. (2002) Rheology and Molecular Weight Distrbution of Hyperbranched Polymers. *Macromolecules* **35**, 9605–9612.

Suzuki, J., Takano, A. and Matsushita, Y. (2008) Topological effect in ring polymers investigated with Monte Carlo simulation. *J. Chem. Phys.* **129**, 034903–1–034903–5.

Teixeira, R. E., Dambal, A. K., Richter, D. H., Shaqfeh, E. S. G. and Chu, S. (2007) The individualistic dynamics of entangled DNA in solution. *Macromoelcules* **40**, 2461–2476.

Tsenoglou, C. (1991) Molecular Weight Polydispersity Effects on the Viscoelasticity of Entangled Linear Polymers. *Macromolecules* **24**, 1762–1767.

Wasserman, S. A. and Cozzarelli, N. R. (1986) Biochemical Topology: Application to DNA recombination and replication. *Science* **232**, 951–960.

Weist, J. M., S. R. Burdette, T. W. L. and Bird, R. B. (1987) Effect of ring closure on rheological behavior. *J.Non-Newt.Flu.Mech* **24**, 279–295.

WIKIPEDIA (2009) Cantor set. http://en.wikipedia.org/wiki/Cantor_set.

Zimm, B. H. (1956) Dynamics of Polymer Molecules in Dilute Solution: Viscoelasticity, Flow Birefringence and Dielectric Loss. *J. Chem. Phys.* **24**, 269–278.

Zimm, B. H. and Stockmayer, W. (1949) The Dimension of Chain Molecules Containing Branches and Rings. *J. Chem. Phys* **17**, 1301–1314.

Appendix C

List of Publications

Balaji Iyer, V. S., Lele, A. K. and Juvekar, V. A. (2006) Flexible ring polymers in an obstacle environment: Molecular theory of linear viscoelasticity, *Phys. Rev. E.*, **74**, 021805-1:12.

Balaji Iyer, V. S., Lele, A. K. and Shanbhag, S. (2007) What Is the Size of a Ring Polymer in a Ring-Linear Blend?, *Macromolecules*, **40**, 5995-6000.

Balaji Iyer, V. S., Shanbhag, S., Juvekar, V. A. and Lele, A. K. (2008) Self-Diffusion Coefficient of Ring Polymers in Semidilute Solution, *J. Polym. Sci. Part B: Polym. Phys.*, **46**, 2370-2379.

Balaji Iyer, V. S., Lele, A. K., Juvekar, V. A. and Mashelkar, R. A. (2009) Self-Similar Dynamics of a Flexible Ring Polymer in a Fixed Obstacle Environment: A Coarse Grained Molecular Model *accepted for publication in Ind. Eng. Chem. Res.*.

Acknowledgments

The course of the time spent in developing the ideas in this thesis were of great value to me, especially so, as it was enriched by interactions with many people in both IIT Bombay and NCL Pune. First and foremost I would like to thank my advisors Prof.Vinay Juvekar and Dr.Ashish Lele for their constant support and encouragement in the course of my thesis work. I consider myself extremely privileged to have worked with an advisor who embodies knowledge and the other who is the best person to work with in terms of gaining a dynamic understanding and an infectious enthusiasm in looking for solutions to problems. Special thanks goes to Prof. Juvekar for being a source of inspiration with his indefatigable spirit to support learning that gave me the extra impetus to strive for the kind of depth and vastness of knowledge Prof. Juvekar embodies. While Prof.Juvekar served as the inspiration I had Dr.Ashish always at my side with his great personal concern towards my well being which made my life during this period on the whole a very pleasant experience. In fact I remember paining him initially with all kinds of requests for which he would personally attend to. He is unsurpassable in his commitment to making life easy for all his students and I personally benefited a lot from this commitment. One other unique feature of Dr. Ashish which I learnt a lot from is his ability to simplify a problem and skill in breaking down an idea into its elements with great clarity of expression. I would also like to thank my RPC members Prof. Hemant and Prof. Khakkar for their support. Special thanks goes to Prof. Rochish of IIT Bombay and Prof. Shankar of IIT Kanpur for equipping me with important ideas in polymer physics which were valuable in bettering my understanding. I am deeply indebted to Mohan anna for sharing his knowledge and ideas in a range of topics, opening me up to some fabulous literature and his timely advise at different stages of my life which did a world of good to me.

I now come to the very special encounters which pertains more to my 'extra curricular' side of life during my stay at IIT Bombay. It was fun to be part of Hostel 6 during my first semester stay. The M.Sc physics population was especially great fun to be with. Special thanks

goes to to Arkajit Burman a great fan of Mohd Rafi and Guru Dutt who introduced me to some of the fantastic songs and classy movies I have heard and seen so far, Dibyendu Hazra for introducing me to rabindra sangeet in his own cheerful way, Saikat Dalvi for being a very good example of simplicity of approach to life and Saikat Chaudhary for the discussions on Swami Vivekananda. The chemistry dudes starting with Biplab, Ramakrishna, Buddha, Pramit, Shukla were all very kind to me and helped me in lot of ways like 'sutta partnership'(Ramakrishna and Pramit), philosophy (Biplab and Shukla) and martial arts (special thanks goes to Buddha who tried to teach me win chun and aikido in spite of my limited physical abilities). Foraging for food was an integral part of IIT life and in that respect I have to thank Murthy who introduced me to the early morning 'maddu' mess in Powai which provided some kind of a stable foraging zone especially at odd times. My Chemical Engineering friends Viknesh, Ananth and Prithvi helped me in bouncing off a few ideas across as a training ground for interaction with students. My IIT Bombay episode would not be complete without the mention of my interaction with Mashuq-un-Nabi from whom I learnt a few of the great principles of Islam.

In NCL I have met some of the people who have been instrumental in developing my own philosophy of relationships. Without the help of these people I would have developed into a complete social misfit. In this respect I would specifically like to thank Sam for her great enthusiasm in showing me the way to be nice to people, her remarkable freshness in approach which was sometimes annoyingly independent of what I thought or advised her, her craze for shopping (so I knew if I wanted something all I need to do is ask her), travel support for my innumerable tea sessions to Siddharth and places in and around NCL and lots of other things of which I have lost count. Among the NCL football legends (infact often injured legend) I had this wonderful opportunity to train under coach Naveen and learn a lot about passion and in fact even more about compassion for which I am grateful to him. I am thankful to Kiran for his commitment towards my emotional well being - like he ensured that on a regular basis sutta was taken care of and also made sure that I listened to his completely biased opinion about everything under the sky before I made any decision. I also would like to thank him for rekindling my interest in rock n roll and specifically for introducing me to Link'n Park and Ledd Zepplin.

I would like to thank Aditya for generally kicking my ass around the ground in the name of army fart parade in his endeavor to get me into shape – which has however continued to be unrelentingly bad. I also would like to thank Omkar for introducing me to 'The Big Bang

Theory' when I was into the thesis writing dry days (literally dry as I did not have enough funding for booze) and ensured that I had that little bit of entertainment that was much needed to ensure that I did not go completely nuts. My thanks to Chirag for all the discussions we have had on physics and physicists (especially the one about G.I. Taylor) that helped me broaden my horizon. The other CFPE members have always chipped in with their valuable time to do some time pass without which life at NCL would have been a terrible bore. I would like to specially thank a couple of the time pass members like Anurag and Vikrant who taught me some of the essentials of being a 'dude' during our fantastic road trip through the hills to Mahad. I would also like to thank Arun, 'Captain' Vijay and Pandu for their sutta-chai and residential support during my return to NCL and for generally making me listen to bad guitar (courtesy Arun) and forcing me to buy Santana, Eagles and Beatles in order to escape the torture. I would also like to thank Virus & Elan for the innumerable party sessions we have had during my transition from IIT to NCL way of life.

Special thanks goes to Kalyani and Ganpat Dahe for their ready support in getting a lot of my official work done in IIT Bombay. Thanks to Meera for proof reading and her valuable suggestions in improving the thesis. Thanks to Harsha for helping me out in preparing the printouts for conference presentation. Thanks to Shailesh for his ready extension of help in anything and lightening up some of my moments in NCL with his good sense of humor. I would like to thank Ajey and Piyush for their help with several of the administrative jobs at NCL and Ashok for being a source of information for all kinds of official details in IIT and NCL. In the course of my stay in IIT and NCL I have met so many people each of whom have patiently suffered me and there are far too many names and special incidents to be mentioned in this acknowledgement. I would like to thank all of them for patiently suffering me.

Date: _____ V. S. Balaji Iyer